ANALYSIS OF A POWER CONVERSION SYSTEM FOR A WAVE ENERGY CONVERTER

David Van der Meeren

Master's thesis
May 2011
Degree Programme in Electrical Engineering
Tampereen ammattikorkeakoulu
Tampere University of Applied Sciences

TAMPEREEN AMMATTIKORKEAKOULU
Tampere University of Applied Sciences

Writer	David Van der Meeren
Thesis	Analysis of a power conversion system for a wave energy converter
Pages	89
Graduation time	June 2011
Thesis supervisor (KHBO)	Isabelle Vervenne
Thesis supervisor (TAMK)	Lauri Hietalahti
Thesis orderer	TAMK

Abstract

In this thesis the energy conversion of a Wave Energy Converter is analysed. To start there is an introduction about wave energy and a short presentation of the project. Throughout the project a permanent magnet generator, powered by a floating buoy, is used. A test setup is made to simulate the incoming movement on the generator with an electric motor. The theoretic values of the generator are tested with reality based on several measurements. The problem with generating energy in this manner is that the axis of the generator stops on the moment that the buoy is on the maximum and minimum of the wave. This results in an irregularly generated voltage with dips.

In this thesis it is researched how this irregular voltage can be smoothened without using a (super) capacitor. A study is made of an electronic circuit of a Boost Converter to solve this problem. These results were used to make PSpice simulations in OrCAD in order to analyse the function and feasibility of this project.

To conclude, the Boost Converter can indeed show an improvement but, in combination with a flywheel on the axis and a smaller capacitor the best results will most likely be achieved. However, this requires further investigation.

Keywords: WEC, ASWEC, wave energy conversion, floating buoy, permanent magnet generator, PSpice simulations, boost converter

Schrijver	David Van der Meeren
Thesis	Analysis of a power conversion system for a wave energy converter
Aantal pagina's	89
Afstudeertijd	Juni 2011
Promotor intern (KHBO)	Isabelle Vervenne
Promotor extern (TAMK)	Lauri Hietalahti
Thesis opdrachtgever	TAMK

Abstract (in Dutch)

In deze thesis wordt de energie omzetting van een Wave Energy Converter bestudeerd. Er wordt gestart met een inleiding over golfslagenergie, waarna kort het project wordt voorgesteld. In het project wordt gebruik gemaakt van een roterende permanente magneet generator aangedreven door een drijvende boei. Een testopstelling is gemaakt om de inkomende beweging op de generator te simuleren met een motor. De theoretische waarden van de generator worden getoetst aan de realiteit aan de hand van enkele metingen. Het probleem bij het opwekken van energie op deze manier is dat de generator as stil staat op het moment dat de boei op het hoogte-en dieptepunt van de golf is. Dit resulteert in een onregelmatige gegenereerde spanning met dips.

In deze thesis wordt bestudeerd hoe deze spanning kan afgevlakt worden zonder gebruik te maken van een (super)condensator. Er is een studie gemaakt van een elektronische schakeling van een Boost Converter om dit probleem op te lossen. Hiervan werden in OrCAD PSpice simulaties gemaakt om de werking en haalbaarheid te onderzoeken.

Als besluit wordt gesteld dat de Boost Converter wel degelijk een verbetering kan zijn, maar gecombineerd met een vliegwiel op de as en een (kleinere) condensator worden wellicht de beste resultaten bereikt. Hiervoor is echter verder onderzoek vereist.

Trefwoorden:	WEC, ASWEC, wave energy conversion, floating buoy, permanent magnet generator, PSpice simulations, boost converter

Preface

This final master thesis is made at Tampere University of Applied Sciences (TAMK). For me, as an Erasmus exchange student, this was a very challenging but interesting experience. During my stay in Finland, I learned a lot about the wave-energy subject as well as the Finnish –and other cultures. This thesis is a part of the ASWEC project, anyone who wants the complete result of this project will have to consult more sources than this thesis.

This Erasmus exchange had never worked without the full support of my home university KHBO (Catholic University College of Bruges–Ostend) and TAMK (Tampere University of Applied Sciences). For which I wish to thank these institutions. I want to thank Mr. Lauri Hietalathi as my supervisor in TAMK and Ms. Isabelle Vervenne as my supervisor in KHBO for the support during my stay. Also thank to Mr. Joan Peuteman who supported this Erasmus exchange from the beginning.

Special thanks to my parents and grandmother for the emotional and financial support during this exchange. Also special thanks to my girlfriend Helena for the lovely support and help with the translations.

Tampere, May 2011

David Van der Meeren

1 CONTENTS

1 CONTENTS 5
2 INTRODUCTION 10
2.1 Waves: where do they come from? 10
2.2 Waves: how much energy they have? 12
2.3 How much energy can we extract from an ideal wave? 14
2.4 Which part of the power can a buoy extract? 16
2.5 Global wave energy possibilities 16
3 THE ASWEC PROJECT 18
3.1 The Floating buoy 18
4 THEORETICAL MODEL 20
5 TEST EQUIPMENT 21
5.1 Permanent Magnet Generator 22
5.1.1 Theoretical generator characteristics 23
5.1.2 Practical generator characteristics 26
5.1.3 Comparison between theoretical and practical values 27
5.2 Servo Motor 27
5.3 Gear 28
6 INDUCED VOLTAGE SHAPING 29
6.1 Step 1: diode bridge 30
6.1.1 Losses in the bridge of diodes 31
6.2 Step 2: DC link voltage 32
6.2.1 Super capacitor 32
6.2.2 DC-DC converter: Boost convertor 32
6.3 Step 1 + 2: Unidirectional boost rectifier 42
6.3.1 Unidirectional rectifier 42
6.3.2 Control of unidirectional rectifier 43
6.3.3 External simulated results 43

6.3.4 Losses 44
6.3.5 Test equipment: theoretical boost converter parameters 45
6.4 Step 3: DC Transport basics 46
6.4.1 Common DC bridge 46
6.4.2 Main HVDC advantage 47
6.4.3 Conclusion 48
6.5 Step 4: Three phase inverter 49
6.5.1 PWM - converter 49
6.5.2 Solution when incoming voltage varies 50
7 BOOST CONVERTER SIMULATION 51
7.1 PSpice boost converter topology 51
7.2 Basic boost converter – DC input 52
7.3 Basic boost converter – saw tooth input 54
7.4 Basic boost convertor – 1 phase wave form input 55
7.5 Basic boost converter – 1 phase rectified input 56
7.6 Three-phase boost converter input 57
7.7 Optimizing simulation Load value 62
7.8 3-phase boost & non-boost comparison 67
7.8.1 3-phase without boost 67
7.8.2 3-phase with boost 69
7.8.3 Comparison 71
7.9 Higher boost switching frequency 72
8 MEASUREMENTS 74
8.1 Optimal power at fixed speed 74
8.1.1 Load seen from generator side 74
8.1.2 Load seen from DC-side 79
8.1.3 Conclusion 82
8.2 First changing speed measurement 82

8.3 Fixed load at changing speed 84

8.3.1 Fixed load - Model simulation 85

8.3.2 Fixed load – Measurements 85

9 CONCLUSIONS 87

10 REFERENCES 89

Abbreviations and symbols

Abbreviations and symbols waves		
Symbol	*Unit*	*Definition*
λ	M	wavelength
T	S	time period of the wave
TA = A	M	Amplitude wave
H = Hc	M	Peak to peak amplitude of the wave= 2A
V	m/s	horizontal velocity wave –
ω	Rad/s	*rotational speed*
N	rpm	*rotational speed*
f	rad/s	Frequency wave
g	m/s²	Gravity = 9.81 m/s²
P	W/m	Total wave energy per unit crest width, under ideal conditions
	kg/m³	Mass per volume

Abbreviations and symbols permanent magnet generator		
Symbol	*Unit*	*Definition*
n_n	rpm	Nominal speed
n_{max}	rpm	Maximum rotational speed
f_s	Hz	Line frequency at 250rpm
P_n	kW	Nominal power
I_n	A	Line current
U_Y	V	Induced voltage at nominal speed

Abbreviations and symbols servo motor		
Symbol	*Unit*	*Definition*
n_n	rpm	Nominal rotational speed
M_n	Nm	Nominal torque
M_k	Nm	Stall torque

Abbreviations and symbols practical generator characteristics		
Symbol	*Unit*	*Definition*
E_{PM}	V	Phase voltage
Ψ	Wb	Magnetic flux
f_s	Hz	Frequency of induced voltage

Abbreviations and symbols load value		
Symbol	*Unit*	*Definition*
P_l	W	Output power
E	V	Induced voltage in no load condition
R_l	Ω	Load resistance
R_g	Ω	Generator resistance
X_s	Ω	Generator coil impedance

2 INTRODUCTION

Note: Because this thesis is based on an existing project, some basic parts were already written down earlier. Parts of this introduction are copied from the thesis of Hannes Stubbe, who was working on this subject before me.

2.1 Waves: where do they come from?

Wave energy is created by wind, as a by-product of the atmosphere's redistribution of solar energy. The rate of energy input to waves is typically 0,01 to 0,1 W/m². This is a small fraction of the gross solar energy input, which averages 350W/m², but waves can build up over oceanic distances to energy densities averaging over 100kW/m (note that the typical measure is power per meter width of wave front). Because of its origin from oceanic winds, the highest average levels of wave power are found on the lee side of temperate zone oceans. [1]

For choosing suitable sites to plant a Wave Energy Converter, it is important to know which wave power is estimated on the optional zones. Therefore, measurements and estimations are set out on a map. The following map in Figure 1 shows the global annual mean wave power estimates in kW/m. Note that this is a 10-year mean annual wave power for all global points in the WorldWaves database. Other maps can show e.g. the wave power in one month, or e.g. just one continent as shown in Figure 2.

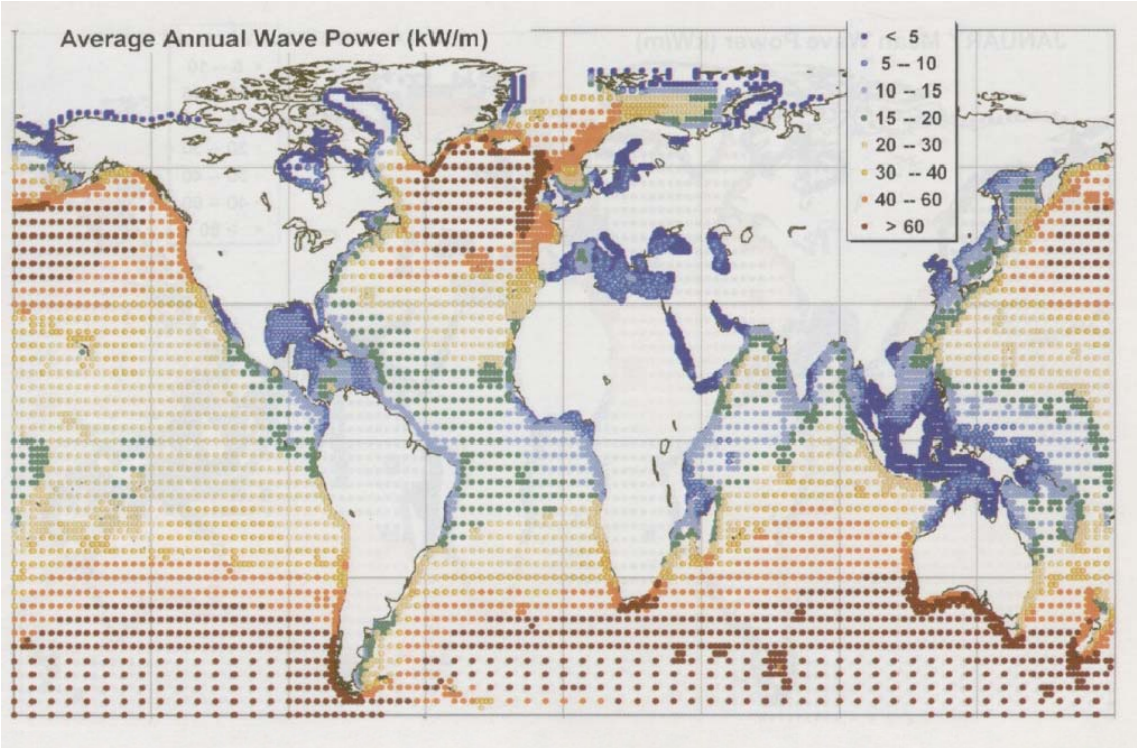

Figure 1: Global annual mean wave power estimates in kW/m [1]

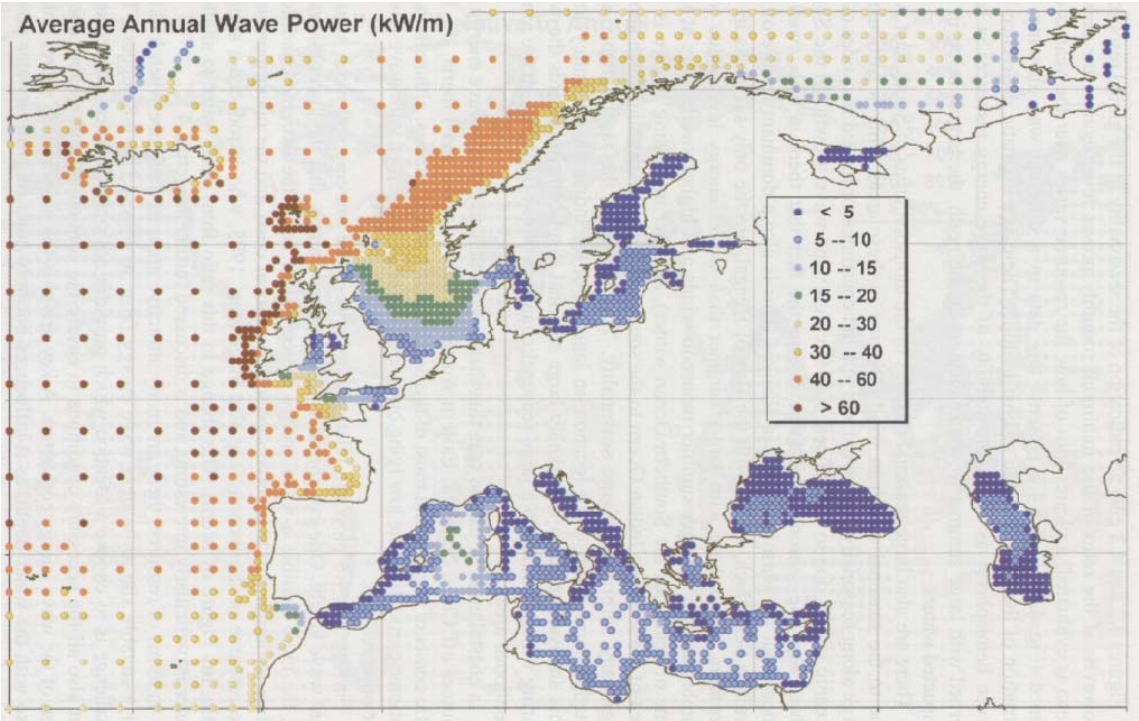

Figure 2: Annual mean wave power estimates (kW/m) for European waters [1]

2.2 Waves: how much energy they have?

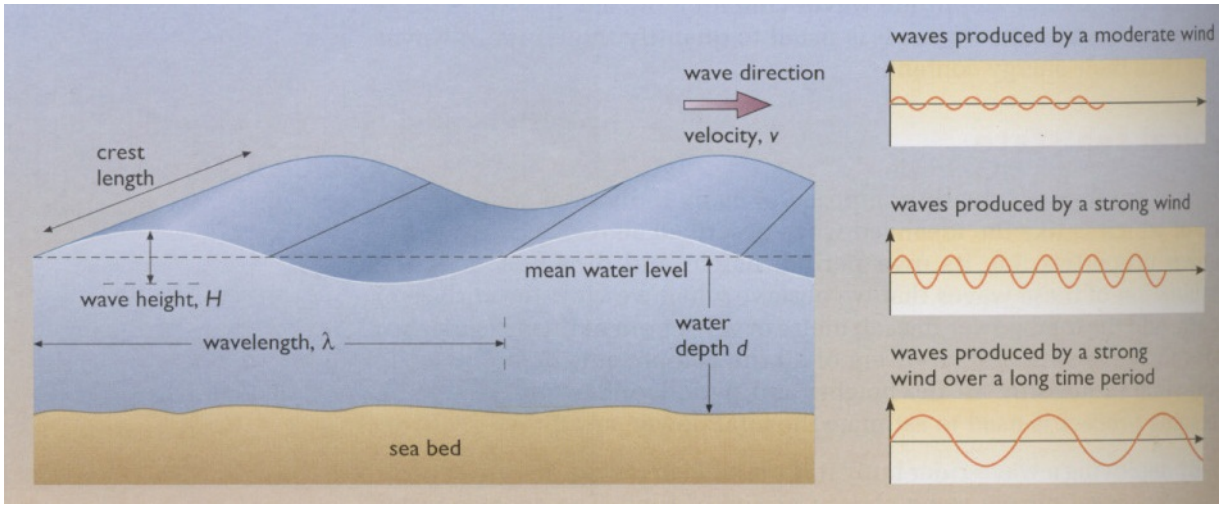

Figure 3: Wave properties [2]

Frequency f is related to the wavelength λ and the horizontal speed v.

λ=wavelength (in m)

T= time period (s)

A= amplitude (in m)

H=Peak to peak amplitude=2A (in m)

Usually A< λ/10

v= wave progresses with a horizontal velocity v (individual particles describe circular paths)

$$v = \frac{\lambda}{\mathrm{T}} = \lambda \mathrm{f} \ \ (\mathrm{in\ m/s}) \tag{1.1}$$

Angular frequency ω:

$$\omega = 2\pi f = \frac{2\pi}{T} \ (\mathrm{rad/s}) \tag{1.2}$$

It can be proven that the wavelength of a surface travelling wave is as follows:

$$\lambda = \frac{2\pi \mathrm{g}}{\omega^2} \ (\mathrm{in\ m}) \tag{1.3}$$

The last two expressions together give us:

$$T = \sqrt{\frac{2\pi\lambda}{g}} \ (\mathrm{s}) \tag{1.4}$$

With g = 9.81 m/s²

In the Atlantic ocean waves typically have periodic times of 10 seconds. This equals a wavelength of approximately 156 meters.

- Horizontal speed.

$$v = \lambda \mathrm{f} = \frac{\omega\lambda}{2\pi} \tag{1.5}$$

$$v = \lambda \mathrm{f} = \frac{2\pi \mathrm{g}}{\omega^2} * \mathrm{f} = \frac{2\pi \mathrm{g}\omega}{\omega^2 2\pi} = \frac{\mathrm{g}}{\omega} = \frac{\mathrm{g}}{2\pi \mathrm{f}} = \frac{\mathrm{gT}}{2\pi}$$
$$= \mathrm{g}\sqrt{\frac{2\pi\lambda}{(2\pi)^2 g}} = \sqrt{\frac{\lambda \mathrm{g}}{2\pi}} \tag{1.6}$$

The velocity v is independent of the wave amplitude H.

What is the total energy in the wave? This is important to know because we cannot extract more than maximum 50% of the energy that the wave contains.

The total energy E (caused by potential and kinetic energy) in each wavelength, per unit width of wave crest of an individual wave is found to be (linear wave theory):

$$E = \frac{\rho g H^2}{8} \ (\mathrm{J/m/\lambda}) \ (\mathrm{J/m2}) \tag{1.7}$$

For a certain wavelength per unit crest width:

$$E = \frac{\rho g H^2 \lambda}{8} \ (\mathrm{J/m}) \tag{1.8}$$

This is the energy per meter coast wave front length

$$\lambda = \frac{2\pi g}{\omega^2} \tag{1.9}$$

$$E = \frac{\rho g H^2}{8} \frac{2\pi g}{\omega^2} (\mathrm{J/m}) \tag{1.10}$$

$$E = \frac{\pi \rho g^2 H^2}{4\omega^2} (\frac{J}{m}) \tag{1.11}$$

And

$$\omega = \frac{2\pi}{T} \tag{1.12}$$

So:

$$E = \frac{1}{16\pi} \rho g^2 H^2 T^2 \ (\frac{J}{m}) \tag{1.13}$$

The theoretical maximum power, P ideal, corresponding to the total energy content, per unit crest width, under ideal conditions (one sinus, deep water) is:

$$P\ ideal = \frac{1}{16\pi} \rho g^2 H^2 T \ (\frac{W}{m}) \tag{1.14}$$

Fill in with common values:

$$\rho = \frac{1000kg}{m^3}$$

$$g = 9{,}81 \frac{m}{s^2}$$

$$P\ ideal = 1915\ H^2 T (\frac{W}{m}) \tag{1.15}$$

2.3 How much energy can we extract from an ideal wave?

In reality, a wave consists of more than one sine, it is a complicated combination of waves having different wavelengths, directions and time-phase displacements.

Mathematically it can be shown that the speed of the overall average wave motion, for random waves, is only half of the power of an individual wave. The energy content of a group of waves is transmitted at only one half of this velocity.

So the practical power extractable per meter of wave front is:

$$Ppract = \frac{1}{8}\rho g H^2 \frac{v}{2} \quad (\text{in W/m}) \tag{1.16}$$

But even this value is not realistic. The best way to determine the overall effect is to measure it repeatedly and use statistical data based on measured previous performance.

To find exact information about a location they use scatter diagrams of wave heights. An example is shown in Figure 4.

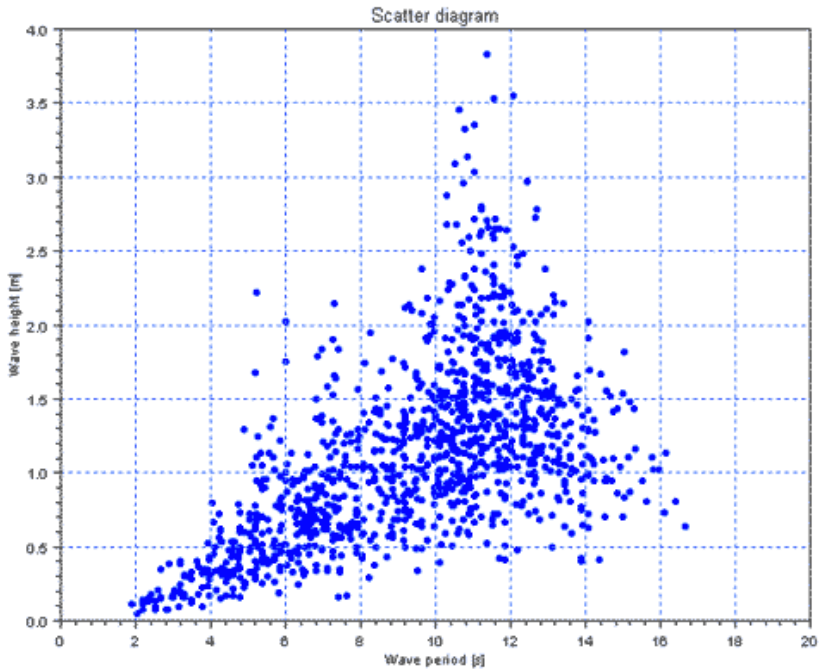

Figure 4: Example of Scatter diagram

When you do 1000 random measurements during one year, you look which time period and wave height occurs. We should take this fact into consideration when building the wave-energy devices for a specific location.

2.4 Which part of the power can a buoy extract?

In this project (ASWEC) we use a buoy as a wave energy convertor. In our models we use another formula. Since a buoy has a certain volume, it can only extract power within its reach. A formula has been developed for the energy that can be collected from a buoy:

$$P = \frac{Hc\,\pi\rho g}{T * 4} = \frac{A\,\pi\rho g}{T * 2}\ (\frac{watt}{m^3}) \qquad (1.17)$$

This formula is used in all of our models.

2.5 Global wave energy possibilities

The theoretical potential is all wave energy there is on earth. As I mentioned before, waves are generated by the wind and the wind energy is produced by solar energy. So the theoretical potential is the amount of energy of the sun that is being used for making waves.

It is logical that we cannot extract it all. The technical potential is what we are able to extract. It takes the overall efficiency, and the available place in count.

And when we use economical potential, we look if it is a good investment in comparison to the other energy sources. The global commercial wave-energy potential is currently zero, only if the price drops with factor 3 it would be economically responsible to use it. [3]

Type of potential	Unit	value
theoretical potential	TW	14
Global theoretical potential	TWh/year	18000
	TW	2
Global technical potential	Twhe/year	1460
	Gwe	556

[3]

Considering these values some calculation can be made.

In 2005 the global electricity consumption was around 15 TW. With a total energy consumption of 131400TWh/year.

$$15TW * 24 * 365 = 131400TWh/year$$

So the technical potential is estimated on 1.1% (1460/131400) of the total electrical energy production. This is not much, but all little efforts can help especially for local consumption and remote places.

According to the world energy council, the global wave energy resource is estimated to be 1-10 TW, we calculated with 2TW. The economic potential for future devices could rise up to 2000TW (1,5%). Nowadays the economic potential is 140-750 TWh/year (0,11% - 0,56%).

When waves move to shallower water, they lose a lot of their energy. But the sea-bed can collect those waves and focus them in so called ‘hot spots’. Those spots are the ideal areas for implementing our devices.

Properties of wave energy:

- Extractable at day – and night-time
- Changes during the year. In Belgium, for example, waves are bigger and contain more energy during wintertime.
- Economic potential, only if the price drops with factor 3.

3 THE ASWEC PROJECT

ASWEC is the name of the machine that we try to develop in the project in TAMK. ASWEC stands for 'Aaltosorvi wave energy convertor'.

Several other students have worked or are working on this project. This means a lot of different things have been done already. While previous tasks were mainly theoretical, I had the luck to do the more practical part. As shown starting from page 21 we started with mounting a test bench. This made us able to do some practical measurements and compare these with previous made estimations.

Thanks to a software program (see servo drive part further on), it was possible to drive our servo motor in such a way that it simulates waves. We were able to measure the generator output and think about how to solve the net connection issues.

3.1 The Floating buoy

In the ASWEC project, the idea is the prototype shown in Figure 5.

Here the upward movement is caused by the floating buoy (1) and the downward movement is due to the mass (5). So we have two different behaviours when going up or down. The downward movement is always the same. The upward movement depends on wave conditions. In previous models there were problems to find a suitable spring, so they changed it by a more easy and predictable application. Also here we convert the movement mechanically in one direction, this is important for the generator, which now

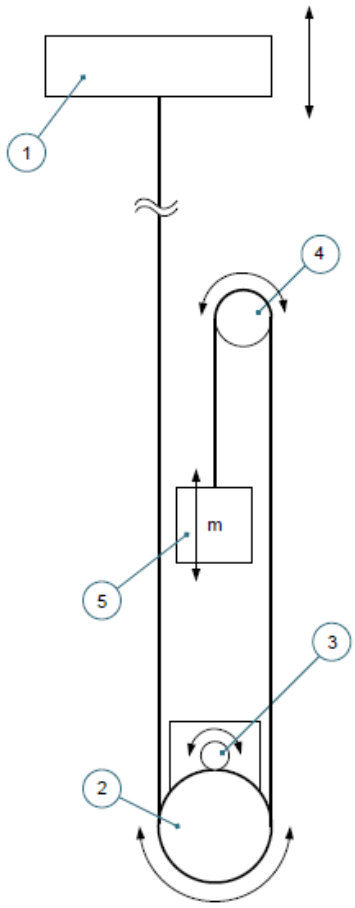

Figure 5: ASWEC principle

turns in only one direction.

This type of convertor has the disadvantage that there is a moment in which the speed becomes zero. This results in a voltage dip at the generator output which is not desirable for grid connection. One of the main issues is to deal with this problem.

4 THEORETICAL MODEL

The generator is simulated in a Matlab model. This model helps us make predictions about e.g. the reaction of the generator when loaded with different loads, when driven by different speeds etc.

One of the goals of the project was to get the theoretical model as accurate as possible. Due to this, a practical test setup was made to measure the generator's practical parameters.

With these values used in our theoretic model, we were able to get this:

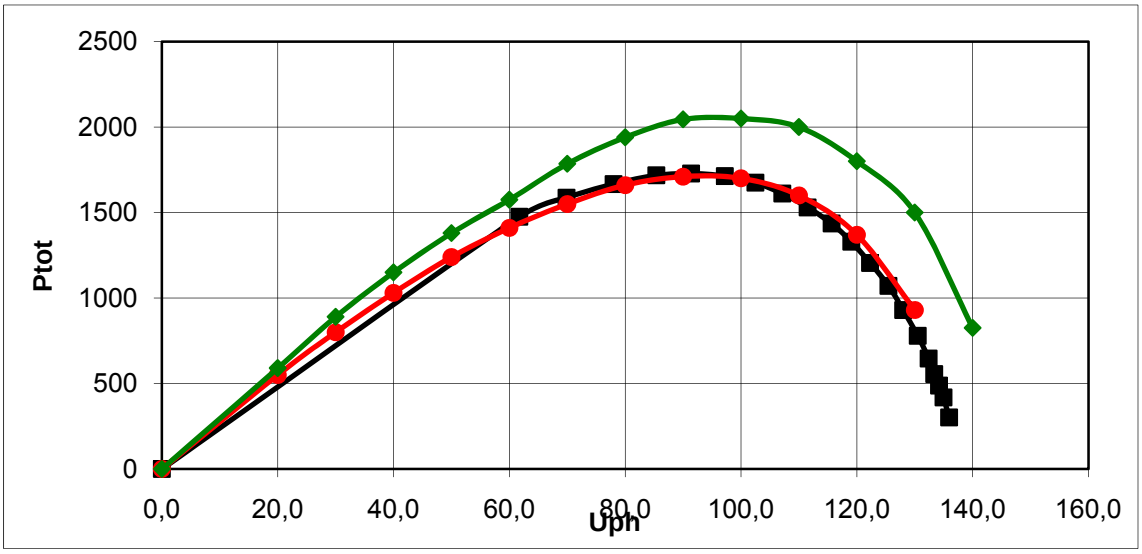

Black (■) line is the curve we measured with the nominal speed in the lab.
Red (●) line is made with matlab using parameters from the measurements.
Green (◆) line is taken from the datasheets.

The Matlab model is as close as possible to the measured motor curve. In order to do this, we used the Lq and Ld values of 0,120mH. Now we are quite sure that the model is reacting as it should be. De difference between the measured values and the datasheet values are probably due to a lower flux, resistance of the cables and measurement errors (rounding results etc). The measuring of the generator values is not always easy with de equipment available in the lab. E.g. the generated voltage frequency at nominal generator speed is 20,8Hz. Because most measurement equipment in the lab is designed for 50Hz, the values were difficult to read because of constant changes.

5 TEST EQUIPMENT

Preliminary to my thesis, a lot of theoretical models and estimations were made. The next step of the project is to compare the theoretical estimations with real measurements. In order to do so, we had to make a test setup, which is shown in Figure 6. This setup exists out of a generator, a gearbox and a motor. The goal is to simulate the waves with the motor and compare the practical generator voltage with the theoretic model.

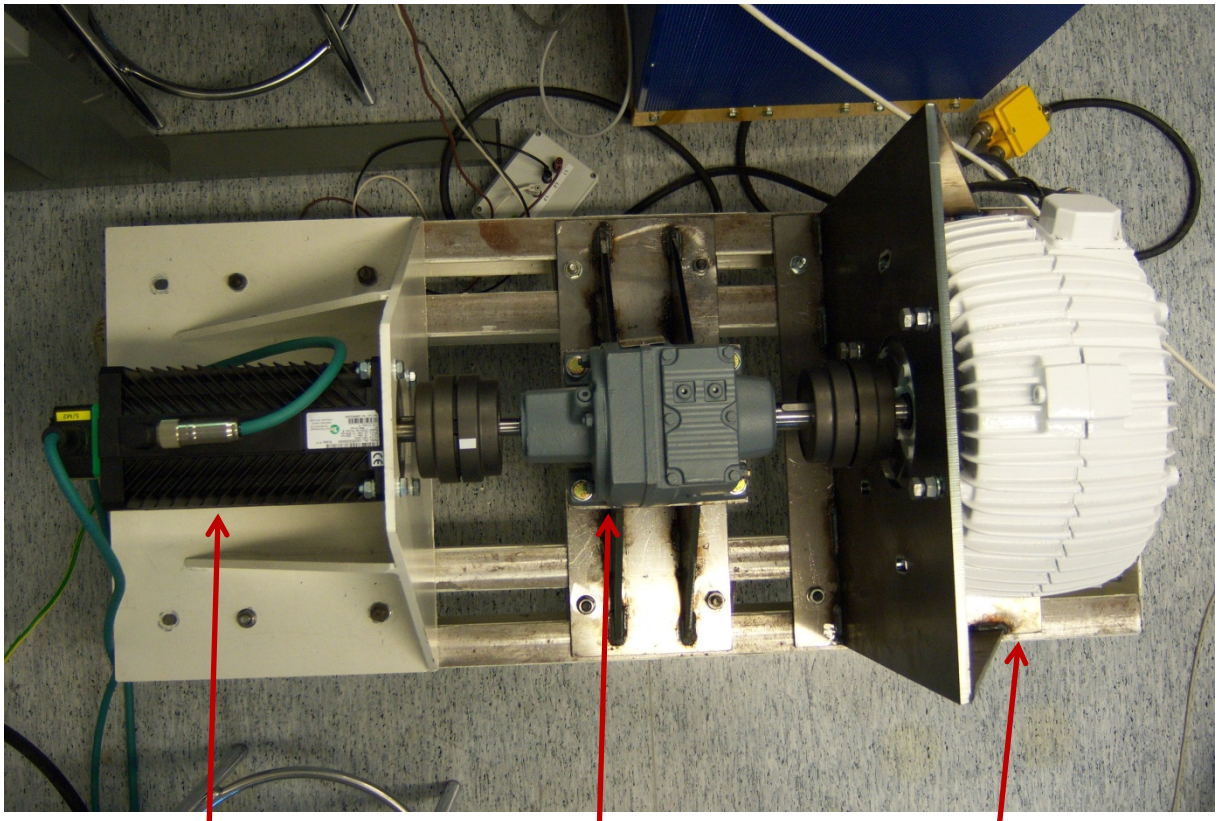

Figure 6: Test equipment

Servomotor

Gearbox 6/1

Permanent Magnet Generator

5.1 Permanent Magnet Generator

Main characteristics:

n_n	n_{max}	f_s	P_n	I_n	U_Y
rpm	rpm	Hz	kW	A	V
250	500	20,8	2,0	5,0	250

The most important part of the setup is the Permanent Magnet Generator. The generator generates an AC voltage. This voltage will change when the generator speed changes.

5.1.1 Theoretical generator characteristics

The manufacturer of the generator gave us following properties of the generator. The full generator datasheet can be found in Annex 1.

There are different characteristics for passive and active loading. A passive load is a load acting as a resistor. An active load is a load which behaves as a non-linear resistor e.g. capacitor or inductance.

Passive loading:

Electrical performance specification – PMG 2.0-250-P – parameters under passive loading

The parameters of the generator.

Parameter	Explanation	Value	Dimension
P	Electric power	2.0	kW
S	Apparent power	2.0	kVA
T	Shaft torque	76	Nm
n	Rotation speed	250	min^{-1}
n_{max}	Maximum allowed rotation speed under full loading	300	min^{-1}
n_{max}	Maximum allowed rotation speed under no-load condition	500	min^{-1}
$2p$	Number of pole-pairs	5	pcs.
f	Line frequency on rotation speed of 250 min^{-1}	20.8	Hz
E_{pm}	PM excited no-load line-to-line voltage at speed 250 min^{-1}	250	V
U	Line-to-line voltage (full load – passive loading)	155 [1)]	V
I_{ph}	Line current	7.6	A

1) Variation interval $0.95 \cdot U \ldots 1.05 \cdot U$ at rated point due to the variation of temperature.

Generator lumped parameters.

Parameter	Value	Dimension
X_d	15.7	Ohm
X_q	15.7	Ohm
L_d	0.12	H
L_q	0.12	H
R_{ph}	1.6	Ohm

Active loading:

Electrical performance specification – PMG 3.0-250-A – parameters under active loading

The parameters of the generator.

Parameter	Explanation	Value	Dimension
P	Electric power	3.0	kW
S	Apparent power	3.1	kVA
T	Shaft torque	115	Nm
n	Rotation speed	250	min^{-1}
n_{max}	Maximum allowed rotation speed under full loading	400 [1)]	min^{-1}
n_{max}	Maximum allowed rotation speed under no-load condition	400 [1)]	min^{-1}
$2p$	Number of pole-pairs	5	pcs.
f	Line frequency on rotation speed of 250 min^{-1}	20.8	Hz
E_{pm}	PM excited no-load line-to-line voltage at speed 250 min^{-1}	250	V
U	Line-to-line voltage (full load – active load)	250 [2)]	V
I_{ph}	Line current	7.2	A

1) Converter protection due to the over voltage is required if rotation speed of 400 min^{-1} is exceeded.
2) Variation interval $0.95 \cdot U \ldots 1.05 \cdot U$ at rated point due to the variation of temperature.

Generator lumped parameters.

Parameter	Value	Dimension
X_d	15.7	Ohm
X_q	15.7	Ohm
L_d	0.12	H
L_q	0.12	H
R_{ph}	1.6	Ohm
X_d	0.61	p.u.
X_q	0.61	p.u.
R_{ph}	0.07	p.u.

Power as a function of phase voltage

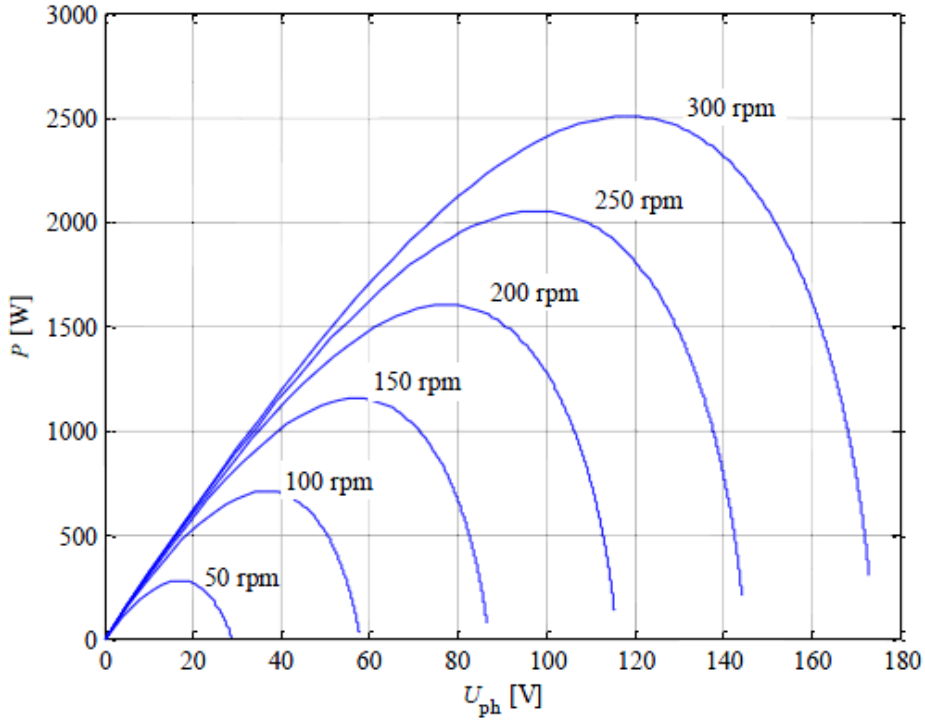

Power as a function of line resistance

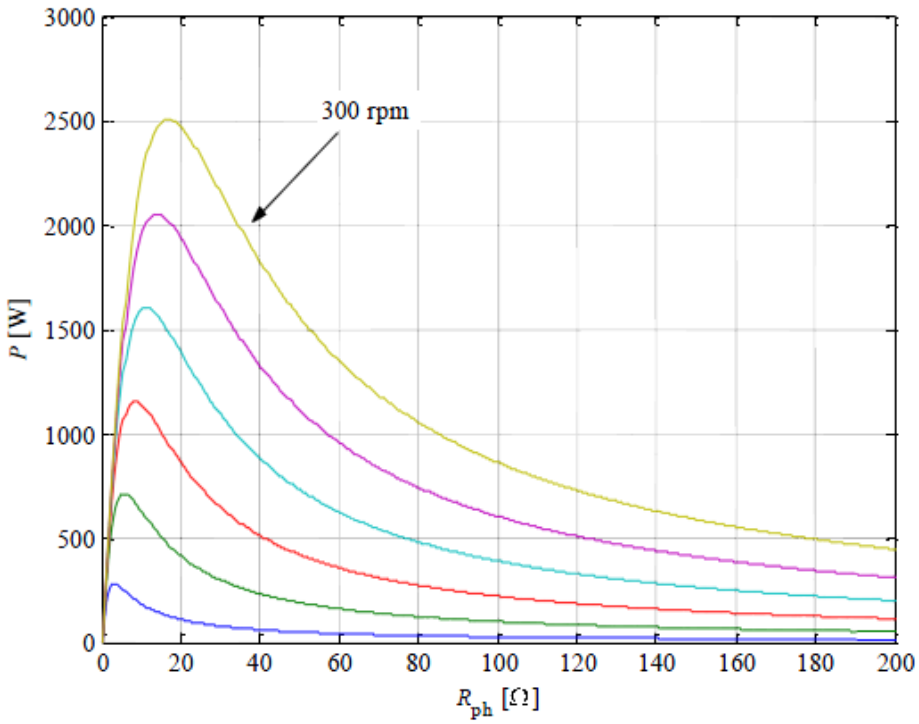

5.1.2 Practical generator characteristics

Out of the datasheet of the manufacturer (Annex 1) we could find some parameters. To be sure we are using the correct parameters; we measured and calculated them from our generator. The flux can vary when the Permanent Magnets are getting older.

	Used	Given by manufacturer	Note
R_s	2,05	1,6	Used value is the value of WARM engine
L_d	0,12	0,12	Found by **testing** different values (fits best)
L_q	0,12	0,12	Found by **testing** different values (fits best)
Flux	1,35	1,56*	Calculated from the no load test

* flux calculated out of datasheet parameters

Resistance: measured with ohm meter and calculated for 1 phase (Calculation is needed since motor is switched in star-connection)

L_d & L_q: found by comparing several values in Matlab, chosen the best fitting one.

L_d is the direct axis inductance and L_q the quadrature axis inductance. These are fundamental inductances of the generator since a permanent magnet generator is usually presented with two axis circuits.

Flux: found by measuring the induced line voltage, then took the average of the three phases, converted it to phase voltage (= E_{pm}) and peak phase voltage (amplitude). Flux is calculated out of this.

$$\hat{E}_{\mathrm{PM}} = \omega_{\mathrm{s}} \cdot \Psi_{\mathrm{PM}} \Rightarrow \Psi_{\mathrm{PM}} = \frac{\hat{E}_{\mathrm{PM}}}{\omega_{\mathrm{s}}} = \frac{\sqrt{2} \cdot E_{\mathrm{PM}}}{2 \cdot \pi \cdot f_{\mathrm{s}}}$$

The flux 1,35Wb is found at constant speed. For changing speed measurements the best fitting flux is 1,38Wb.

5.1.3 Comparison between theoretical and practical values

To be sure the generator is reacting as it should be; we reproduced the measurements found in the generator datasheet and compared them with the theoretical values. Since this was not the subject of this thesis, results of those measurements are not written down here. Anyone who is interested in these results can find them in the thesis of Henri Toijala.

[Henri Toijala, Aaltovoimalaitteiston PM generaattorin ja tasasuuntauksen mallintaminen ja testaus, Tampere University of Applied Sciences, 2011]

5.2 Servo Motor

Characteristics:

n_n	M_n	M_k
rpm	Nm	Nm
3000	18	23,4

In a real sea-wave situation, the generator is driven by waves. This means the buoy goes up and down and stands still for a short moment when changing direction. The generator axis stands still as well. To simulate this, the servomotor is controlled by a computer program, which enables the motor to act like real waves. The program is made by another student. It is possible to load an Excel-file with wave data in the program. This way, different waves (high, low,…) can be simulated. A print screen of the program is shown in Figure 7.

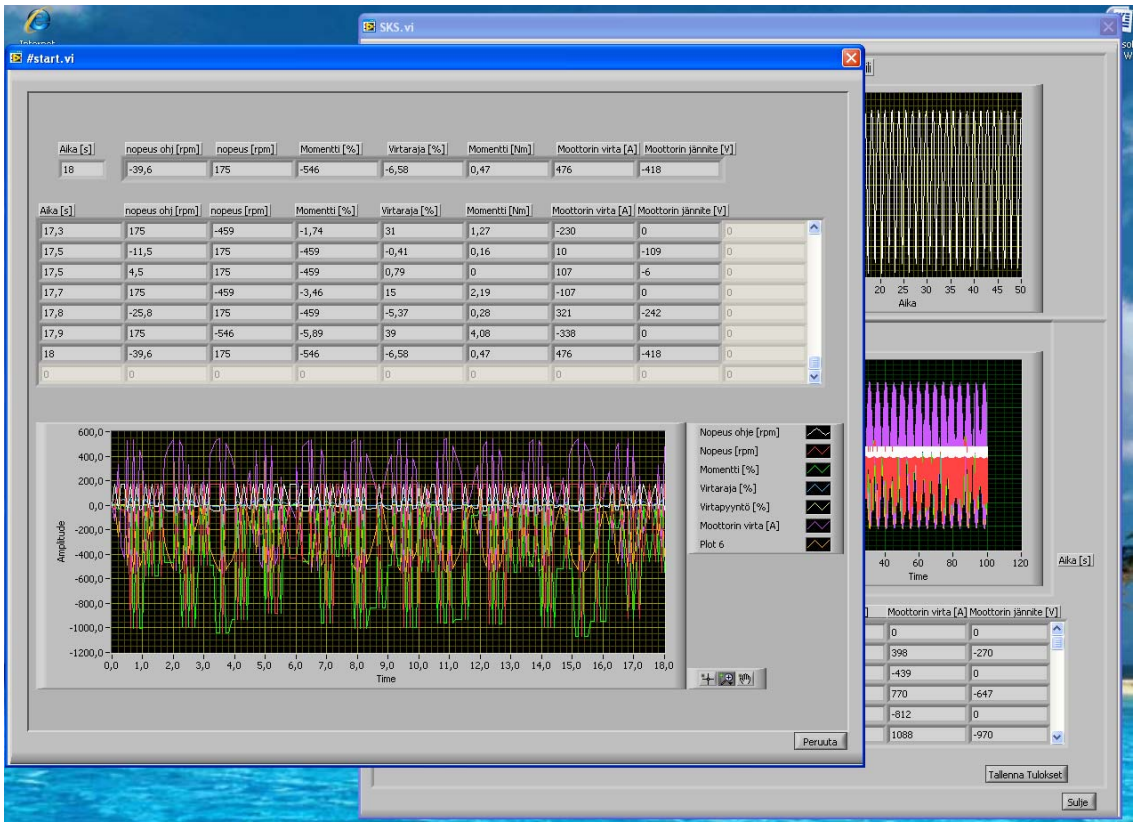

Figure 7: Print screen of the servomotor control program

5.3 Gear

The gearbox is used because the nominal generator speed is 250rpm while the servomotors' nominal speed is 3000rpm. The ratio of the gearbox is 6/1.

Characteristics:

Manufacturer:	SEW-EURODRIVE
Model:	R47 AD2
n1:	*1400 rpm*
n2:	*233 rpm*

6 INDUCED VOLTAGE SHAPING

To inject the generated energy into the grid, the power has to be smooth enough. This means that the unwanted oscillations are minimized. The goal is a perfect sinus with a frequency of 50Hz. The first step is rectifying the voltage, and then we try to keep this DC voltage as constant as possible, even if the generated voltage varies. The next step is to produce a sine wave of 50Hz to inject the generated energy in the grid. These three steps are explained hereafter.

Theoretically the DC link and net connection can be schematized as follows in Figure 8:

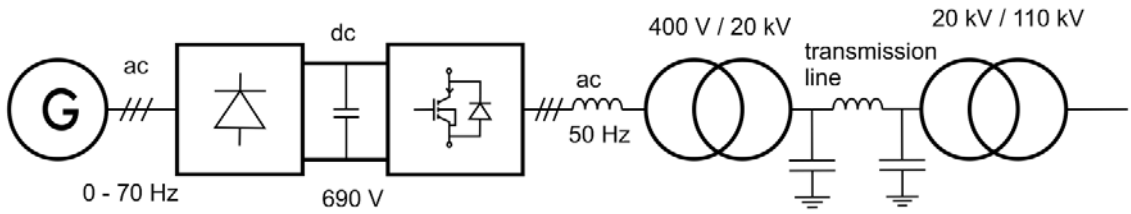

Figure 8: DC link and net connection

The power available for extraction varies dramatically depending on the sea-state, leading to a high ratio of peak powers to the long term average value. The end requirement of any grid-connected electrical generation system is a positive power-flow of sinusoidal AC at the appropriate line frequency (in our case 50Hz). Power flow should be substantially constant over a time period of minutes or more, so as to provide a stable (and saleable) contribution of energy to the grid.

A conventional strategy for conditioning the output of a variable frequency generator is controlled rectification of its output. This provides a steady DC-link voltage, which is then used to feed the main grid via a 3-phase inverter bridge.

6.1 Step 1: diode bridge

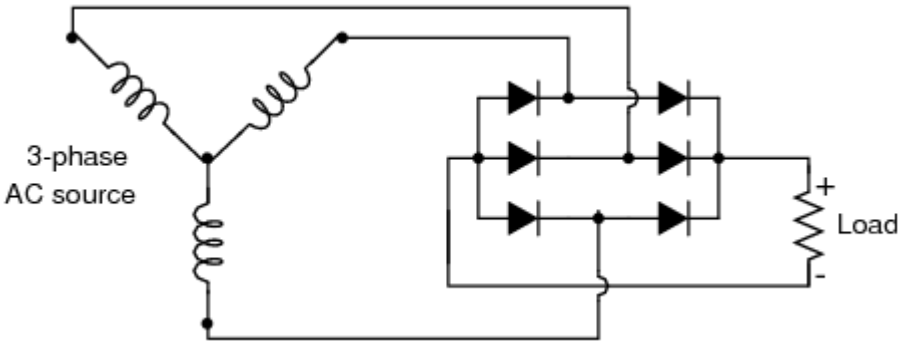

Figure 9: Basic diode bridge

The first step is rectifying the voltage. A 3-phase diode bridge is used for this purpose. A basic diode bridge is shown in Figure 9. As we can see on Figure 10, the generated voltage has dips. This is caused by the tops and bottoms of the waves. That moment, the buoy does not move, so the induced voltage is zero.

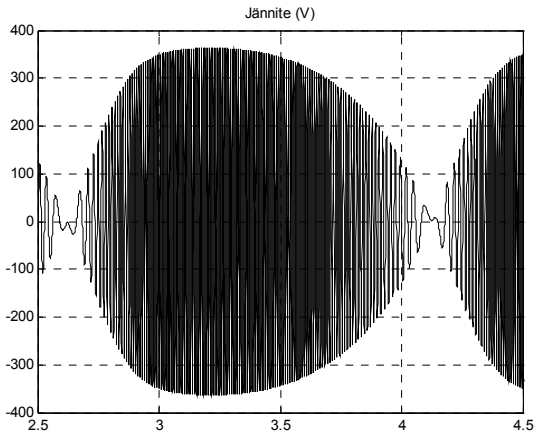

Figure 10: Generated voltage

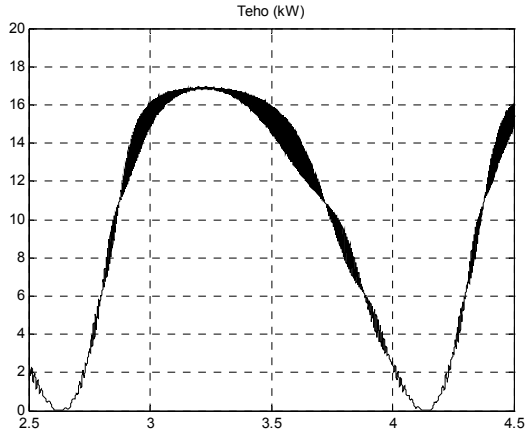

Figure 11: Rectified generator voltage

After rectification, the voltage dips are still visible as shown in Figure 11. Due to grid connection, this problem has to be solved. Some possibilities are explained in 6.2.

6.1.1 Losses in the bridge of diodes

To measure the practical losses in the diode bridge, we compare the ingoing power with the outgoing power. The differences between both are the losses. The efficiency can be easily calculated by dividing the outgoing power by the incoming power.

The measurements learn us that the diode bridge efficiency at peak generated power is 0,93. At other speeds and powers, the efficiency is between 0,90 and 0,93.

For example:

At the nominal speed of 250rpm, the generator's generated peak power is 1709W. After the bridge of diodes, we have left 1597,5W. So, there is a loss of 111,6W. Out of this we can calculate the efficiency, which is 0,93 in this case.

6.2 Step 2: DC link voltage

When this voltage is rectified, the voltage-dips are still visible. Before we transform the DC-voltage in to a 50Hz AC voltage which is suitable for the grid, we want to make the DC-voltage as smooth as possible.

6.2.1 Super capacitor

One of the ways to smoothen the DC-voltage is to implement a super capacitor. Theoretically, this is a good solution, but there are some practical disadvantages. The biggest issue is that the estimated life of the capacitor is too short, which results in an increased maintenance level and higher costs, especially if this is implemented in off-shore applications. If we use the super capacitor only in extreme wave conditions, we can extend the lifetime of the capacitor. Another solution is to mount the capacitor at the coastline, which facilitates the maintenance.

In our project we try to avoid the super capacitor because of the expensiveness and sensitivity.

6.2.2 DC-DC converter: Boost convertor

Another way to smoothen the DC side can be a boost convertor. A basic boost converter is shown in Figure 12. As said, the main problem was the voltage-dips in the rectified voltage. As the name implies, the output voltage of a boost convertor is always greater than the input voltage. So, if we can use the boost convertor to increase the voltage in the dip points, this could result in a more smooth voltage. The boost-converter is a type of DC-DC converter. The output voltage of DC-DC converters can be adjusted by changing the duty cycle D.

$$D = \frac{T_{on}}{T_{off}}$$

Here, the switches are treated as being ideal, and the losses in the inductive and the capacitive elements are neglected. Such losses can limit the operational capacity of the converter. The DC input voltage to the converters is as-

sumed to have zero internal impedance. In our case, the voltage is generated by the generator and will have an internal impedance, one of the difficulties of this subject is the question how we can use this impedance as part of the converter.

Basic principle

When the switch is on, the diode is reversed biased, thus isolating the output stage. The input supplies energy to the inductor. When the switch is off, the output stage receives energy from the inductor as well as the input. In the steady-state analysis presented here, the output filter capacitor is assumed to be very large to ensure a constant output voltage $v_o(t) \cong V_o$.

Continuous-conducting mode

Figure 13 shows the steady-state waveforms for this mode of conduction where the inductor current flows continuously [$i_L(t) > 0$]. Since in steady state the time integral of the inductor voltage over one time period must be zero,

$$V_d t_{on} + (V_d - V_0)t_{off} = 0$$

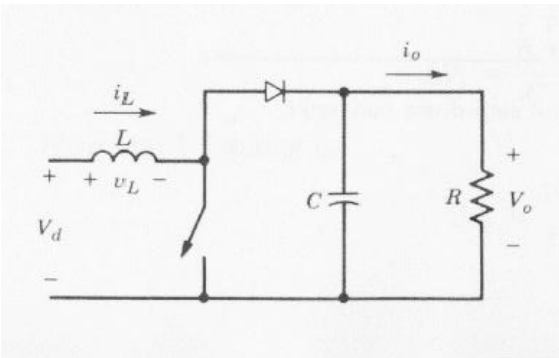

Figure 12: Step-up DC-DC convertor [4]

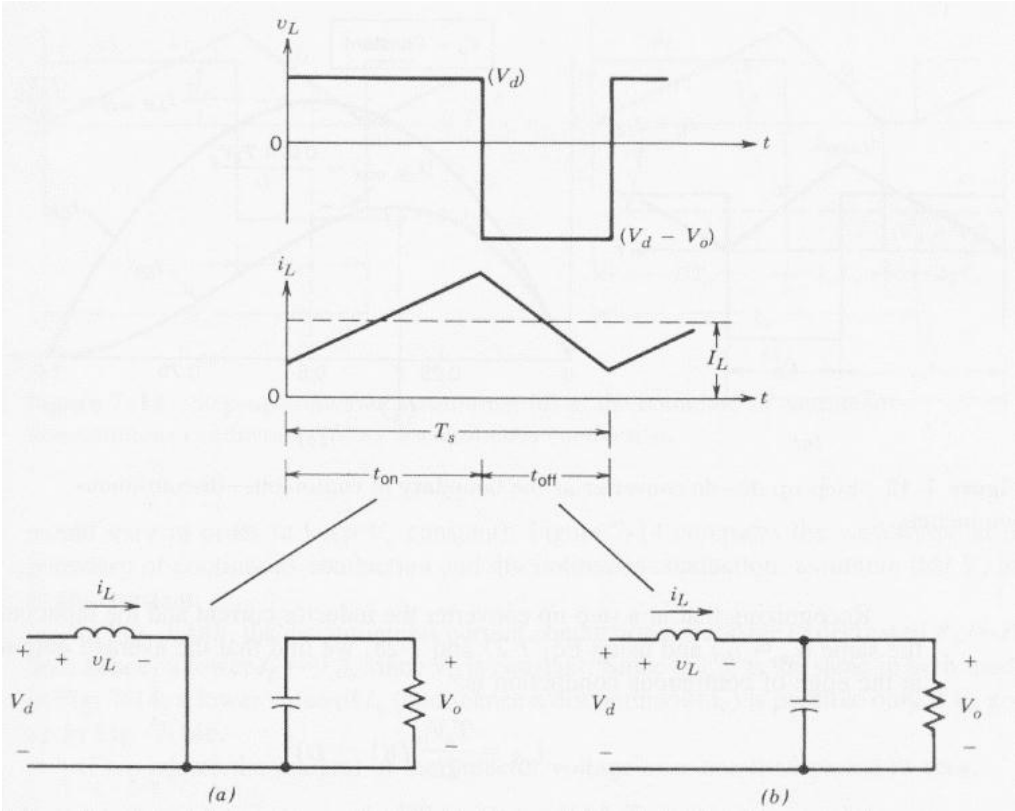

Figure 13: Continuous-conducting mode: (a) switch on; (b) switch off. [4]

Dividing both sides by T_s and rearranging terms yields:

$$\frac{V_O}{V_d} = \frac{T_s}{t_{off}} = \frac{1}{1-D} \tag{2.1}$$

Assuming a lossless circuit, $P_d = P_0$,

$$V_d I_d = V_0 I_0 \tag{2.2}$$

And

$$\frac{I_0}{I_d} = (1-D) \tag{2.3}$$

Boundary between continuous and discontinuous conduction

Figure 14a shows the waveforms at the edge of continuous conduction. By definition, in this mode i_L goes to zero at the end of the off interval. The average value of the inductor current at this boundary is

$$I_{LB} = \frac{1}{2} i_{L,peak} \tag{2.4}$$

$$= \frac{1}{2}\frac{V_d}{L}t_{on} \tag{2.5}$$

$$= \frac{T_s V_0}{2L}D(1-D) \tag{2.6}$$

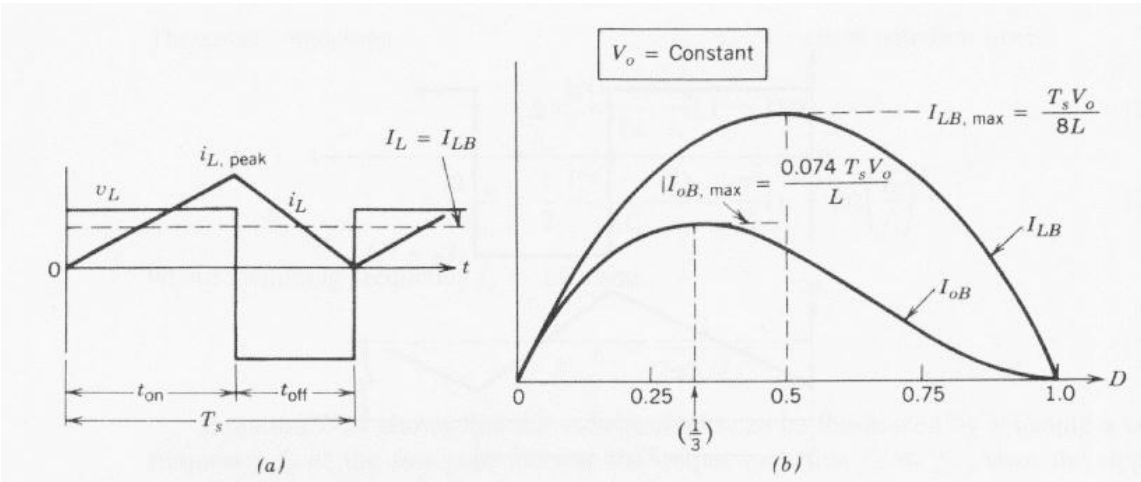

Figure 14: Step-up DC-DC converter at the boundary of continuous-discontinuous conduction. [4]

Recognizing that in a step-up converter the inductor current and the input current are the same ($i_d = i_L$) and using Eq.(2.3) and (2.6), we find that the average output current at the edge of continuous conduction is

$$I_{0B} = \frac{T_s V_0}{2L}D(1-D)^2 \tag{2.7}$$

Most applications in which a step-up converter is used require that V_0 be kept constant. Therefore, with V_0 constant, I_{0B} are plotted in Figure 14b as a function of duty ratio D. Keeping V_0 constant and varying the duty ratio imply that the input voltage is varying.

Figure 14b shows that I_{LB} reaches a maximum value at D = 0,5:

$$I_{LB,max} = \frac{T_s V_0}{8L} \tag{2.8}$$

Also, I_{0B} has its maximum at D = $\frac{1}{3}$ = 0,333:

$$I_{0B,max} = \frac{2}{27}\frac{T_s V_0}{L} = 0{,}074\,\frac{T_s V_0}{L} \tag{2.9}$$

In terms of their maximum values, I_{LB} and I_{0B} can be expressed as

$$I_{LB} = 4D(1-D)I_{LB,max} \tag{2.10}$$

And

$$I_{0B} = \frac{27}{4} D(1-D)^2 \, I_{0B,max} \tag{2.11}$$

Figure 14b shows that for a given D, with constant V_0, if the average load current drops below I_{OB} (and, hence, the average inductor current below I_{LB}), the current conduction will become discontinuous.

Discontinuous conducting mode

To understand the discontinuous-current-conduction mode, we would assume that as the output load power decreases, V_d and D remain constant (even though, in practice, D would vary in order to keep V_0 constant).

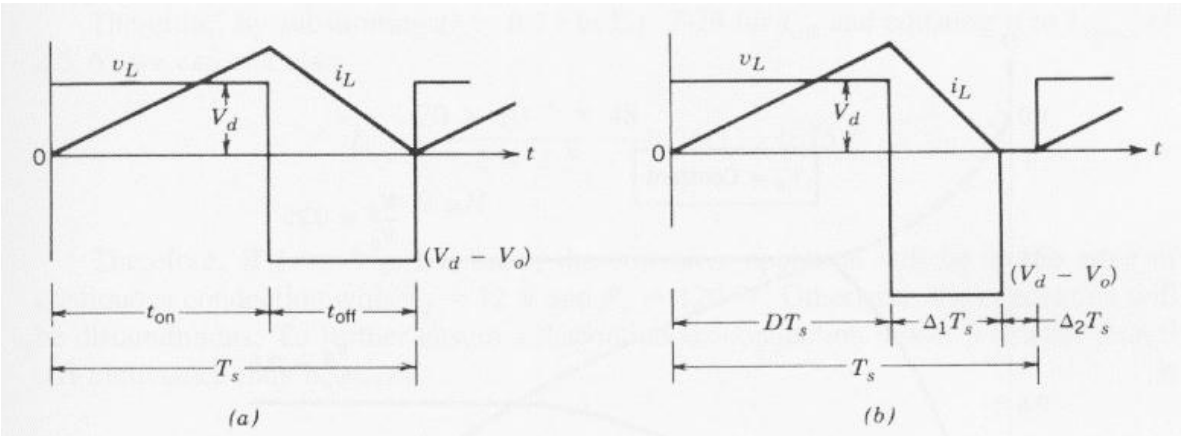

Figure 15: Step-up converter waveforms: (a) at the boundary of continuous-discontinuous conduction; (b) at discontinuous conduction. [4]

Figure 15 compares the waveforms at the boundary of continuous conduction and discontinuous conduction, assuming that V_d and D are constant. In Figure 15b, the discontinuous current conduction occurs due to decreased P_0 (=P_d) and, hence, a lower I_L (=I_d), since V_d is constant. Since $I_{L,peak}$ is the same in both modes in Figure 15, a lower value of I_L (and, hence a discontinuous i_L) is possible only if V_0 goes up in Figure 15b.

If we equate the integral of the inductor voltage over one period to zero,

$$V_d D T_s + (V_d - V_0) \Delta_1 T_s = 0$$

$$\frac{V_0}{V_d} = \frac{\Delta_1 + D}{\Delta_1} \tag{2.12}$$

And

$$\frac{I_0}{I_d} = \frac{\Delta_1}{\Delta_1 + D} \; (since\ P_d = P_0) \tag{2.13}$$

From Figure 15b, the average input current, which is also equal to the inductor current, is

$$I_d = \frac{V_d}{2L} D T_s (D + \Delta_1) \tag{2.14}$$

Using equation (2.13) in the foregoing equation yields

$$I_0 = \left(\frac{T_s V_d}{2L}\right) D \Delta_1 \tag{2.15}$$

In practice, since V_0 is held constant and D varies in response to the variation in V_d, it is more useful to obtain the required duty ratio D as a function of load current for various values of V_0/V_d. By using Eqs. (2.12), (2.15) and (2.9), we determine that

$$D = \left[\frac{4}{27}\frac{V_0}{V_d}\left(\frac{V_0}{V_d} - 1\right)\frac{I_0}{I_{0B,max}}\right]^{\frac{1}{2}} \tag{2.16}$$

In Figure 16, D is plotted as a function of $I_0/I_{0B,max}$ for various values of V_d/V_0. The boundary between continuous and discontinuous conduction is shown by the dashed curve.

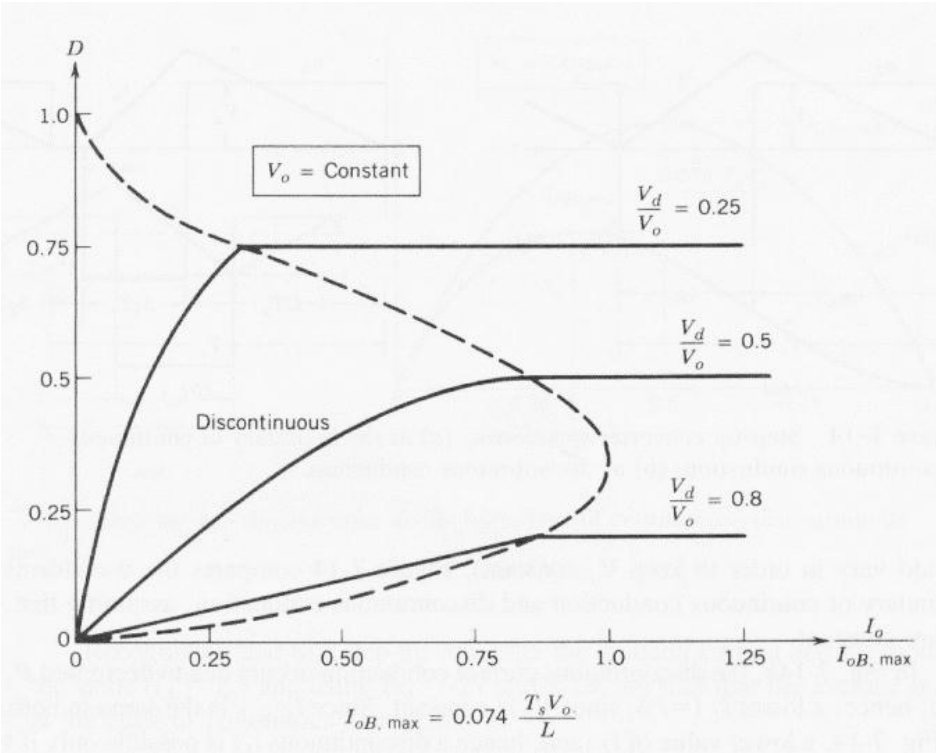

Figure 16: Step-up converter characteristics keeping V_0 constant [4]

In the discontinuous mode, if V_0 is not controlled during each switching time period, at least

$$\frac{L}{2} i_{L,peak}^2 = \frac{(V_d D T_s)^2}{2L} \qquad \text{W-s}$$

are transferred from the input to the output capacitor and to the load. If the load is not able to absorb this energy, the capacitor voltage V_0 would increase until an energy balance is established. If the load becomes very light, the increase in V_O may cause a capacitor breakdown or a dangerously high voltage to occur.

Effect of parasitic elements

The parasitic elements in a step-up converter are due to the losses associated with the inductor, the capacitor, the switch, and the diode. Figure 17 qualitatively shows the effect of these parasitics on the voltage transfer ratio. Unlike the ideal characteristic, in practice, V_0/V_d declines as the duty ratio approaches unity. Because of very poor switch utilization at high values of duty ratio, the curves in this range are shown dashed. These parasitic elements have been ignored in the simplified analysis presented here; however, these can be incorporated into circuit simulation programs on computers for designing such converters.

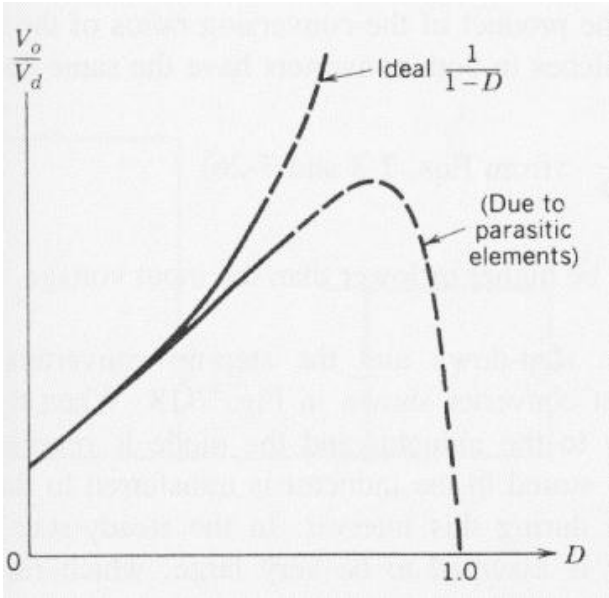

Figure 17: Effect of parasitic elements on voltage conversion ratio (step-up converter) [4]

Output voltage ripple

The peak-to-peak ripple in the output voltage can be calculated by considering the wave-forms shown in Figure 18 for a continuous mode of operation. Assuming that all the ripple current component of the diode current i_D flows through the capacitor and its average value flows through the load resistor, the shaded area in Figure 18 represents charge ΔQ. Therefore, the peak-peak voltage ripple is given by

$$\Delta V_0 = \frac{\Delta Q}{C} = \frac{I_0 D T_s}{C} \text{ (assuming a constant output current)}$$

$$= \frac{V_0}{R}\frac{DT_s}{C} \tag{2.17}$$

$$\frac{\Delta V_0}{V_0} = \frac{DT_s}{RC}$$

$$D\frac{T_s}{\tau} \text{ (where } \tau \text{ = RC time constant)} \tag{2.18}$$

A similar analysis can be performed for the discontinuous mode of conduction.

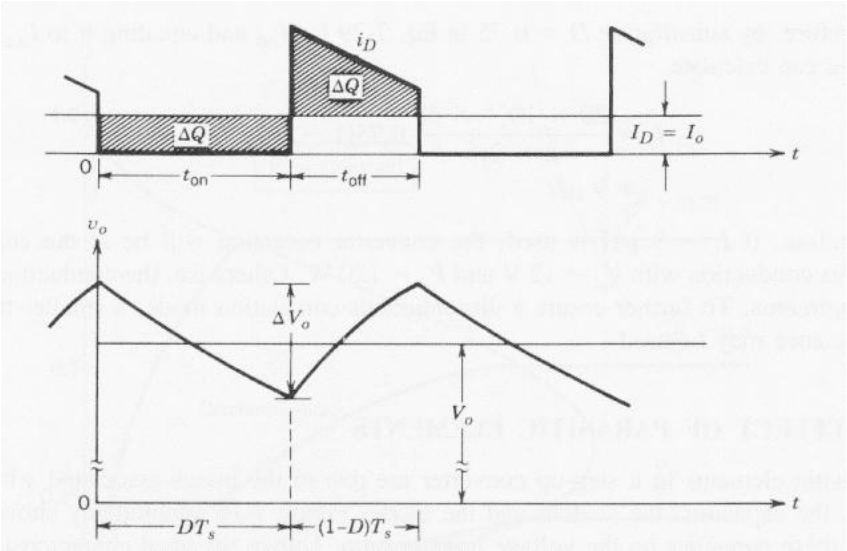

Figure 18: Step-up converter output voltage ripple [4]

Boost Converter Control

One of the methods for controlling the output voltage employs switching at a constant frequency (hence, a constant switching time period $T_s = t_{on} + t_{off}$) and adjusting the on duration of the switch to control the average output voltage. In this method, called pulse-width modulation (PWM) switching, the switch duty ratio D, which is defined as the ratio of the on duration to the switching time period, is varied.

Another control method is more general, where both the switching frequency (and hence the time period) and the duration of the switch are varied. This method is used only in DC-DC converters utilizing force-commutated thyristors.

In our PSpice simulation control, we use the first method with constant switching frequency.

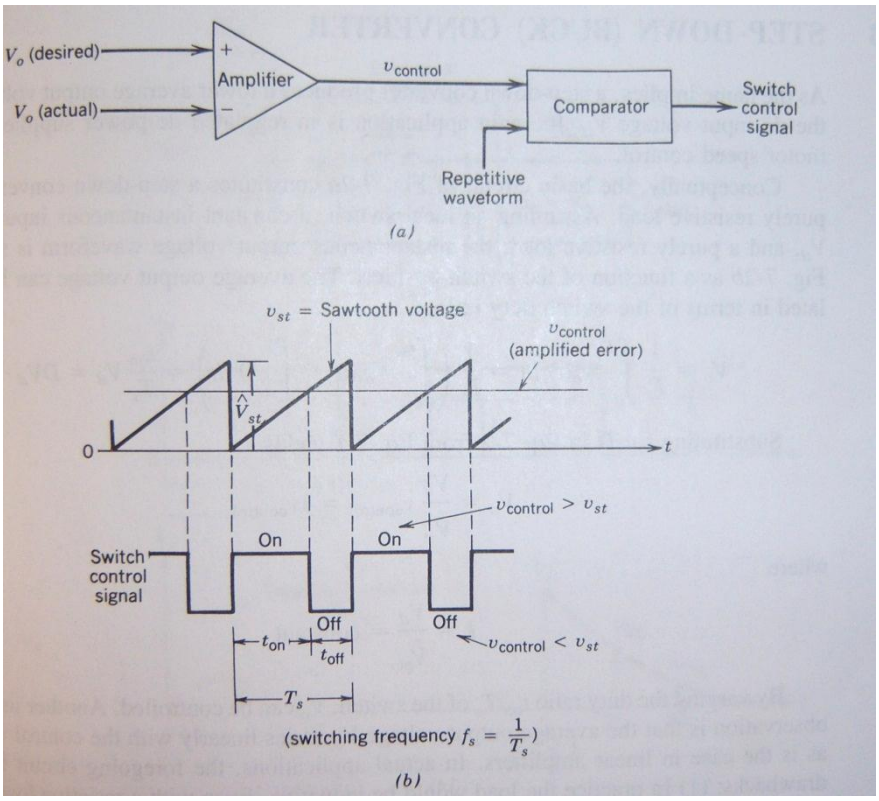

Figure 19: Pulse-width modulator: (a) block diagram; (b) comparator signals [4]

In the PWM switching at a constant frequency, the switch control signal, which controls the state (on or off) of the swith, is generated by comparing a signal-level control voltage $v_{control}$ with a repetitive waveform as shown in Figure 19 (a) and (b). The control voltage signal generally is obtained by amplifying the error, or the difference between the actual output voltage and its desired value. The frequency for the repetetive waveform with a constant peak, which is shown to be a sawtooth, establishes the switching frequency. This frequency is kept constant in a PWM control and is chosen to be in a 1kHz to 8kHz range in our case. When the amplified error signal, which varies very slowly with time relative tot the switching frequency, is greater than the sawtooth waveform, the switch control signal becomes high, causing the switch to turn on. Otherwise, the switch is off. In terms of $v_{control}$ and the peak of the sawtooth waveform V_{st} in Figure 19, the switch duty ratio can be expressed as

$$D = \frac{t_{on}}{T_s} = \frac{V_{control}}{V_{st}}$$

The DC-DC converters can have two distinct modes of operation: (1) continuous current conduction and (2) discontinuous current conduction. In practice, a converter may operate in both modes, which have significantly

different characteristics as shown in 6.2.2. Therefore, a converter and its control should be designed based on both modes of operation. [4]

6.3 Step 1 + 2: Unidirectional boost rectifier

This information is taken from a wave energy conversion example with a linear generator. Because our voltage and current have similar shapes, we can use the same technology.

6.3.1 Unidirectional rectifier

If the mechanical power take-off system can achieve the desired response to input waves without the need for bi-directional power flow with the generator, a unidirectional rectifier topology can potentially be used to afford cost savings in the power electronics. For machines with sufficiently high intrinsic power factor, such as an air-cored tubular linear generator a unidirectional Power Factor Converter stage can achieve the desired current shaping.

The boost topology shown in Figure 20 has been proposed and demonstrated by Ran et al. [5]; where each generator coil is connected to its own boost converter feeding an intermediate DC-link. We can use a single boost converter per phase, operating directly into a high voltage DC-link.

The topology consists of an uncontrolled rectification stage, followed by a boost mode Power Factor Correction circuit, where the generator's phase inductance is used as the boost inductor, placed before the input diodes.

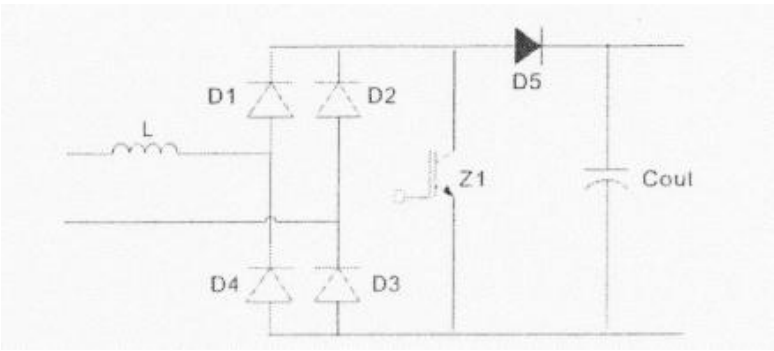

Figure 20: Unidirectional boost rectifier [6]

6.3.2 Control of unidirectional rectifier

Referring to Figure 21, the instantaneous generator Electro Magnetic Force (EMF), v_{sense} is used with load scaling factor a, to control the input current, i_{sense}. The current is made to track proportionally to the EMF by switching Z1, as a result of comparing v_{sense} and a x i_{sense}. When the measured current is lower than demanded, Z1 is turned on and inductor current rises. When higher, Z1 switches off, and inductor current falls. The comparison process is clocked and latched at a rate of e.g. 5kHz, setting an upper limit to the switching frequency. This is chosen to be comfortably below the self-resonant frequency of the generator coils whose inductance is being exploited. Protection logic will inhibit the gate drive for one clock cycle should a pre-set current limit be exceeded between samplings.

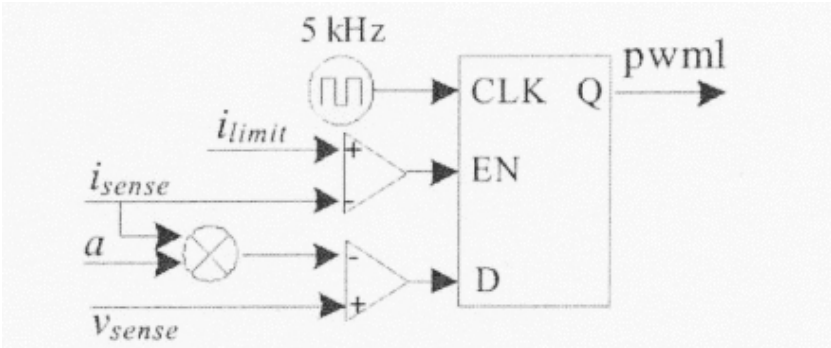

Figure 21: Control of unidirectional boost rectifier [6]

6.3.3 External simulated results

Figure 22 and Figure 23 show the simulation and experimental results of the unidirectional boost rectifier. As desired, inductor current is controlled to track the voltage waveform from the emulator. The DC link voltage is maintained at 300V with a fluctuation of 100V. Since the source reactance is relatively small compared to its resistance (at the generator frequency), there is only small natural phase shift (measured to be less than 6 degrees) between the emulator voltage and inductor current. This causes a short dead-band following each phase reversal of the input voltage.

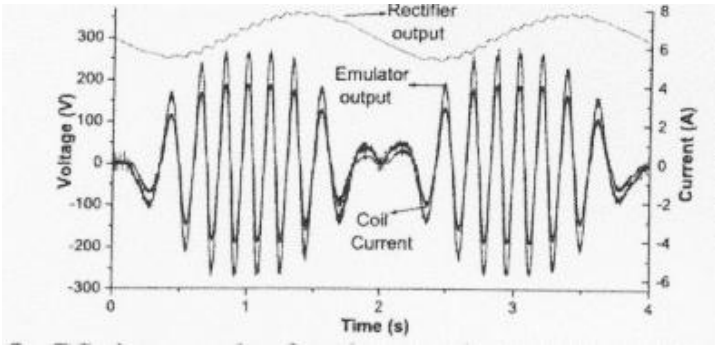

Figure 22: PSpice results for the emulator voltage, coil current and output voltage for the unidirectional rectifier [6]

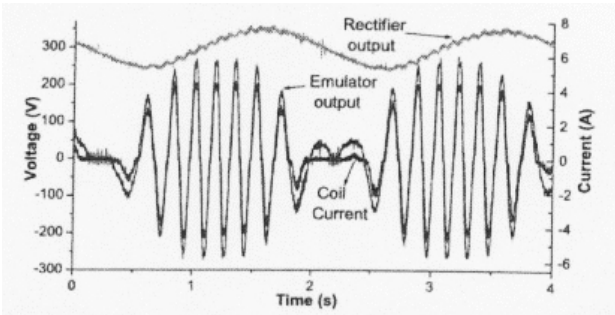

Figure 23: Experimental results for the emulator voltage, coil current and output voltage for unidirectional rectifier [6]

6.3.4 Losses

One system design challenge is to balance the trade-off between system efficiency and maximum power extraction. In conventional generation, system efficiency is a critical concern due to the cost of wasted fuel. However, in renewable generation, the “fuel” is free, skewing the economics to focus more on capital and operating costs for a given output rating. Due to this, it is possible to choose to operate with high losses in order to increase power output for a given size generator. [6]

6.3.5 Test equipment: theoretical boost converter parameters

The externally simulated results indicate that we should be able to get our voltage much better with the boost converter. To simulate this for our equipment, we need a realistic value of boost converter's L.

Out of Eq. (2.8) and our equipment parameters we are able to define the L value which should be used in our boost converter simulation.

$$I_{LB,max} = \frac{T_s V_0}{8L}$$

$$L = \frac{T_s V_0}{8 I_{LB,max}}$$

With

$I_{LB,\ max}$= 8A

T_s= 1/f with f = 10000Hz

V_o= 326V

Which leads to

$$L = \frac{\frac{1}{10000} \cdot 326}{8.8}$$

$$L = 0{,}50938\ mH$$

6.4 Step 3: DC Transport basics

Instead of thinking in the traditional way and transport the energy in AC, the choice of DC transportation has its benefits. Especially; because we already use a boost converter which should make a smooth DC-voltage. This means that we are converting the energy back to AC only when the energy is on land already. If we try to use a boost converter to get a smoother DC voltage, if correctly designed, we might be able to use this output voltage directly as High Voltage Direct Current transport line. An example of DC transportation is shown in Figure 24.

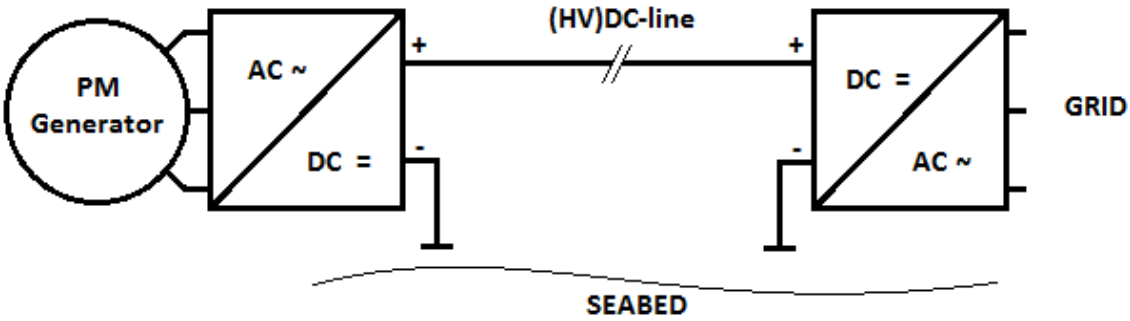

Figure 24: DC topology

Using a DC transport line has its benefits, especially for longer distances e.g. at sea. The biggest benefit is the absence of a third cable. This means a lower copper price, or, if used the same amount of copper for 2 lines: less losses. In some cases, there is only one DC line used, the seabed acts as the 2nd line. If so, the copper price is even lower.

6.4.1 Common DC bridge

As shown on Figure 25, one option can be that the DC transport line is used to couple different wave energy conversion devices. In this case the fluctuation of the DC voltage might be minimalized. Another advantage is that we need only one HVDC cable for several devices.

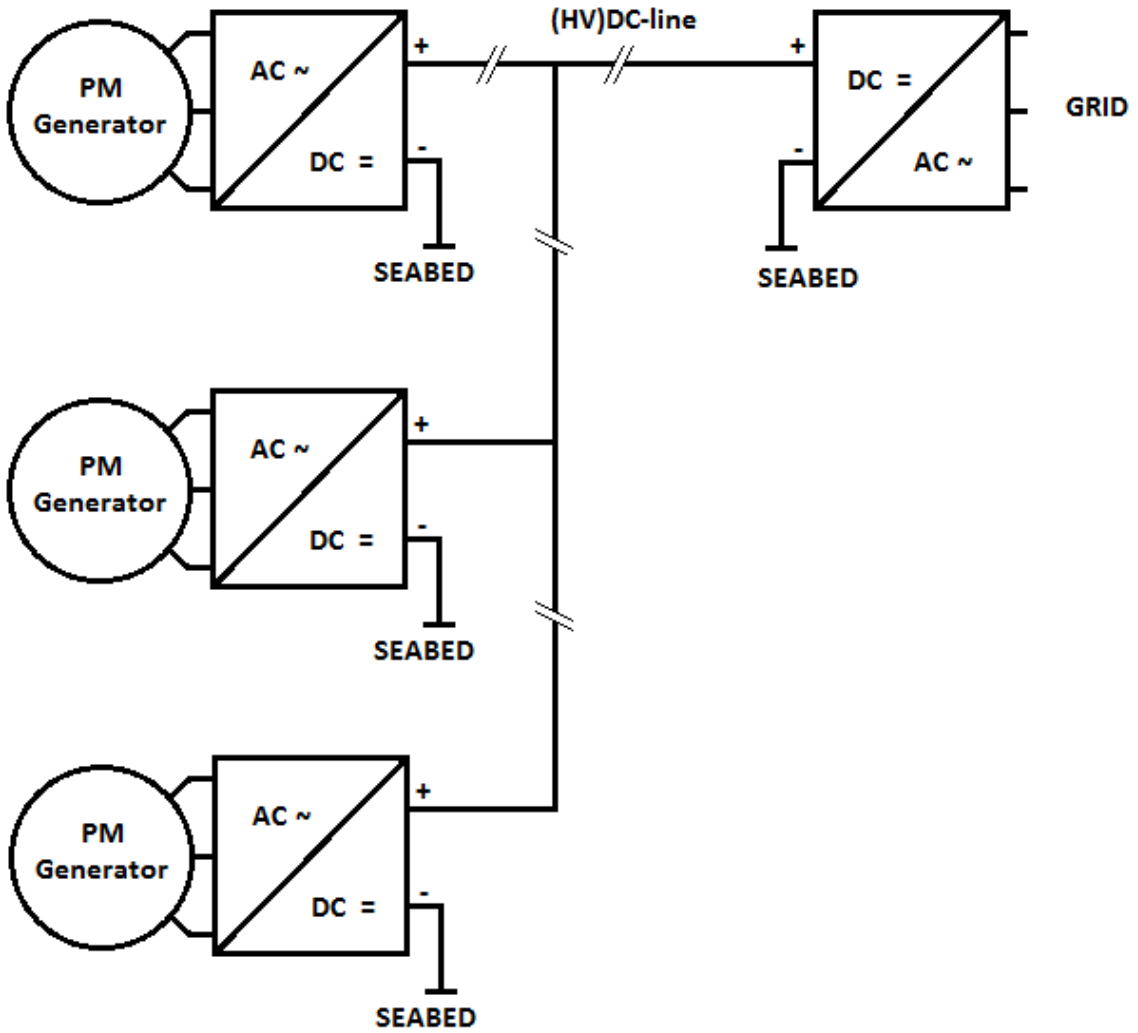

Figure 25: DC connection + transportation

6.4.2 Main HVDC advantage

The advantage of HVDC is that long distance transmission is more efficient as there is no need to charge the capacitance of a transmission line with the alternating voltage.

HVDC has a number of properties which make it different from AC-transmission. The most important are:

- The two stations can be connected to networks that are not synchronized or do not even have the same frequency.

- Power can be transmitted over very long distances without compensation for the reactive power. Reactive power is power that does not add to the transmitted power, but is a by-product at AC-transmission as the line or cable capaci-

tances have to be charged 50 or 60 times per second. As HVDC has a constant voltage it does not generate reactive power.

- Only two conductors are needed (or even one conductor if the ground or the sea is used as return) for HVDC compared to three conductors for alternating current. [7]

6.4.3 Conclusion

A DC transporting line can have benefits for the wave energy, but many parameters influence the choice. First we have to know the distance, power, etc. before a good decision can be made.

6.5 Step 4: Three phase inverter

6.5.1 PWM - converter

In applications such as uninterruptible AC power supplies and AC motor drives, three-phase inverters are commonly used to supply three-phase loads. It is possible to supply a three-phase load by means of three separate single-phase inverters, where each inverter produces an output displaced by 120° (of the fundamental frequency) with respect to each other. Though this arrangement may be preferable under certain conditions, it requires either a three-phase output transformer or separate access to each of the three phases of the load. In practice, such access is generally not available. Moreover, it requires 12 switches.

The most frequently used three-phase inverter circuit consists of three legs, one for each phase, as shown in Figure 26. The output of each leg, for example v_{AN} (with respect to the negative DC bus), depends only on V_d and the switch status; the output voltage is independent of the output load current since one of the two switches in a leg is always on at any instant. Here, we ignore the blanking time required in practical circuits by assuming the switches to be ideal. Therefore, the inverter output voltage is independent of the direction of the load current.

Most frequency converters are using a PWM control, which is obtained by using a sawtooth voltage and a control voltage. Its working is not discussed here.

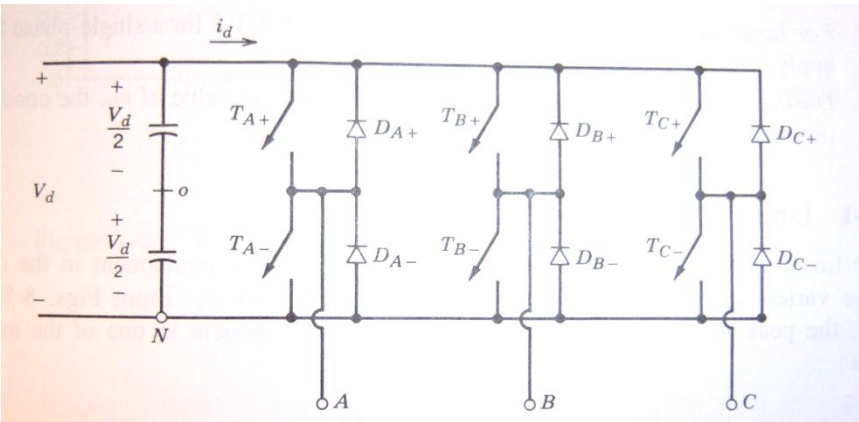

Figure 26: a three-phase converter [4]

6.5.2 Solution when incoming voltage varies

Because it is not easy to get a perfect smooth DC-voltage in the DC-link, the converter which transforms the DC into 50Hz AC can have a slightly variable voltage. To deal with this, we can use a ‘Feed Forward’ PWM converter. This is a PWM converter which can directly change the duty cycle. In this way, the output voltage stays the same, when the input voltage varies. Voltage Feed Forward regulation is shown in Figure 27.

This technique is realized by adding the input voltage to the PWM-control. The only difference with the normal PWM-converter is that now the amplitude of the sawtooth voltage V_T is not constant, but changes proportionally with the input voltage.

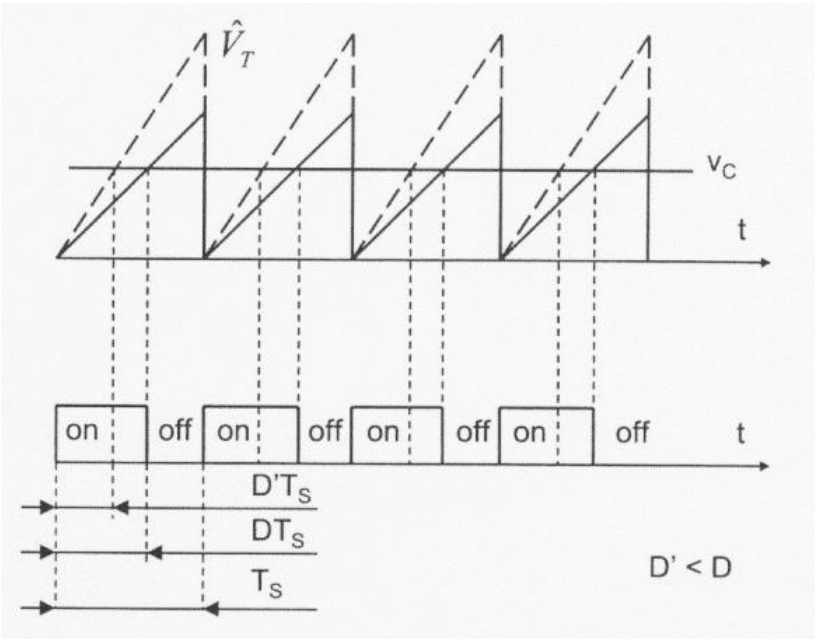

Figure 27: Voltage 'Feed-Forward' PWM regulation [8]

Since we are expecting to have a not perfect smooth DC-link, this can be very useful.

7 BOOST CONVERTER SIMULATION

As said in 6.3.3, others were able to simulate a boost converter on a voltage which has the same shape as in our case. We know they have it, and it might be a solution for our case. But, in the found external result, nothing was said about the transmitted power and eventually used capacitors. A simulation suitable for our case has to be made to ensure this.

Note: In the simulation schemes colored pins are used to show where measurements are taken. The colours of the pins do not match with the colours of the lines in the result graphs.

7.1 PSpice boost converter topology

Both Matlab and PSpice simulations are commonly used. Because a working boost converter simulation in PSpice was available, I tried to work with this.

Figure 28 shows the first made boost converter simulation topology. There are four main components. The generator, DC-bridge, boost converter, and the load.

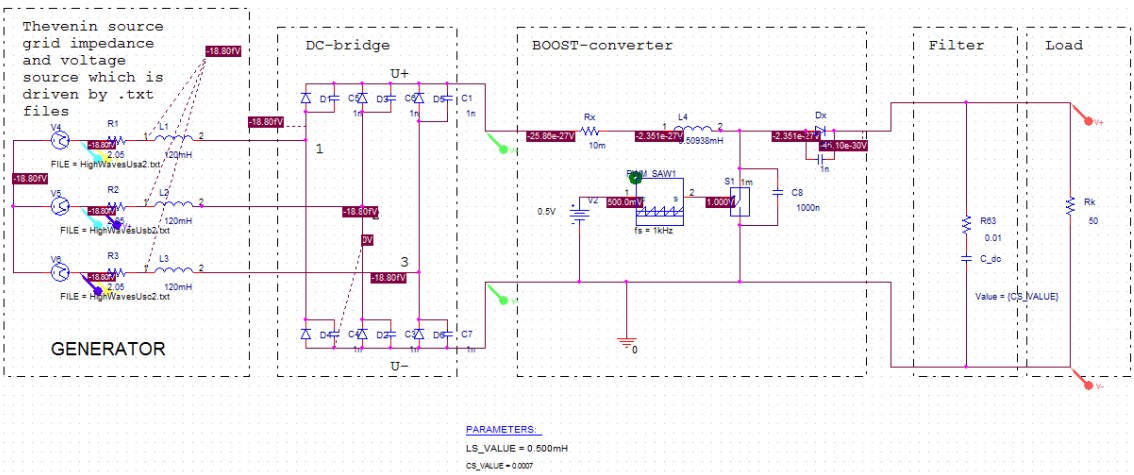

Figure 28: Boost Converter Topology

The model shown in Figure 28 had a lot of errors, because of undefined reasons the model did not recognize the switching part of the boost converter. Many alternatives were tried, but the result was always the same. The model was not running at all, or it was running with a non-active boost converter.

7.2 Basic boost converter – DC input

Since the first model was not working, another model was made; starting from a different working boost converter model. The difference here is the boost converter which is build out of alternative parts. Comparison between Figure 28 and Figure 29 show this difference.

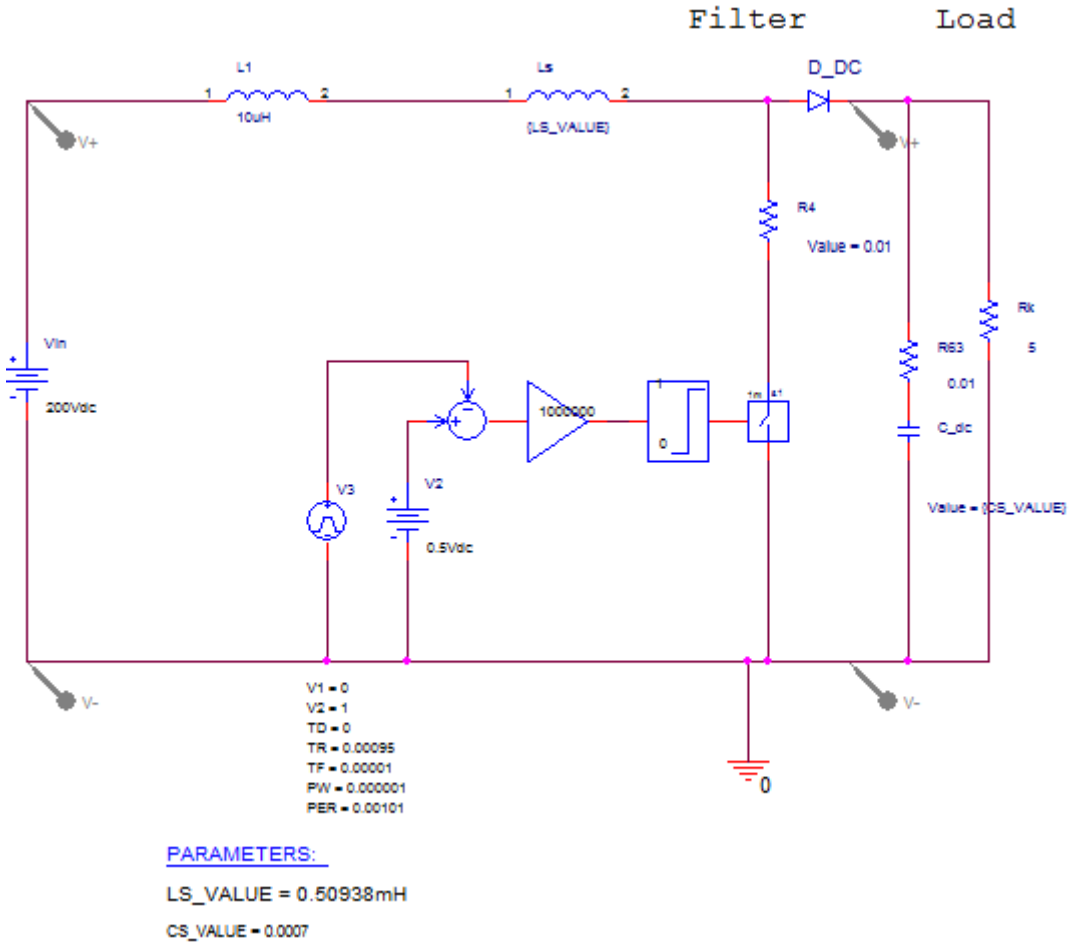

Figure 29: Basic boost converter

To test if this converter is working, a 200V DC voltage is placed at the input. The simulation result is given in Figure 30. As shown, the output voltage varies around the 400V DC, while the input voltage is 200V DC. One leads to the conclusion this boost converter is working.

In Figure 31 a zoom of the result is given. As shown, the switching moments of the boost converter are clearly detected in the output voltage. The output voltage varies approximately 50V.

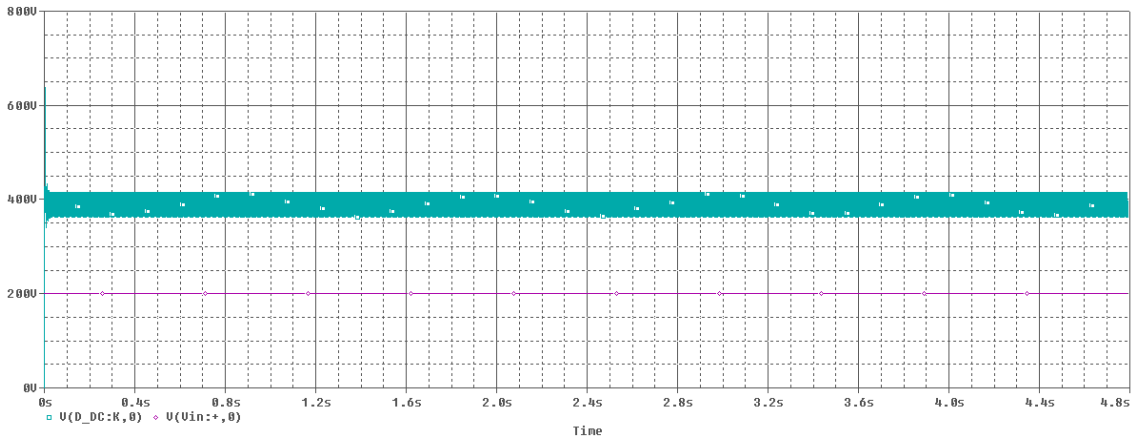

Figure 30: Basic DC boost result

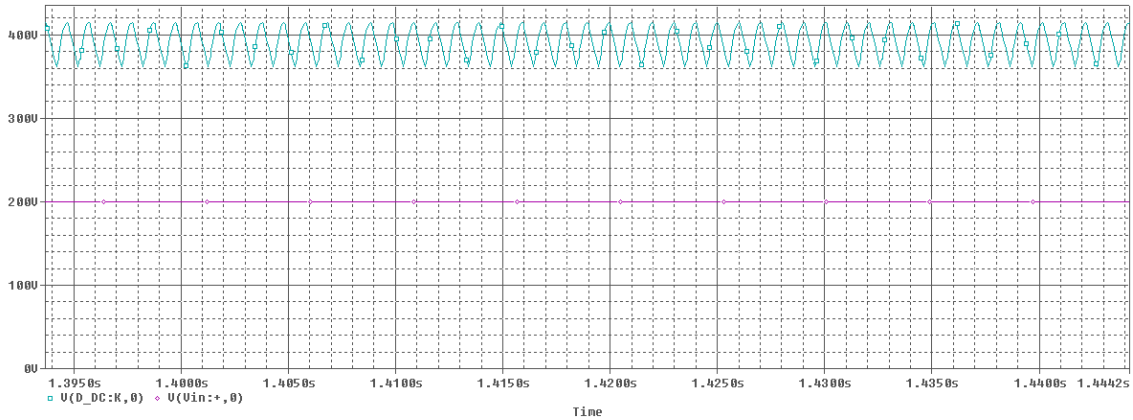

Figure 31: Zoom of basic DC boost result

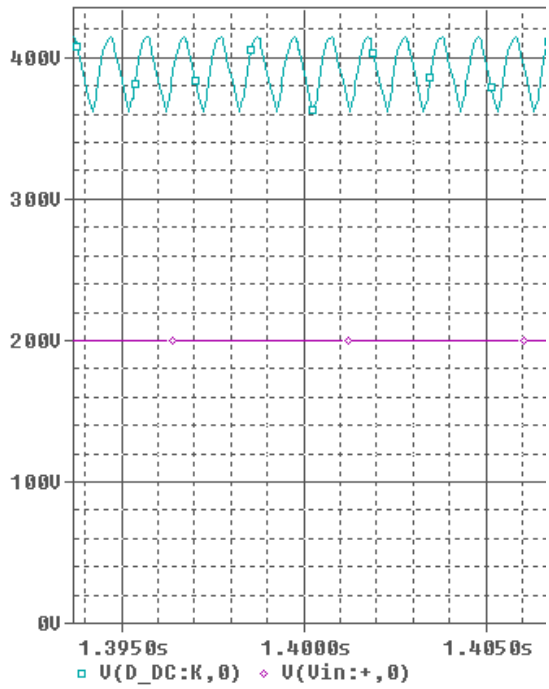

Figure 32: Close up of basic DC boost result

7.3 Basic boost converter – saw tooth input

When the DC source is replaced by an AC source as shown in Figure 33, the boost converter is still working. An important fact is that the output voltage has zero point when the input voltage is zero. This means this system is not able to store energy.

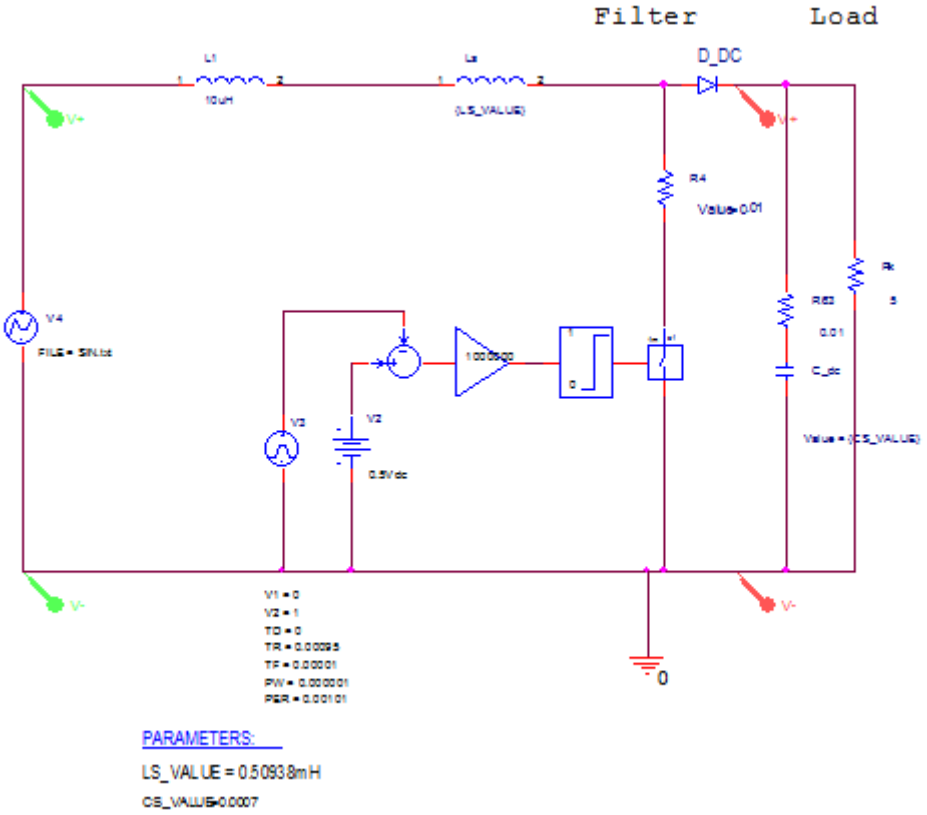

Figure 33: Basic boost converter – AC input

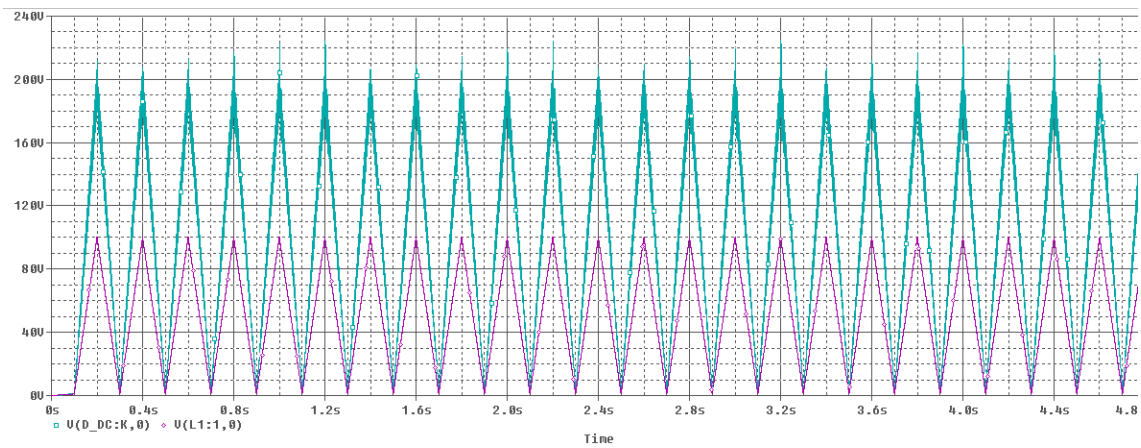

Figure 34: Basic boost converter saw tooth result

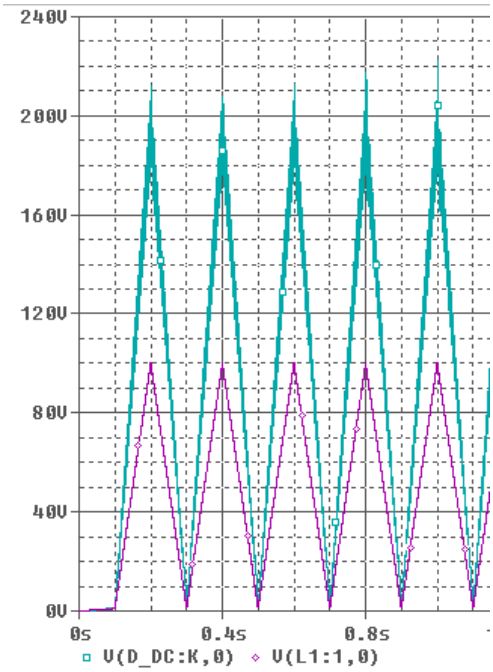

Figure 35: Close up of saw tooth result

7.4 Basic boost convertor – 1 phase wave form input

As shown on Figure 36, the boost converter is still doing its job, but the zero points are still present.

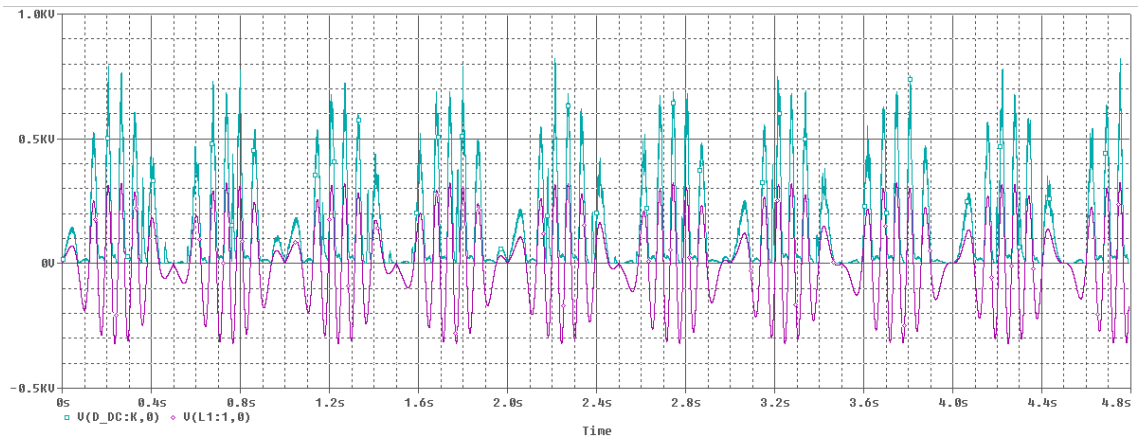

Figure 36: Basic boost converter - wave form input

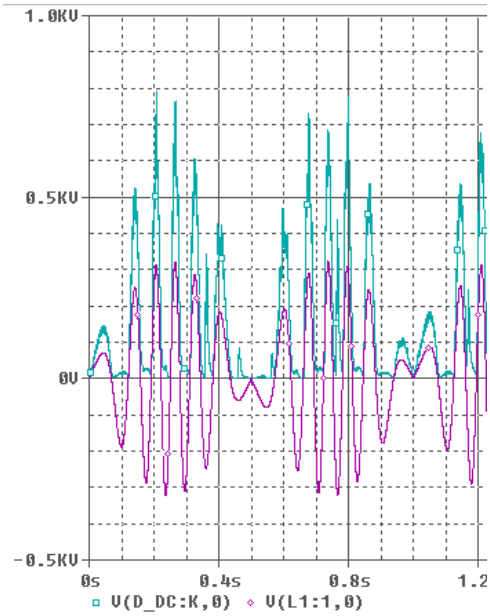

Figure 37: Close up from wave form result

7.5 Basic boost converter – 1 phase rectified input

By adding a one phase diode bridge as shown in Figure 38, the input voltage is now rectified.

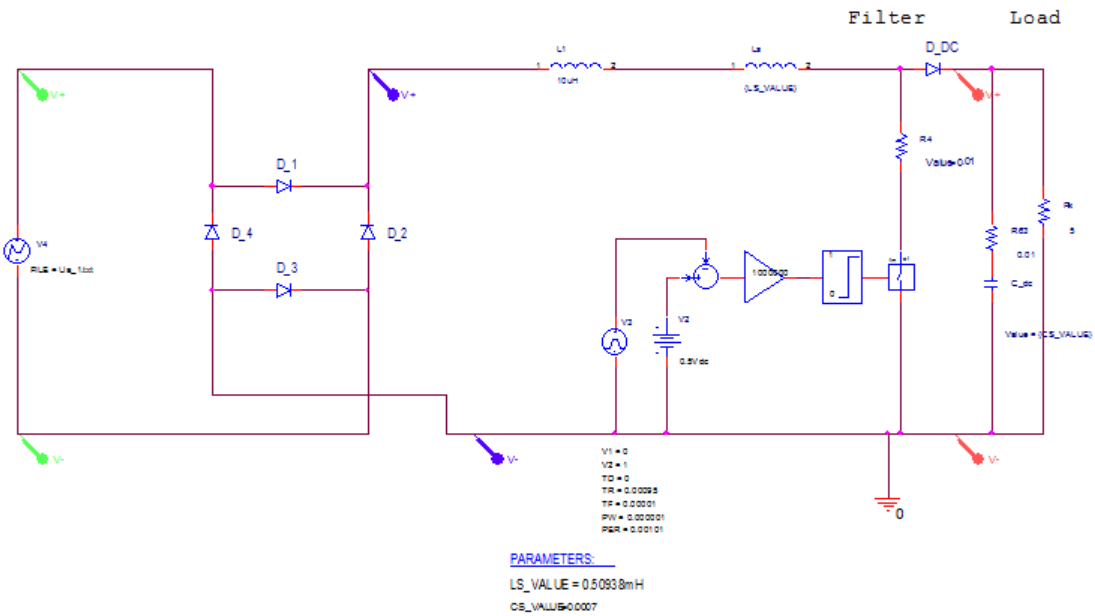

Figure 38: Basic boost converter - one phase rectified input

The output result is shown in Figure 39. Compared with Figure 36, the average output power is increased.

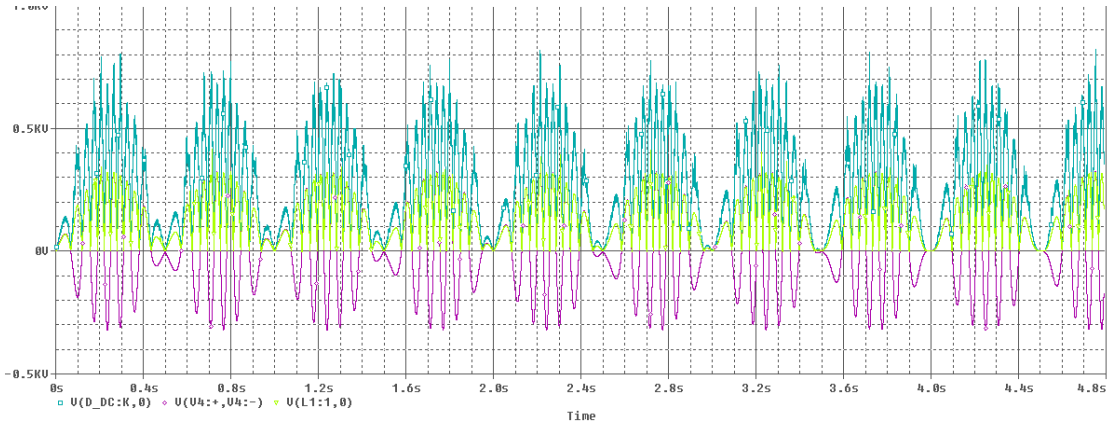

Figure 39: 1 phase rectified output

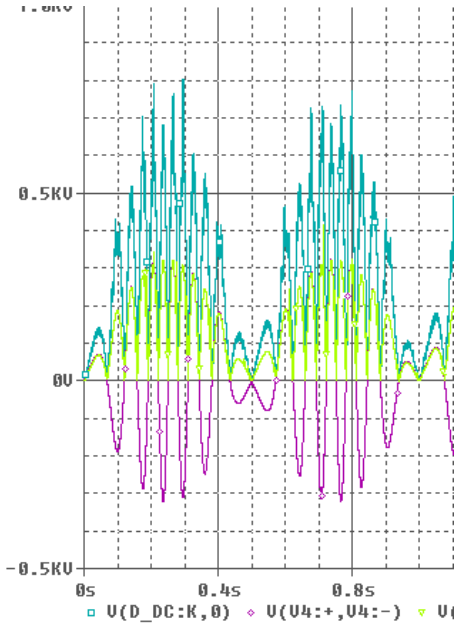

Figure 40: Close up of phase rectified result

7.6 Three-phase boost converter input

Since we know the boost converter is working, we can now try to simulate again with the generator. This part is copied from the first –not working- simulation. Generator parameters are set on L=120mH and R=2,05Ω for each line. A 3-phase bridge rectifies the induced voltage.

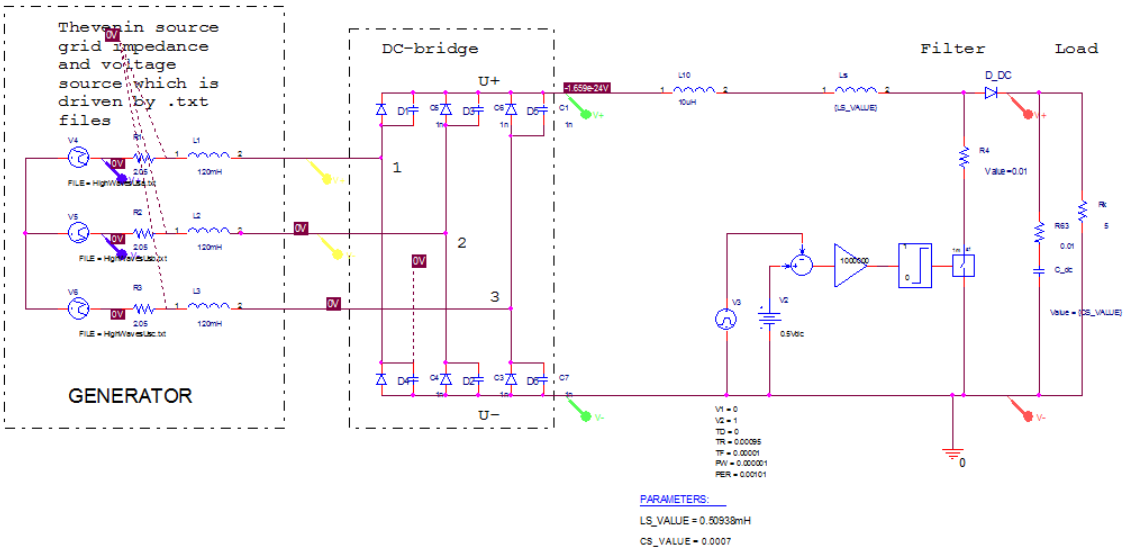

Figure 41: 3-phase basic boost converter

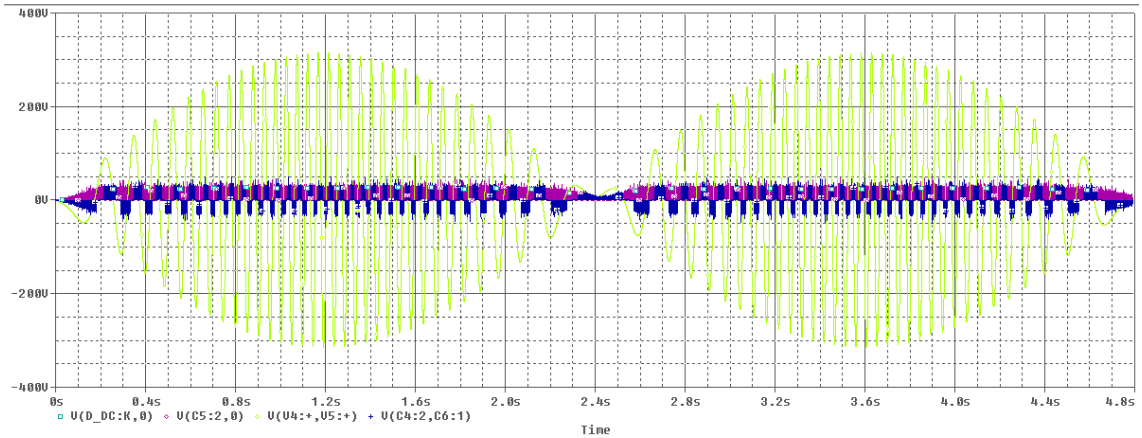

Figure 42: 3-phase boost converter result

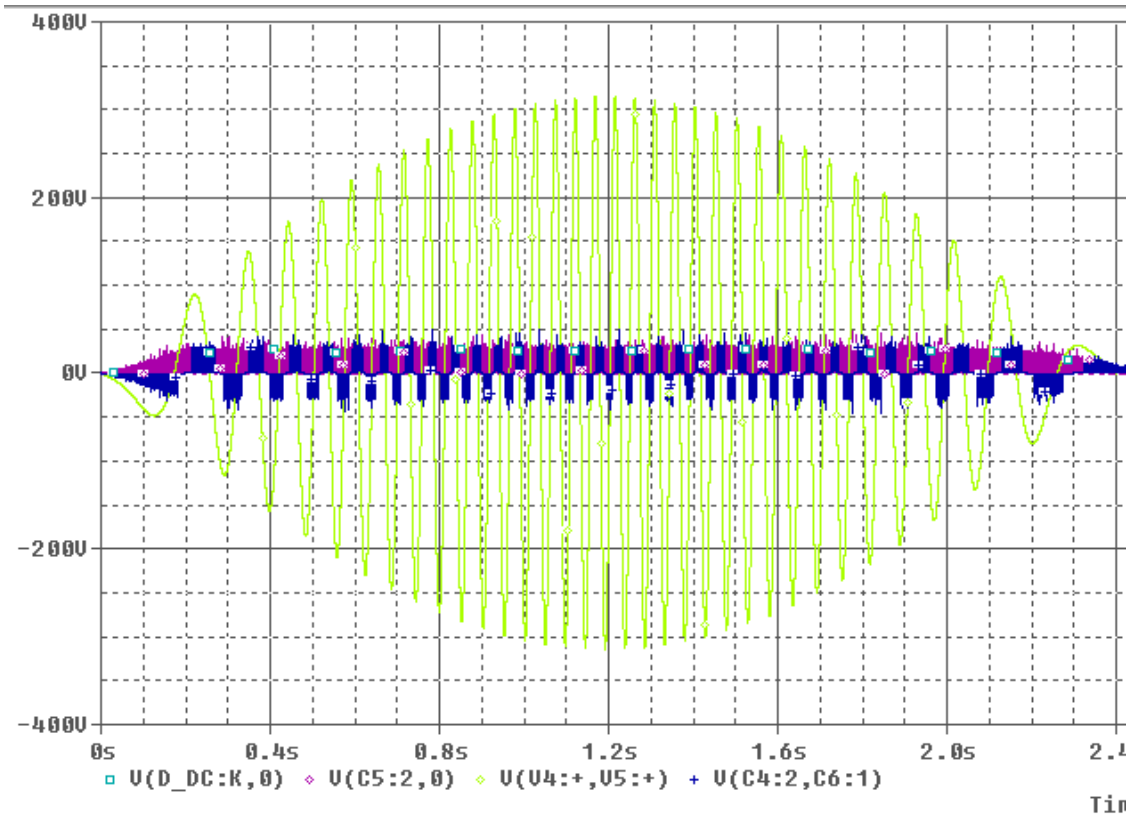

Figure 43: Close up of 3 phase boost converter result

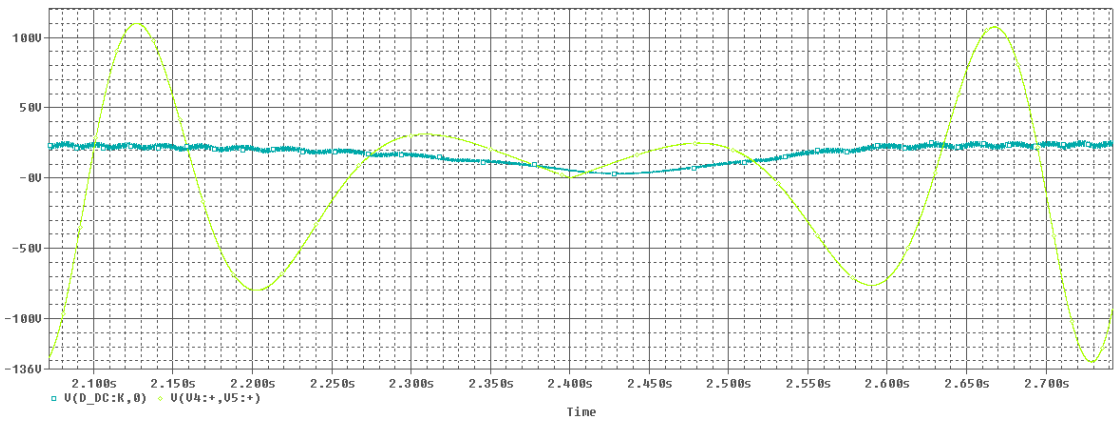

Figure 44: 3-phase boost converter result zoom

As we look closer to the output voltage, we see the output voltage is still very close to zero on the crucial moment. The boost converter simply has no voltage to boost.

Trying to avoid this, a capacitor was added.

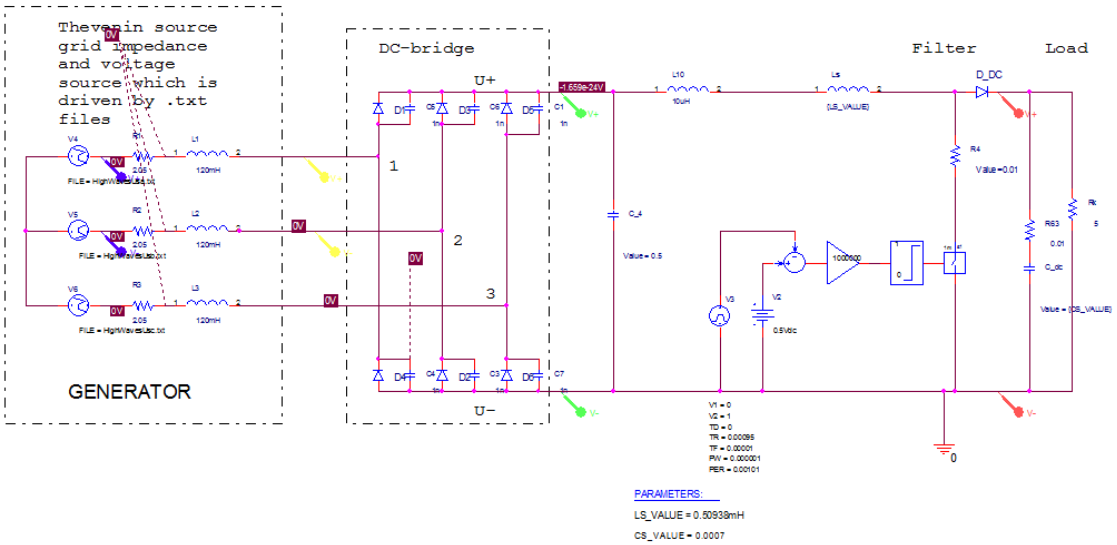

Figure 45: 3-phase boost converter with DC capacitor

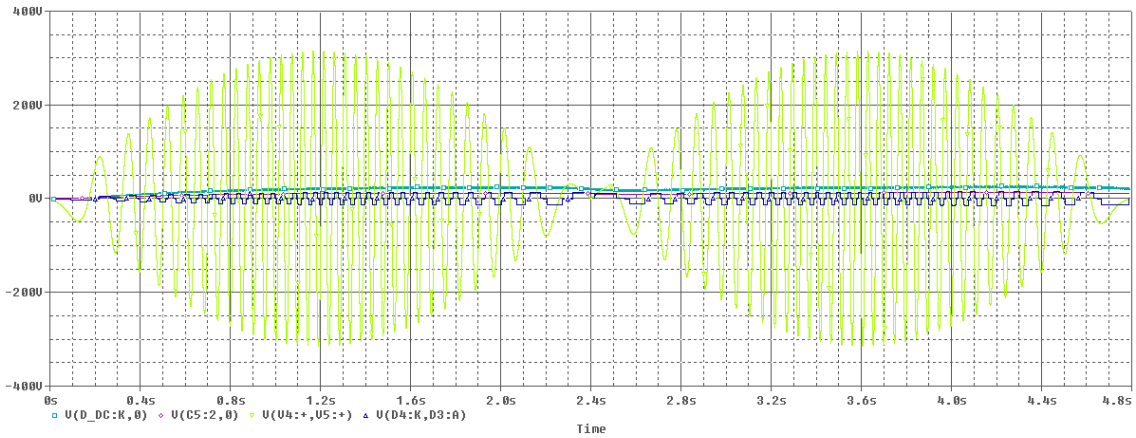

Figure 46: 3-phase boost converter with DC-capacitor result

Another option was placing a capacitor at the load side of the boost converter, as shown in Figure 47.

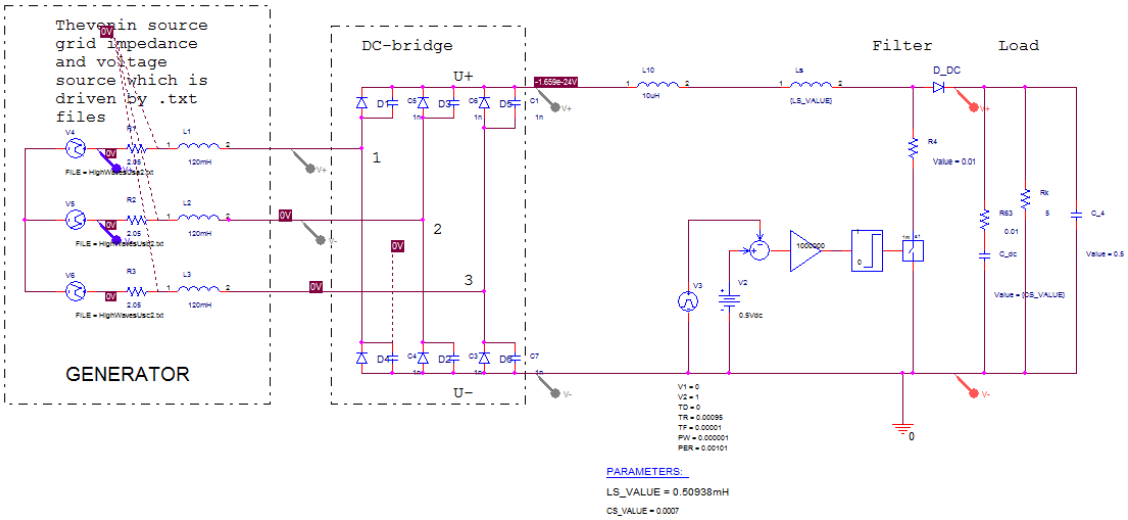

Figure 47: 3-phase basic boost converter with extra C at load side

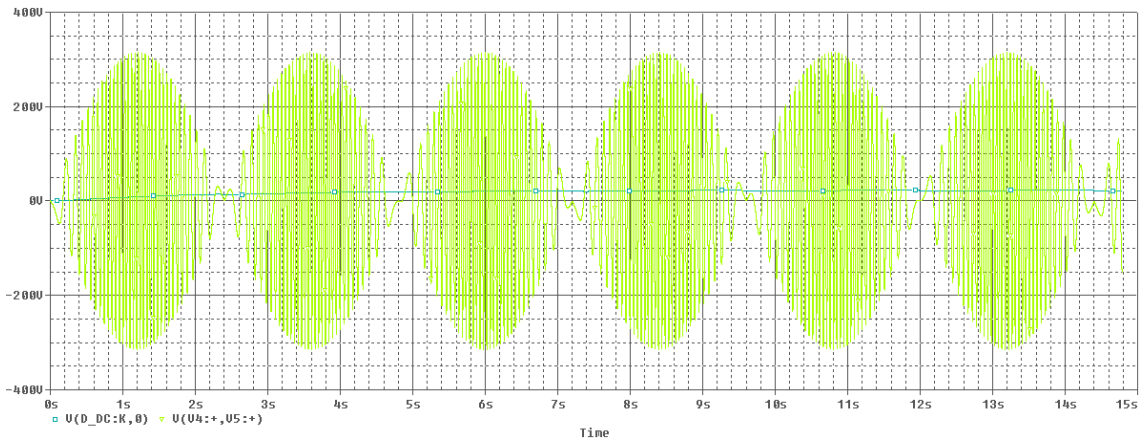

Figure 48: 3-phase boost converter with extra C at load side - result

As shown in Figure 48, the output voltage is now more constant, but still very low.

7.7 Optimizing simulation Load value

Previous simulations showed the influence of the parameters is not that big. Only one parameter is left, the load value. To calculate the optimal load we can use a formula from wave energy converters with linear generators. Knowing the components of the lumped circuit the active power in the load can be calculated:

$$P_l = E^2 \left(\frac{R_l}{(R_l + R_g)^2 + (X_s + X_l)^2} \right) \tag{3.1}$$

With

P_l = output power (W)
E = induced voltage (no load)
R_l = Load resistance
R_g = Generator resistance
X_s = 2.π.f.L with L = generator coil inductance 120mH
X_l = assumed zero

The active output power of a generator depends on the induced emf, the synchronous reactance, the armature winding resistance and the load. The induced emf varies with the translator speed (which we take constant 200rpm in this example) and the output power will thus vary as the translator changes speed during a wave period. By changing the load the output power for a given translator speed can also change. By varying the load, the damping of the generator can be varied. This can be used as control strategy to control the power absorbed by the Wave Energy Converter. [1]

Since we want extract maximum power out of the generator, the optimal load has to be found using (3.1). We assume a constant induced voltage of 111,8V.

Rload (Ω)	Rgen (Ω)	Xs (Ω)	Xl (Ω)	E (V)	Pphase (W)	3*Pphase (W)
1	2,05	12,59	0	111,8	74,5	223,4
5	2,05	12,59	0	111,8	300,1	900,3
6	2,05	12,59	0	111,8	335,8	1007,3
7	2,05	12,59	0	111,8	363,9	1091,6
8	2,05	12,59	0	111,8	385,3	1155,8
9	2,05	12,59	0	111,8	400,8	1202,5
10	2,05	12,59	0	111,8	411,5	1234,5
11	2,05	12,59	0	111,8	418,1	1254,3
12	2,05	12,59	0	111,8	421,4	1264,2
13	2,05	12,59	0	111,8	422,0	1266,0
14	2,05	12,59	0	111,8	420,5	1261,5
15	2,05	12,59	0	111,8	417,3	1252,0
16	2,05	12,59	0	111,8	412,9	1238,7
17	2,05	12,59	0	111,8	407,5	1222,5
18	2,05	12,59	0	111,8	401,4	1204,1
19	2,05	12,59	0	111,8	394,7	1184,2
20	2,05	12,59	0	111,8	387,7	1163,2

Out of the calculations we see the highest output power is with a load of 13Ω. Using this value in a simulation with constant input voltage, we should get a total output power of 1266W.

This is the output power of a load directly connected to a generator rotating at constant speed. If we replace the generator and the diode bridge by a DC-source, the value of this source can be calculated:

$$U_{dc} = 1{,}35 \,.\sqrt{3}\,.E \tag{3.2}$$

$$U_{dc} = 1{,}35 \,.\sqrt{3}\,.111{,}8$$

$$U_{dc} = 261{,}42V$$

The load R_{dc} in a DC-simulation is calculated

$$P = 3.\frac{E^2}{R} = \frac{{U_{dc}}^2}{R_{dc}} \tag{3.3}$$

$$R_{dc} = R.\frac{{U_{dc}}^2}{3.E^2} \tag{3.4}$$

$$R_{dc} = 13.\frac{261{,}42^2}{3.111{,}8^2}$$

$$R_{dc} = 23{,}69\Omega$$

Optimized load scheme is shown in Figure 49.

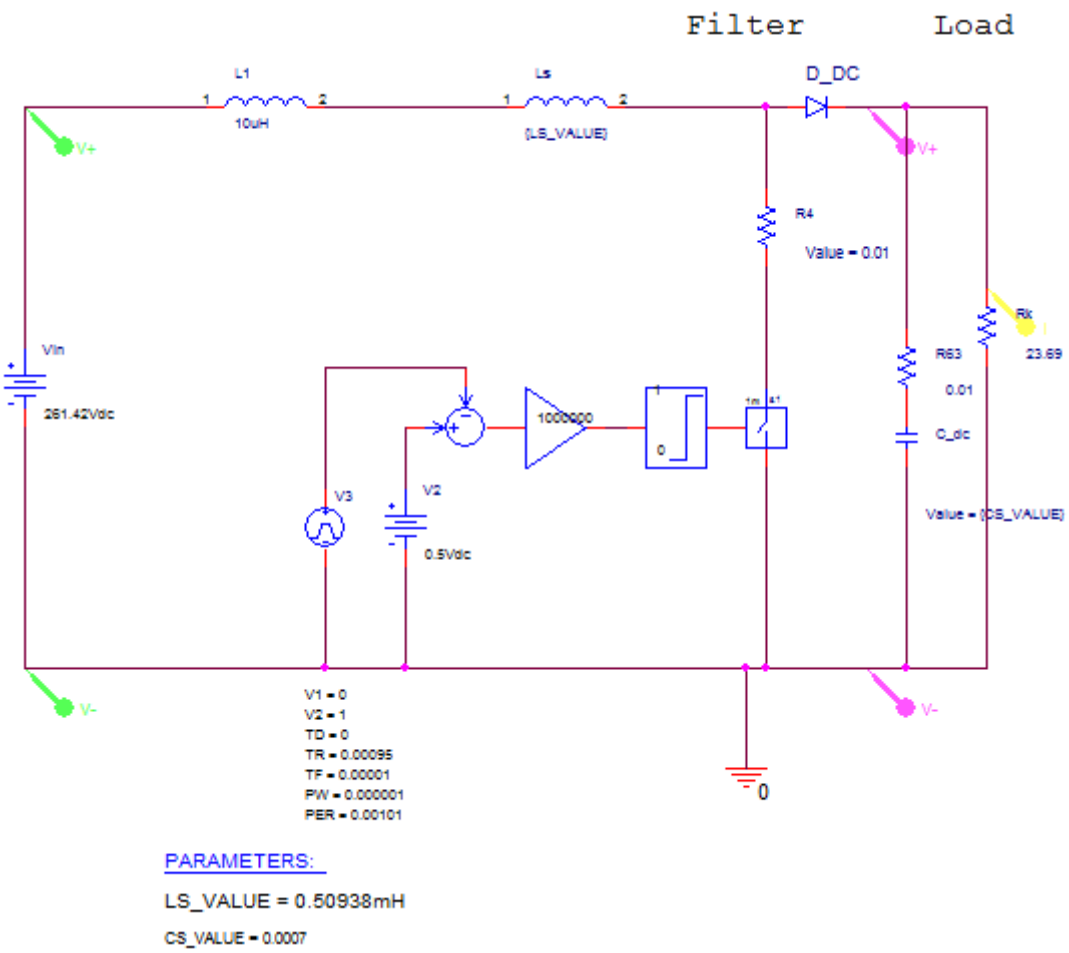

Figure 49: Optimized load scheme

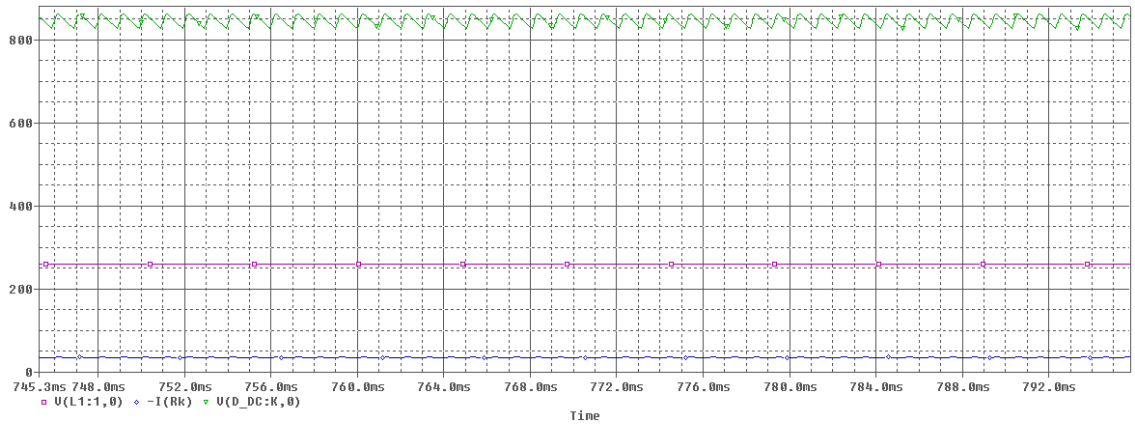

Figure 50: Optimized load result – part 1

Figure 50 shows an output voltage of approximately 850V. The next step is designing the output resistance for an output voltage of 850V and a power of 1266W.

$$R_{dc} = \frac{U^2}{P} \tag{3.5}$$

$$R_{dc} = \frac{850^2}{1266}$$

$$R_{dc} = 570{,}70\Omega$$

The scheme with the optimized resistance is shown in Figure 51.

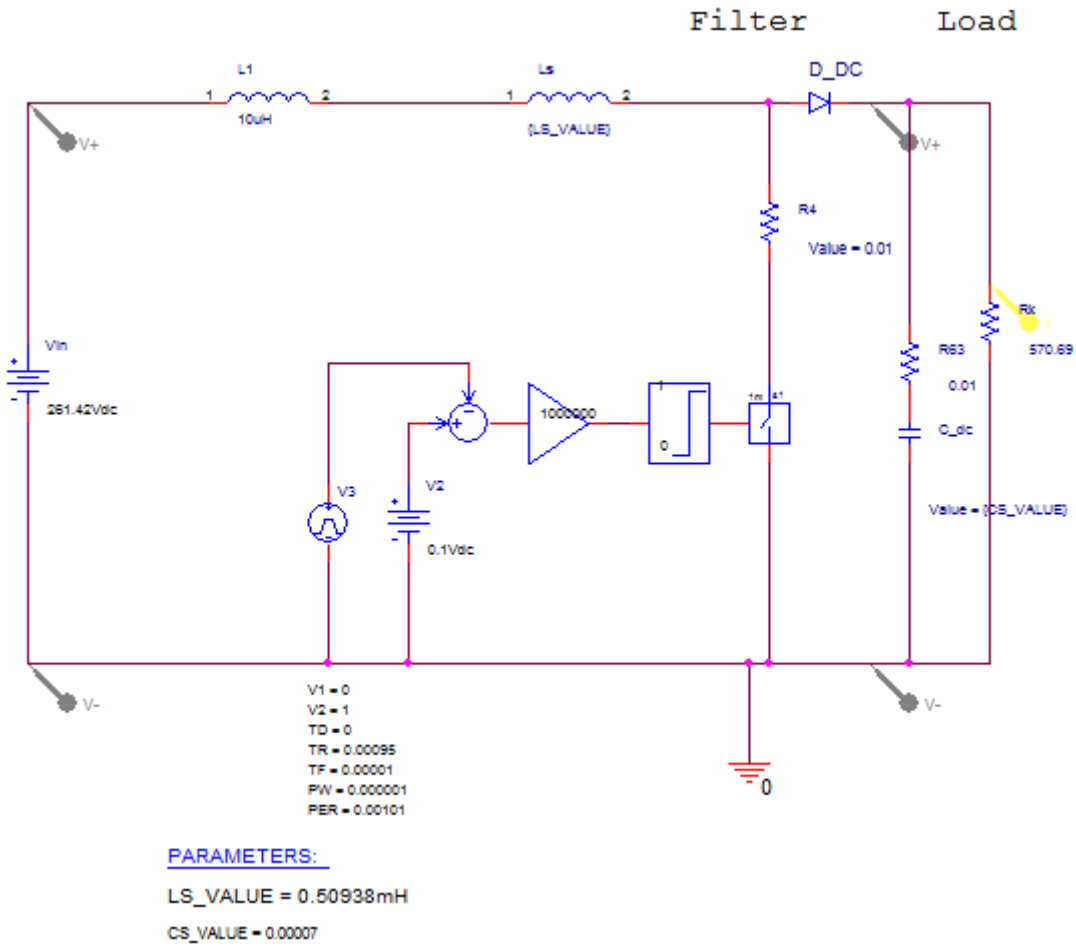

Figure 51: Scheme with optimized resistance

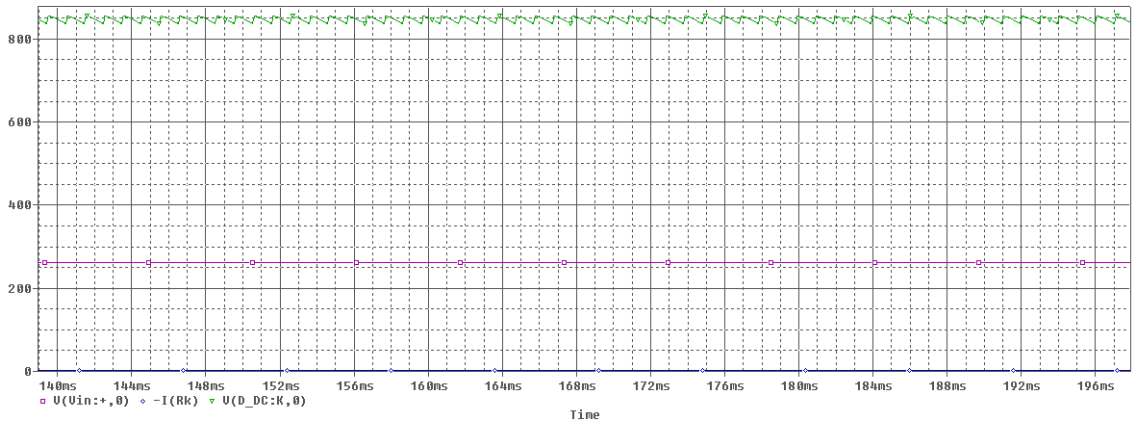

Figure 52: Optimized load result – part 2

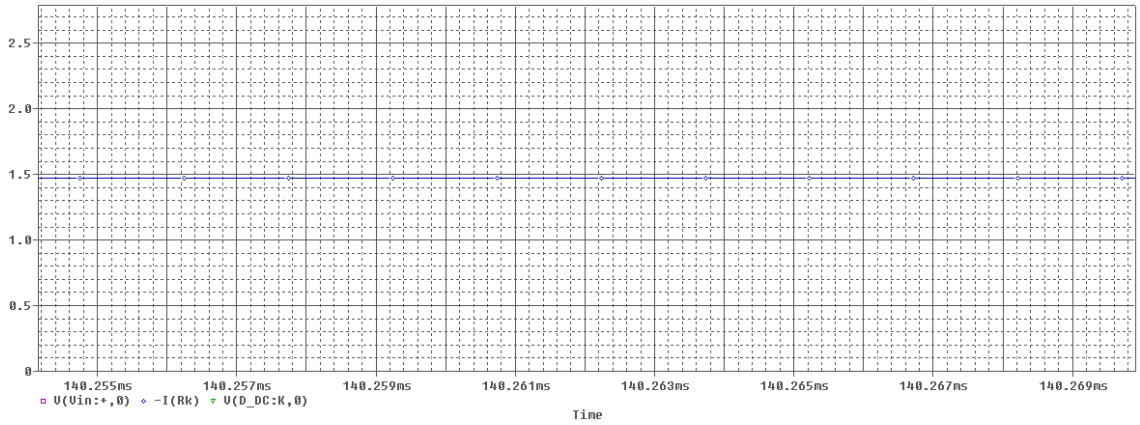

Figure 53: Optimized load result, zoom in on current

Figure 52 and Figure 53 show the result of the simulation with the optimized load resistance of 570,69Ω. An output voltage of approximately 850V and an output current of approximately 1,5A lead to an output power of approximately 1250W, which is close to the calculated value of 1266W.

Important is that we had to adjust the duty cycle of the boost converter by changing the control voltage from 0,5V to 0,1V manually to get the simulation running correctly. This proves the need of a good control which should do this automatically.

7.8 3-phase boost & non-boost comparison

To see the effect of the boost converter in the three phase system, a comparison is made here.

7.8.1 3-phase without boost

3-phase without boost converter scheme is shown in Figure 54.

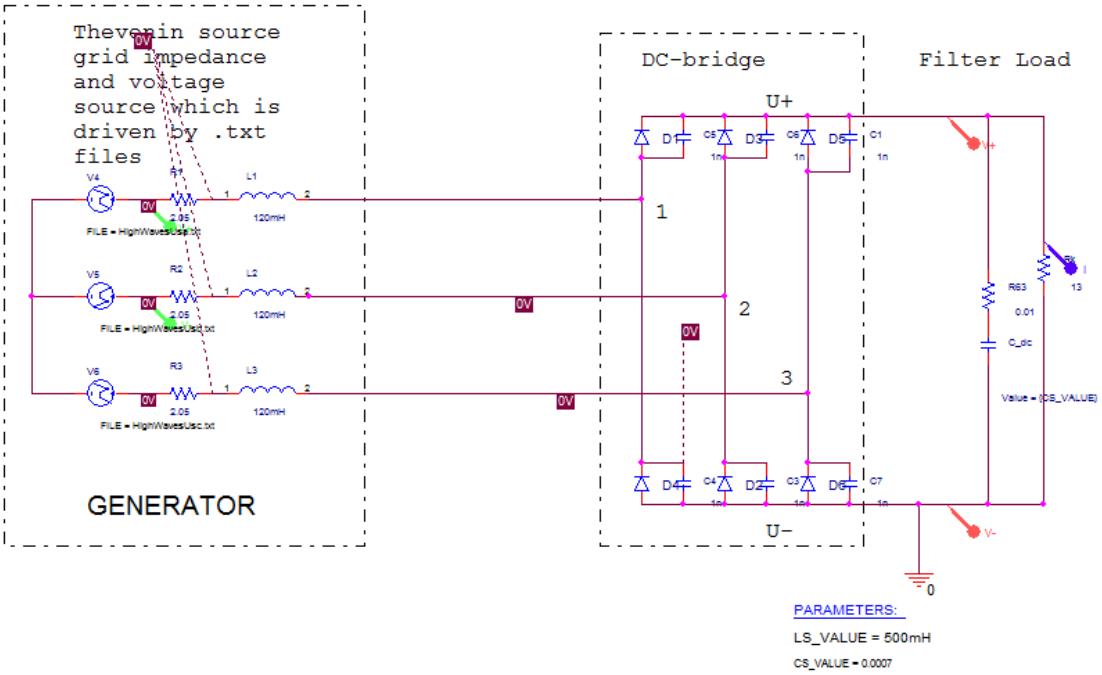

Figure 54: 3-phase no boost converter scheme

This leads to

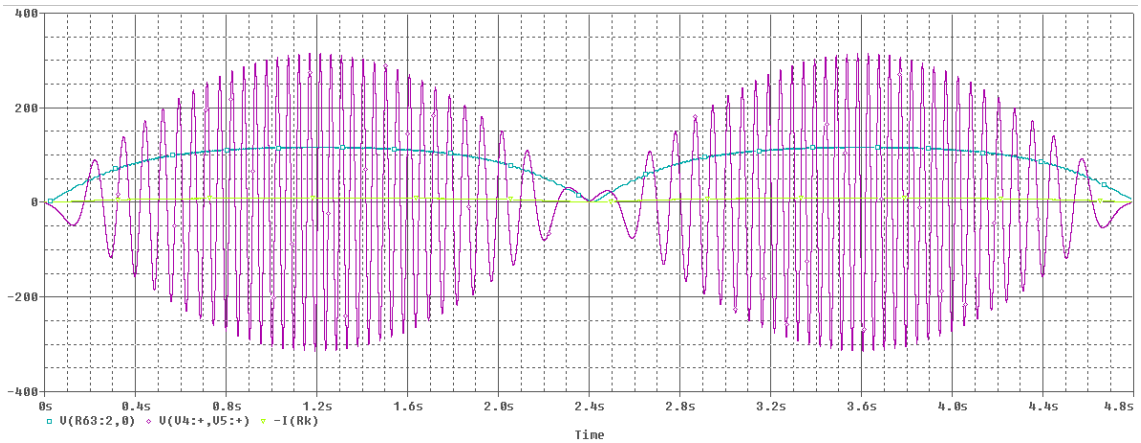

Figure 55: 3-phase no boost converter result

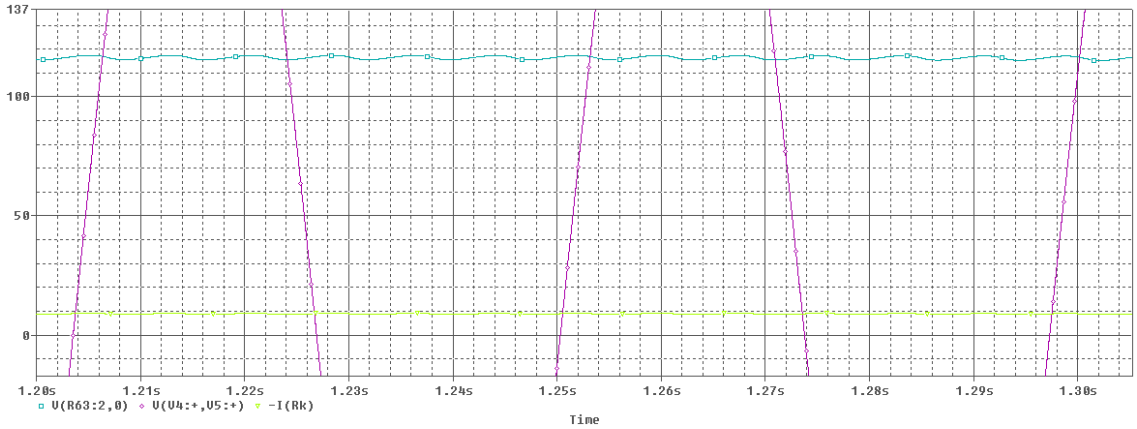

Figure 56: zoom in on 3-phase no boost converter result

In Figure 56 it is shown that the maximum output voltage is approximately 117V, the maximum output current is 9A.

If we zoom in on the voltage dip, this is what we see:

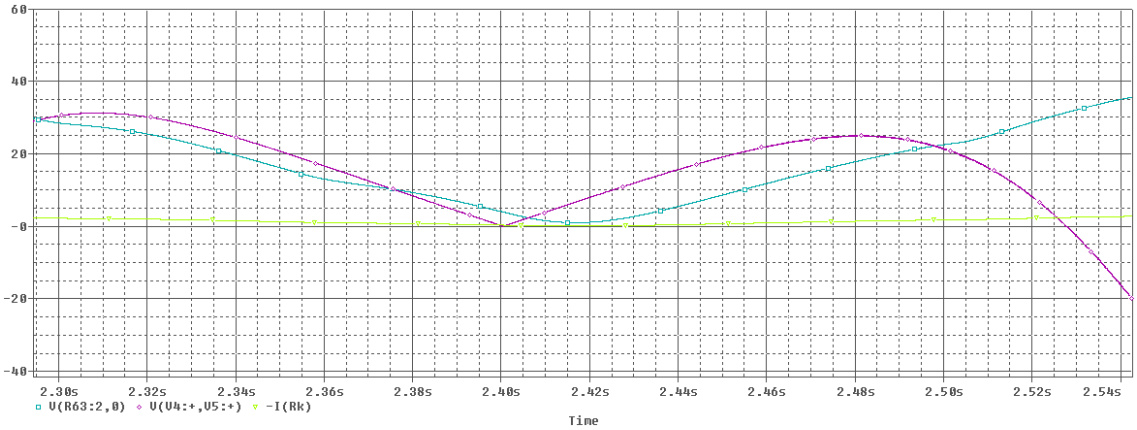

Figure 57: zoom in on voltage and current dip of 3-phase no boost converter result

In Figure 57 we can see the voltage and current drop very close to zero. The current at the lowest point is less than 0,1A.

7.8.2 3-phase with boost

3-phase with boost scheme is shown in Figure 58.

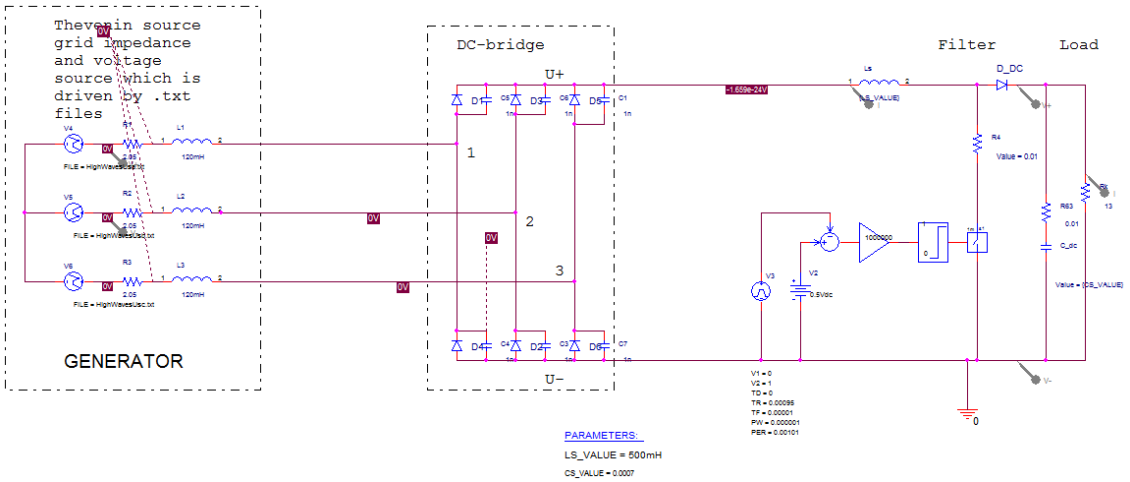

Figure 58: 3-phase with boost converter scheme

This leads to

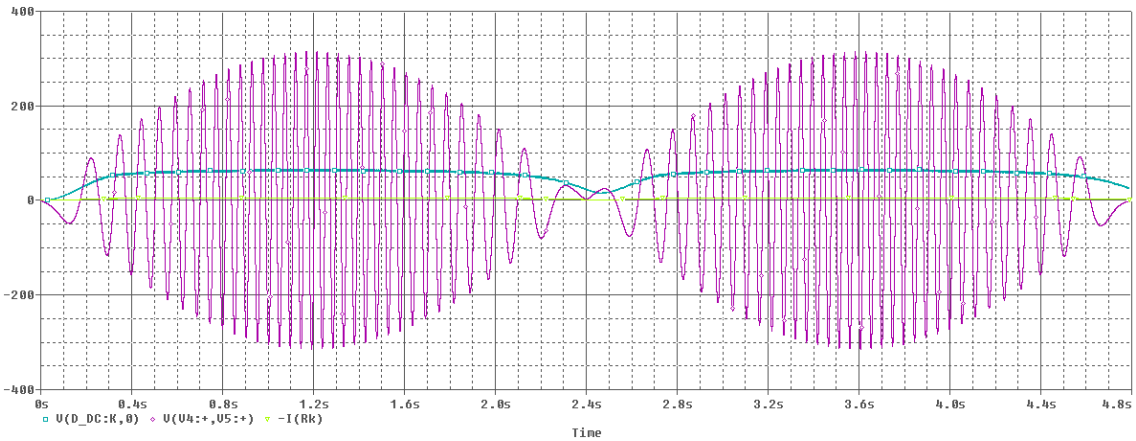

Figure 59: 3-phase with boost converter result

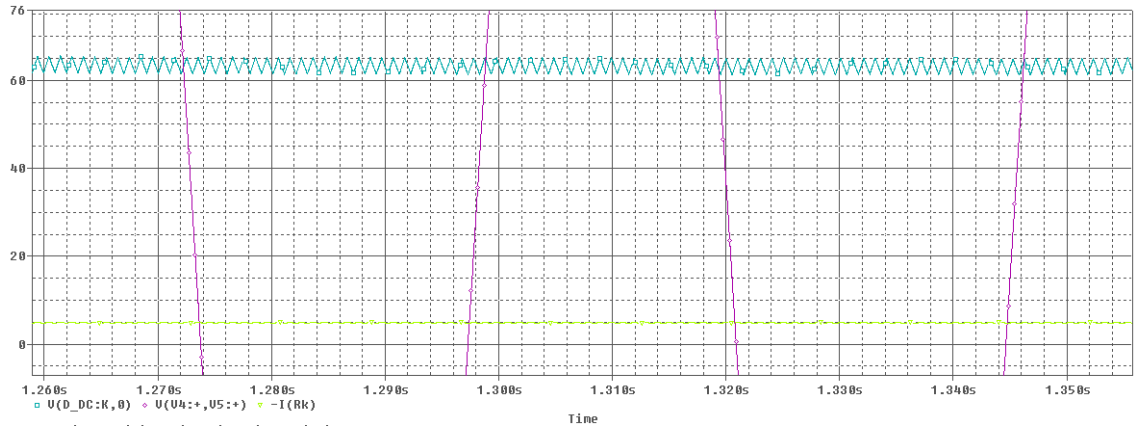

Figure 60: zoom in on 3-phase with boost converter result

As we can see in Figure 60, there is a maximum output voltage of approximately 62V. The output current is 5A.

If we zoom in on the voltage dip, this is what we see:

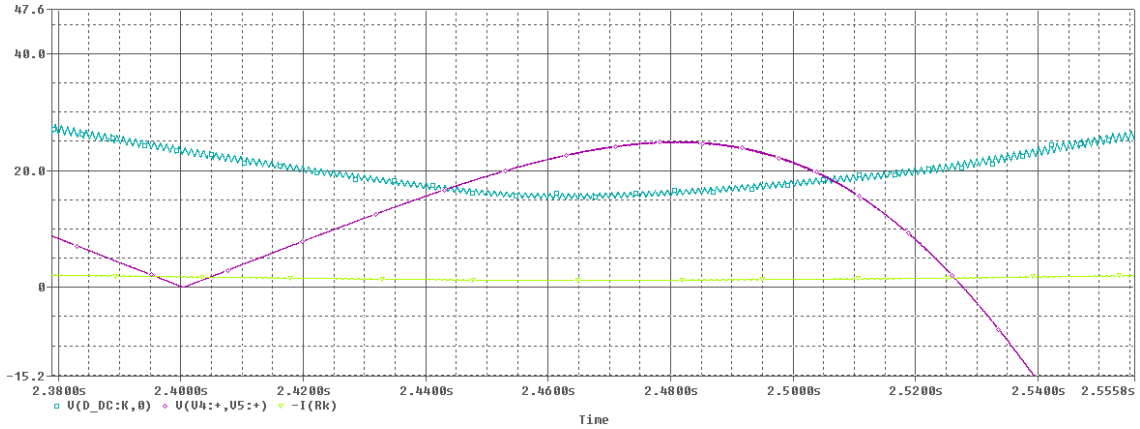

Figure 61: zoom in on voltage and current dip of 3-phase with boost converter result

Figure 61 shows the output voltage drops to 18V, and the output currents' lowest point is 1,2A.

7.8.3 Comparison

Both results are listed in following table.

	NO boost	**With boost**
Max. voltage	117V	62V
Max. current	9A	5A
Min. voltage (dip)	2V	18V
Min. current (dip)	0,1A	1,2A

It is clear that the voltage and current drop without the boost converter is lower than with the boost converter. The maximum voltage and current without the boost converter is higher, this is logic, because the boost converter stores energy, so less energy is at the output with a boost converter.

The main conclusion we can make is that the boost converter is working and the dip is not as low as before.

7.9 Higher boost switching frequency

All previous simulations are made with a boost switching frequency of 1 kHz. In our calculation of the L value of the boost converter in 6.3.5 we used a frequency of 10 kHz. A simulation using this frequency might give better results.

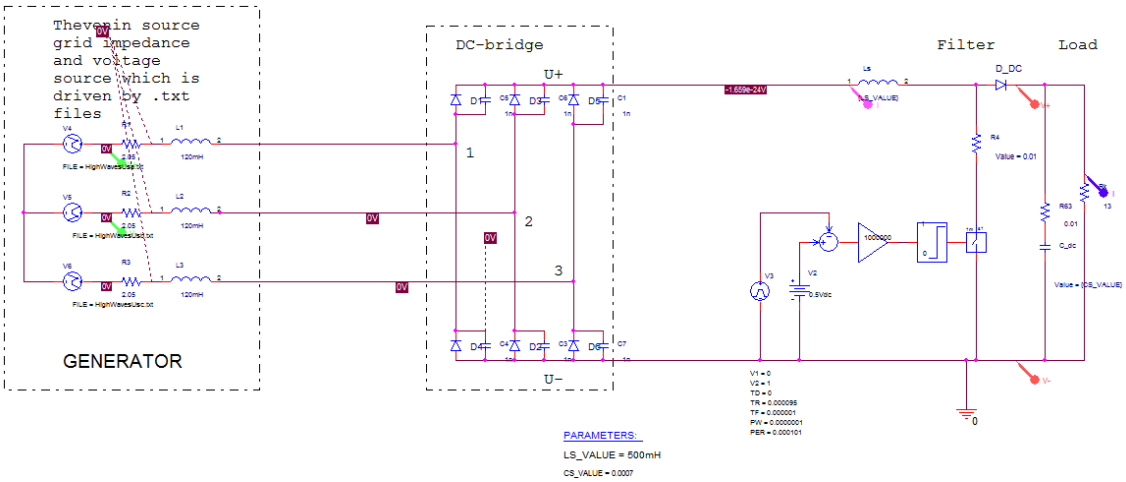

Figure 62: 3-phase with 10 kHz boost frequency

As shown in Figure 62 nothing changes in the scheme. Only the boost converter parameters shown in Figure 63 are adjusted.

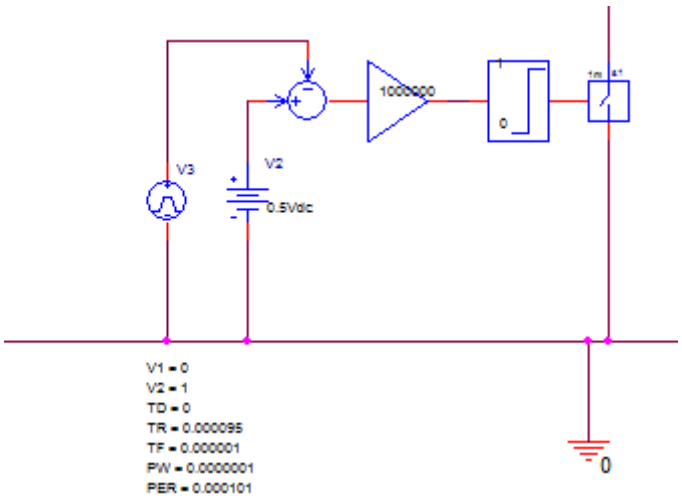

Figure 63: Boost converter parameters

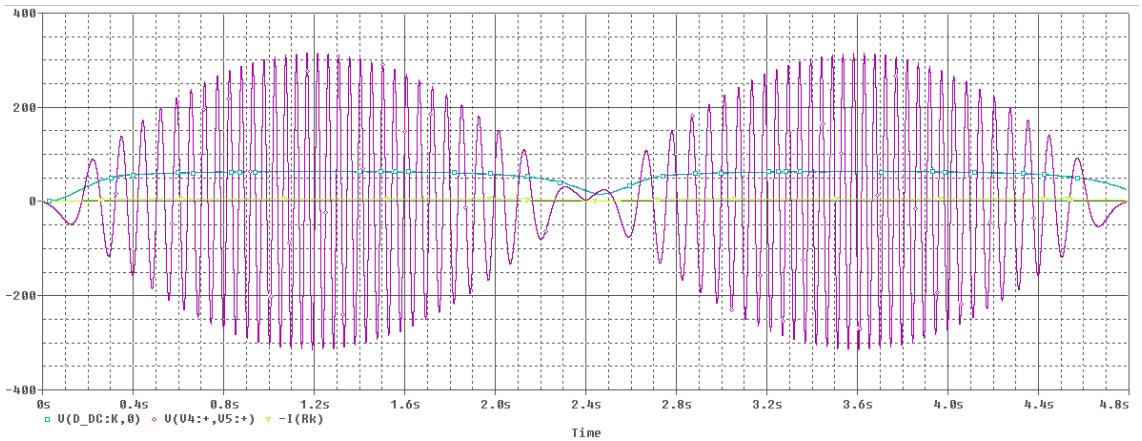

Figure 64: 10 kHz boost converter result

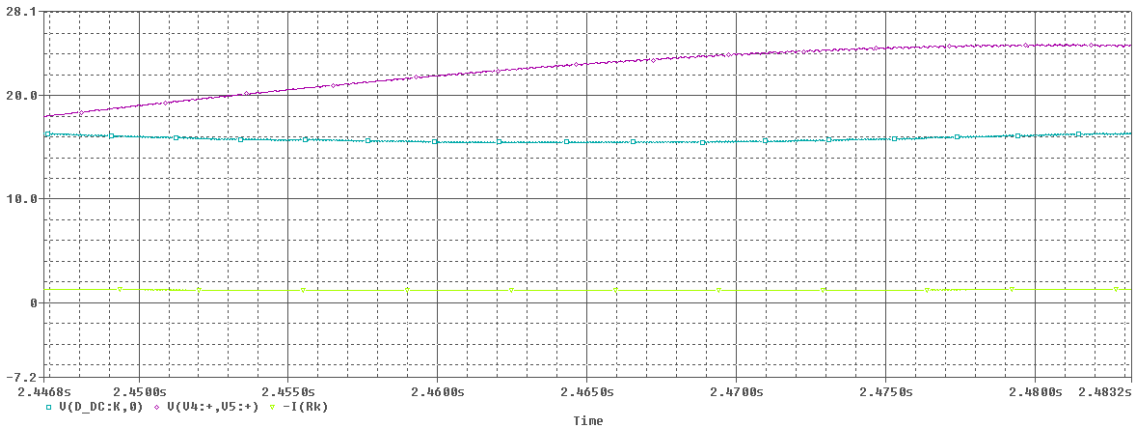

Figure 65: Close zoom of voltage and current dip of 10 kHz boost converter

In Figure 65 we can see the lowest current is less than 0,8A and the lowest voltage is approximately 16V. This is lower than the simulation with 1 kHz (18V and 5A). So increasing of the switching frequency to 10 kHz means no direct improvement.

8 MEASUREMENTS

8.1 Optimal power at fixed speed

In order to extract maximum energy from the ocean, we have to find the optimal load value. A dynamic boost DC-DC converter is used to control the optimal power extraction from the generator. These measurements and optimal power are not linked to the previous simulations.

To perform these measurements, we kept the generator speed fixed. Then we used an adjustable resistive load (connected in triangle). By measuring the generator's phase current I_{ph} and voltage over the resistor U_r we were able to calculate the power. Doing this for different speeds we found the optimal power at those speeds.

The total power which is given in the graphics is calculated by:

$$P = U_{f,gen} I_{ph} 3 \tag{4.1}$$

with

$$U_{f,gen} = \frac{U_r}{\sqrt{3}} \tag{4.2}$$

8.1.1 Load seen from generator side

Loaded with only resistance

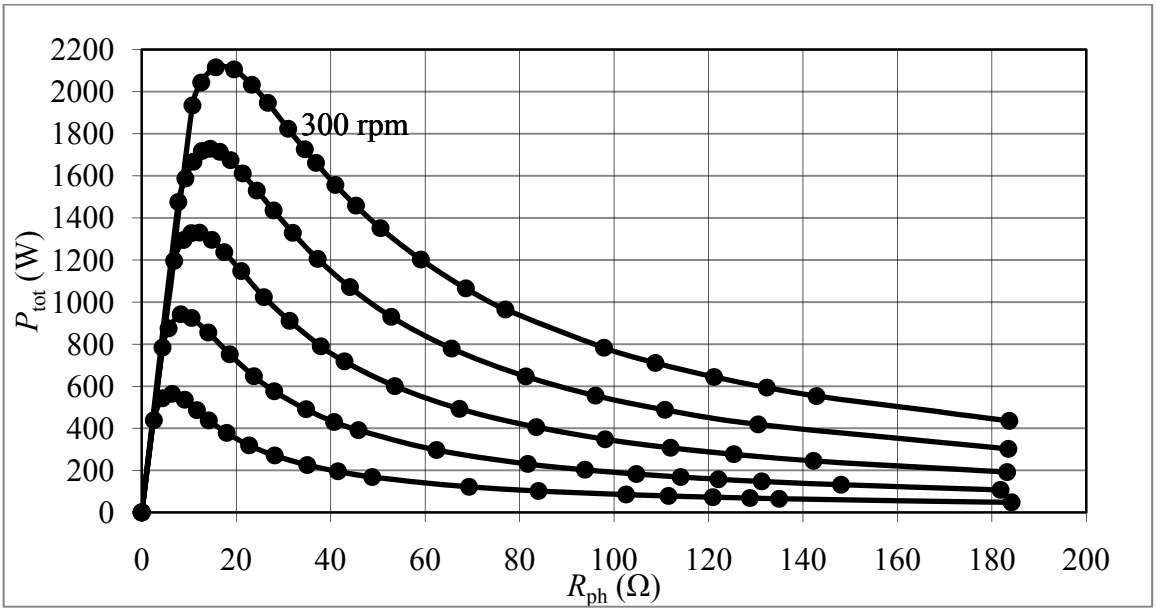

Optimized points:

Resistance

n	R_{ph}
rpm	Ω
300	17
250	14
200	11
150	9
100	6
0	0

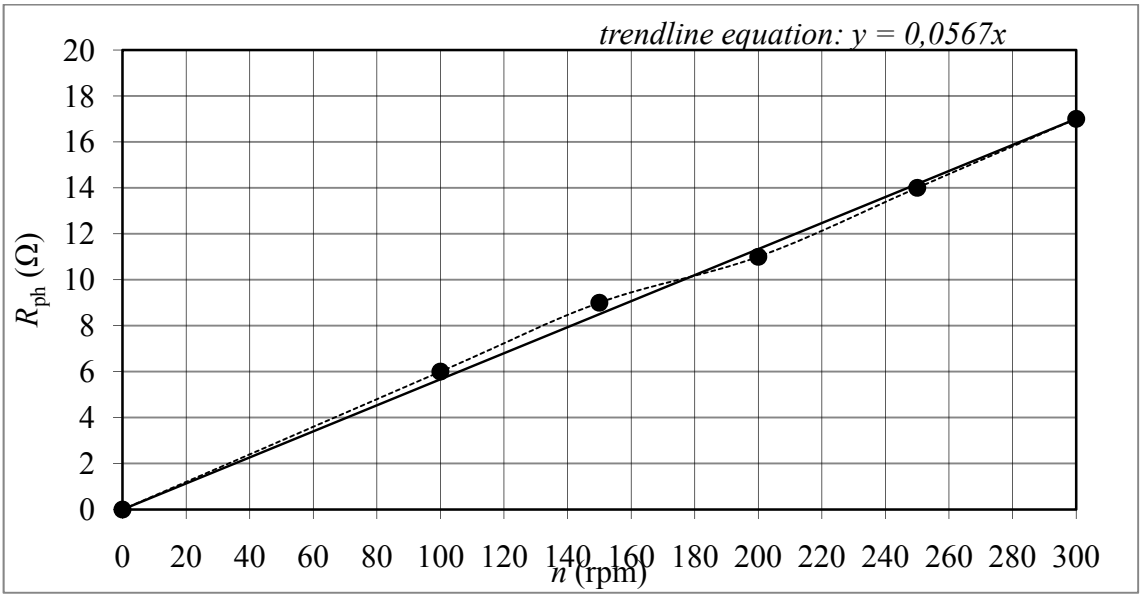

Loaded with resistance + diode bridge

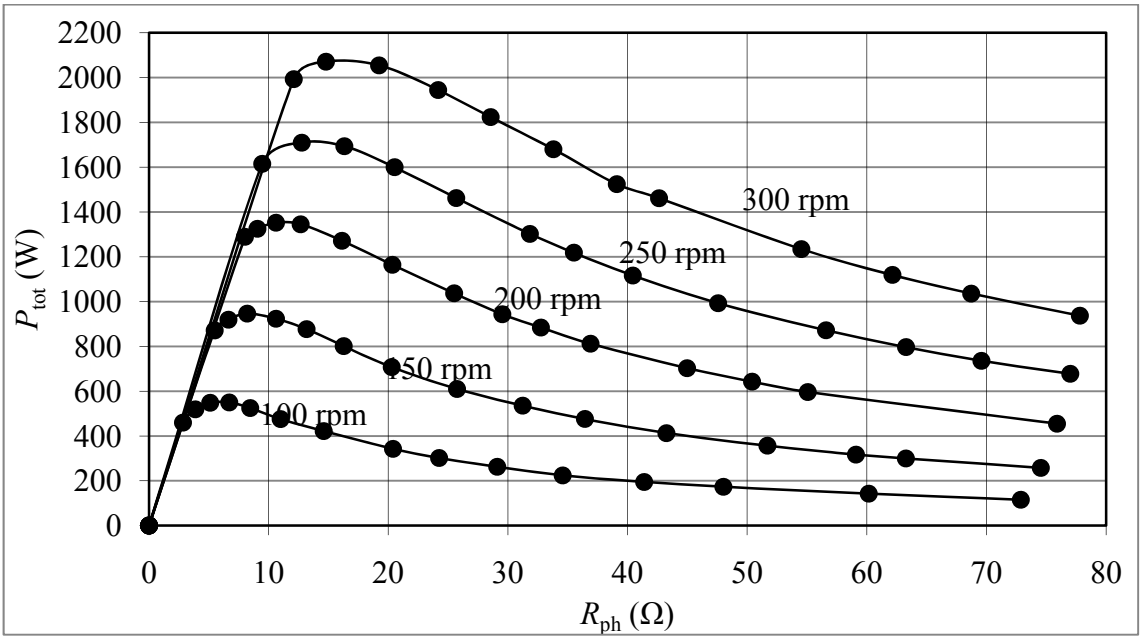

Optimized points

Resistance + bridge

n	R_{ph}
rpm	Ω
300	16
250	14
200	11
150	9
100	6
0	0

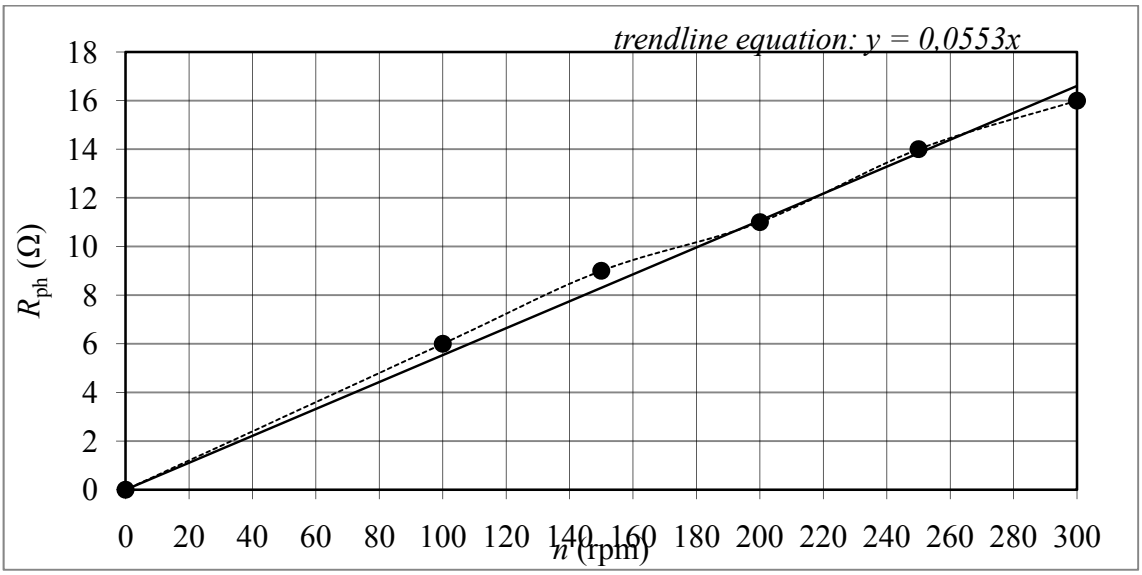

Loaded with only capacitance

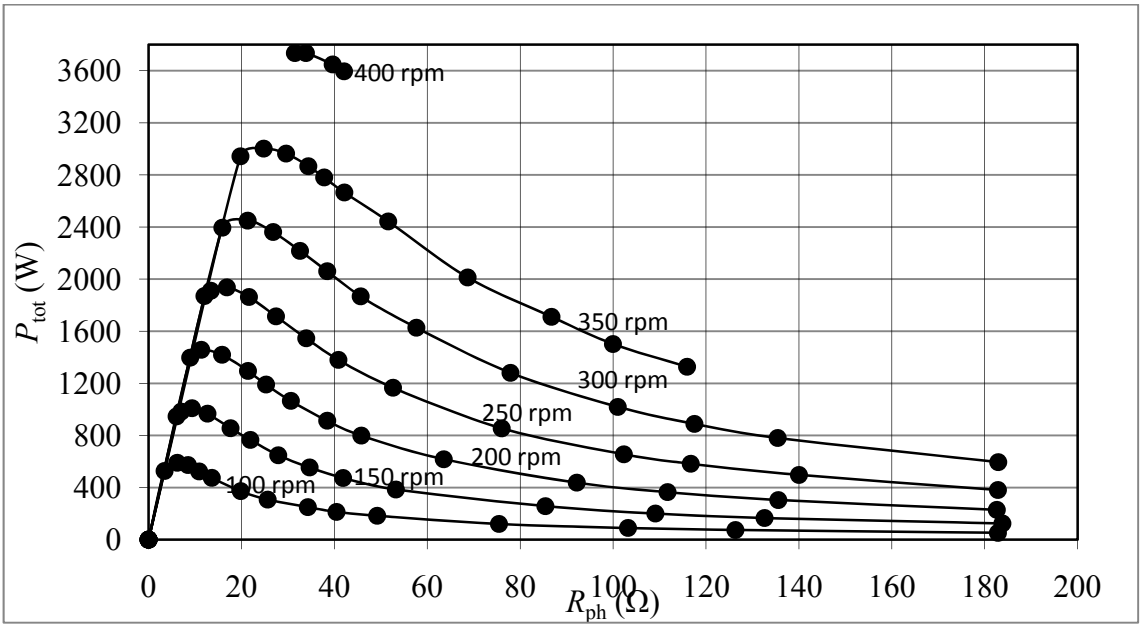

Optimized points

Capacitance

n	R_{ph}
rpm	Ω
400	29
350	23
300	18
250	16
200	12
150	9
100	6
0	0

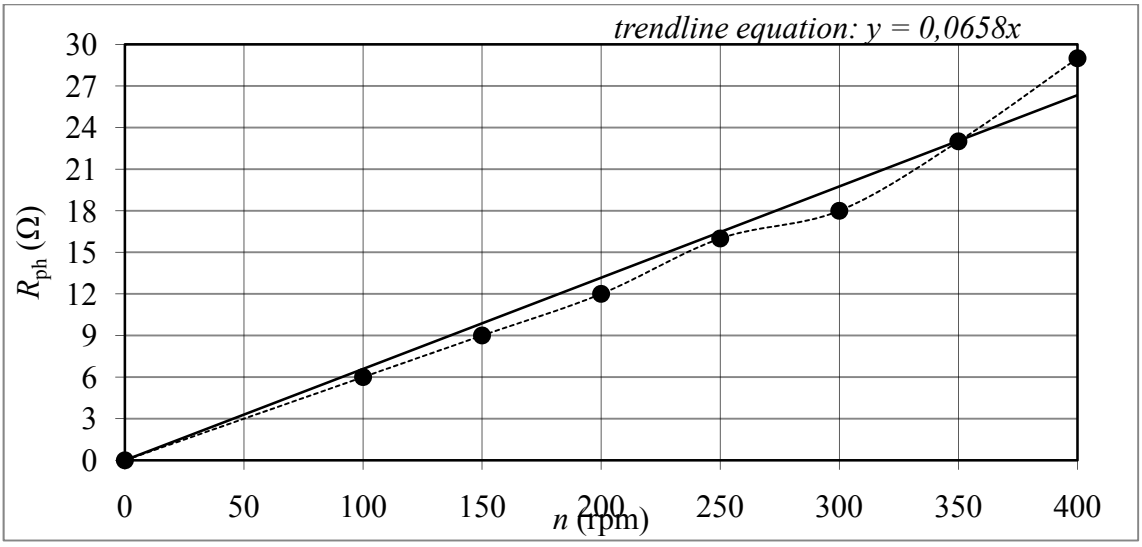

Loaded with capacitance and bridge

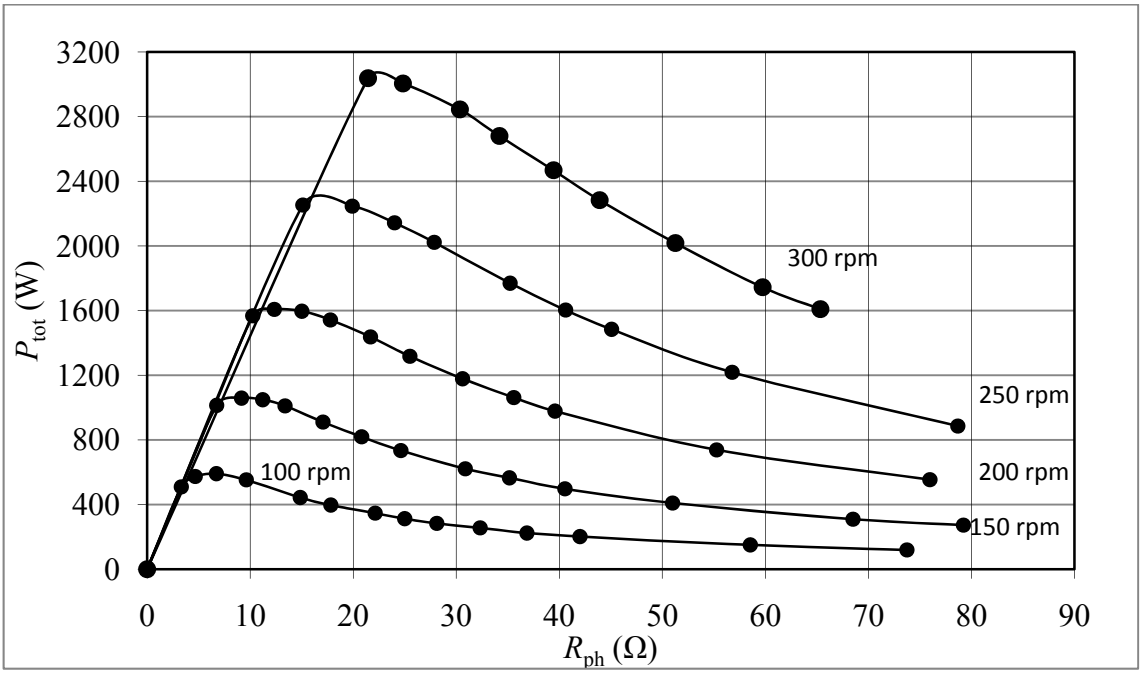

Optimized points

Capacitance + bridge

n	R_{ph}
rpm	Ω
300	21
250	16
200	13
150	9
100	6
0	0

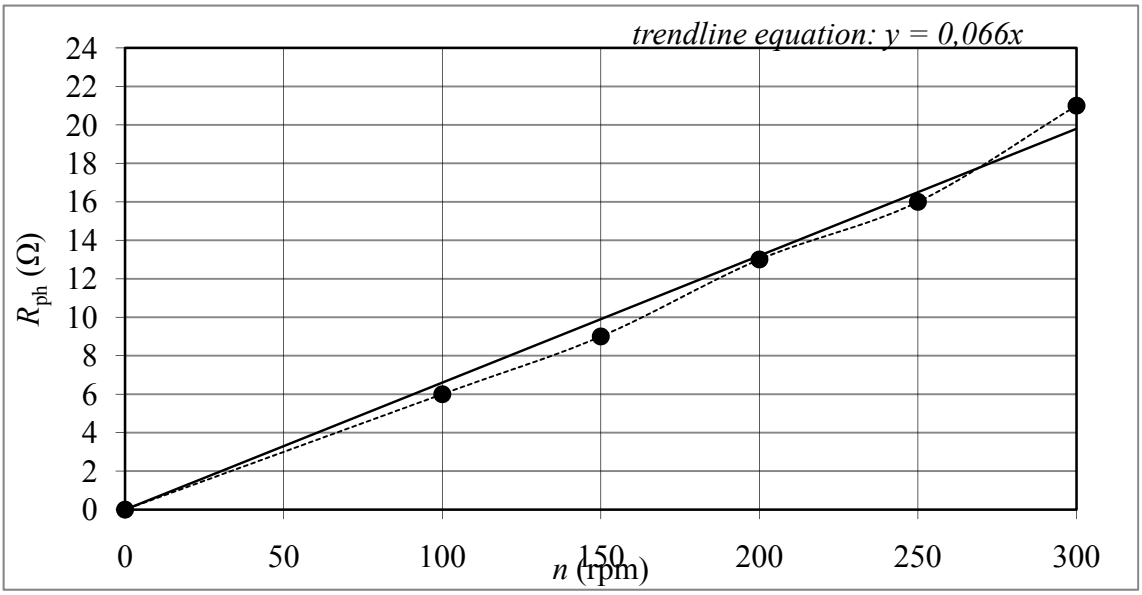

8.1.2 Load seen from DC-side

Note: depends on DC-bridge, these are measurements with our DC-bridge.

Lines with ● show the power measured before the DC-bridge, lines with ■ show the power after the DC-bridge. The difference between the two are the losses.

DC-side without capacitance

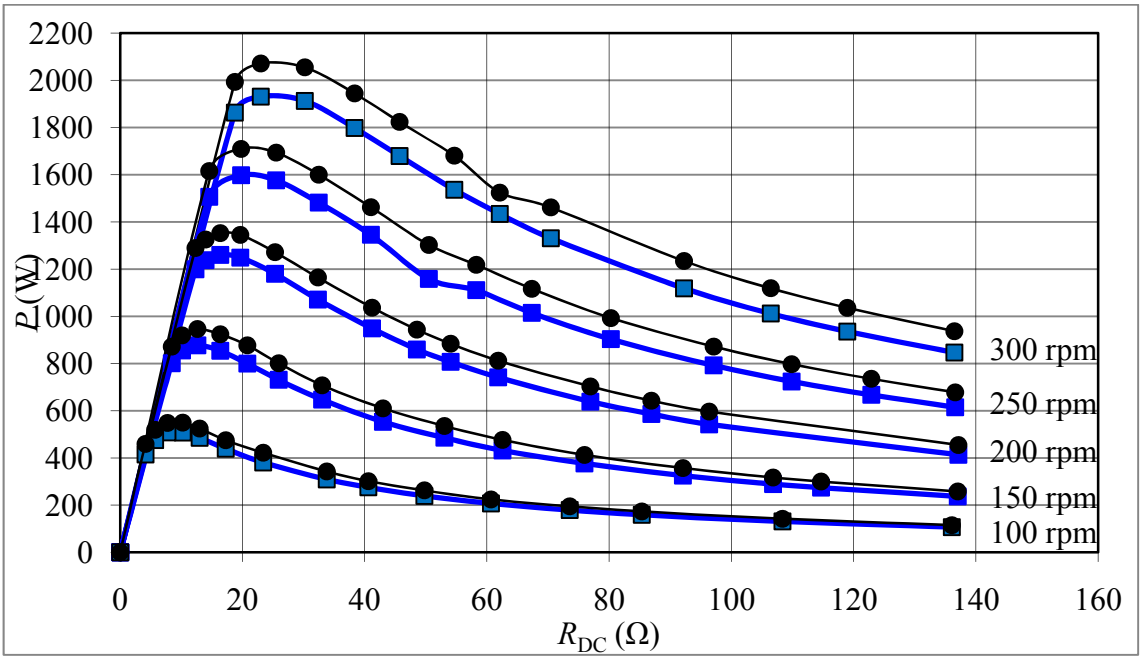

Optimized points

DC - side

n	R_{DC}
rpm	Ω
300	24
250	21
200	17
150	13
100	9
0	0

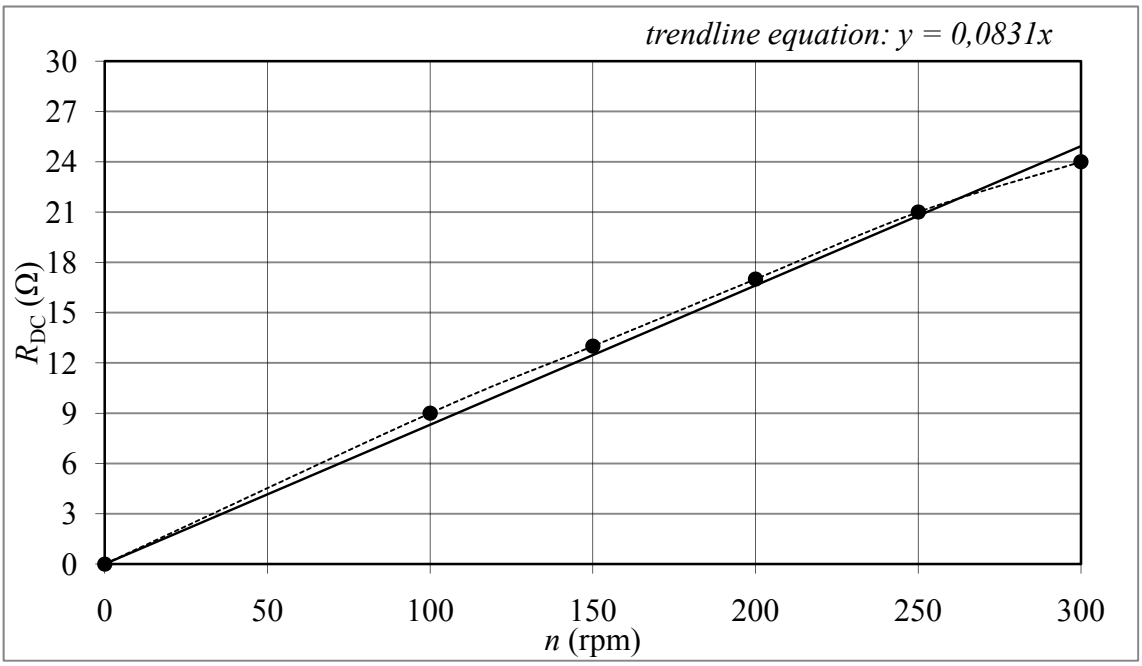
trendline equation: y = 0,0831x
30
27
24
21
18
15
12
9
6
3
0
R_{DC} (Ω)
0
50
100
150
200
250
300
n (rpm)

DC-side with capacitance

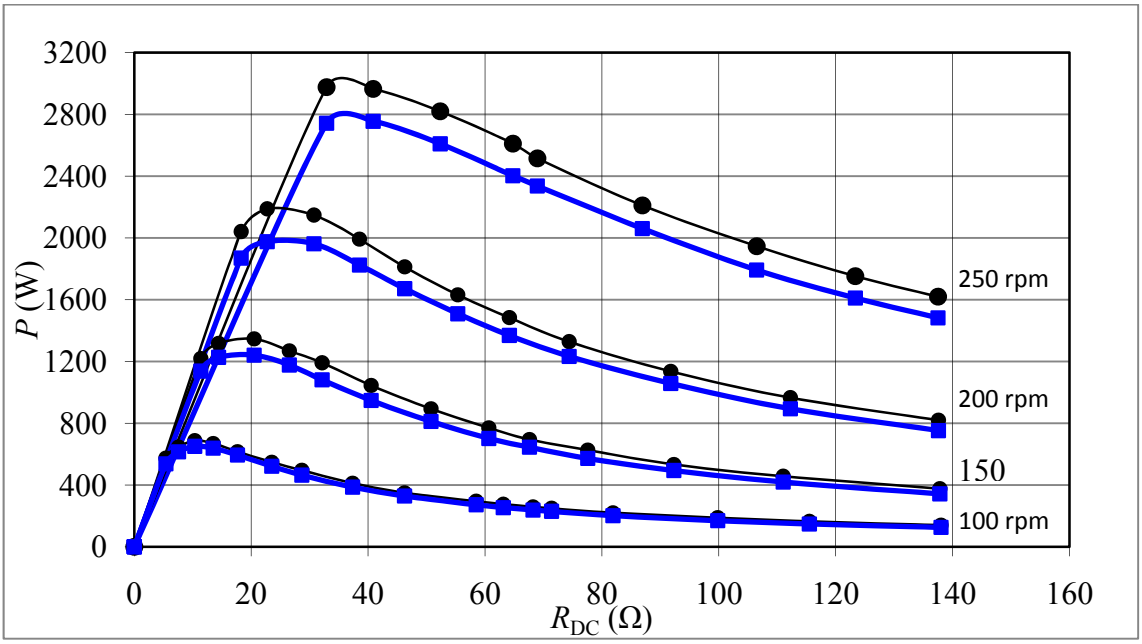

Optimized points

DC-side + Capacitance

n	R_{DC}
rpm	Ω
300	35
250	27
200	21
150	16
100	11
0	0

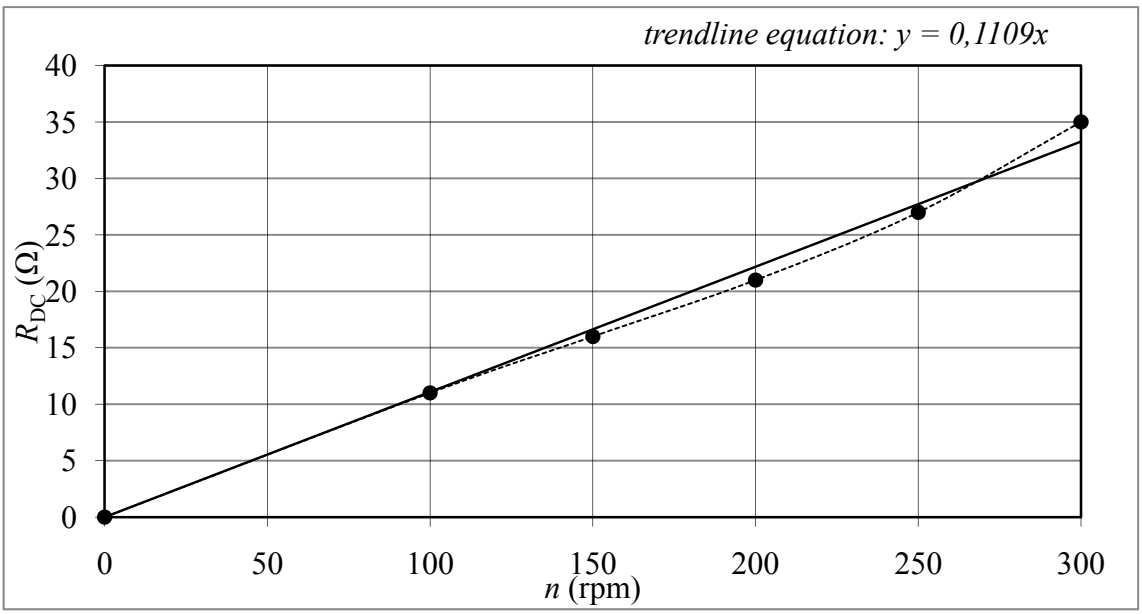

8.1.3 Conclusion

We can see clearly that the total power is changing depending on speed and load. We have to notice that the capacitance, which is switched directly after the generator at the AC side, can boost the total available power to a higher level. This is due to the neutralization of some generator inductance.

We also notice that the curve with load as a function of the speed is near to linear. The trend line is shown and the trend line's equation is calculated. This equation might be useful when the load has to become adjusted to the generator speed. A dynamic system using these equations might be a solution.

8.2 First changing speed measurement

This is the first measurement we did with the generator driven by a changing speed.

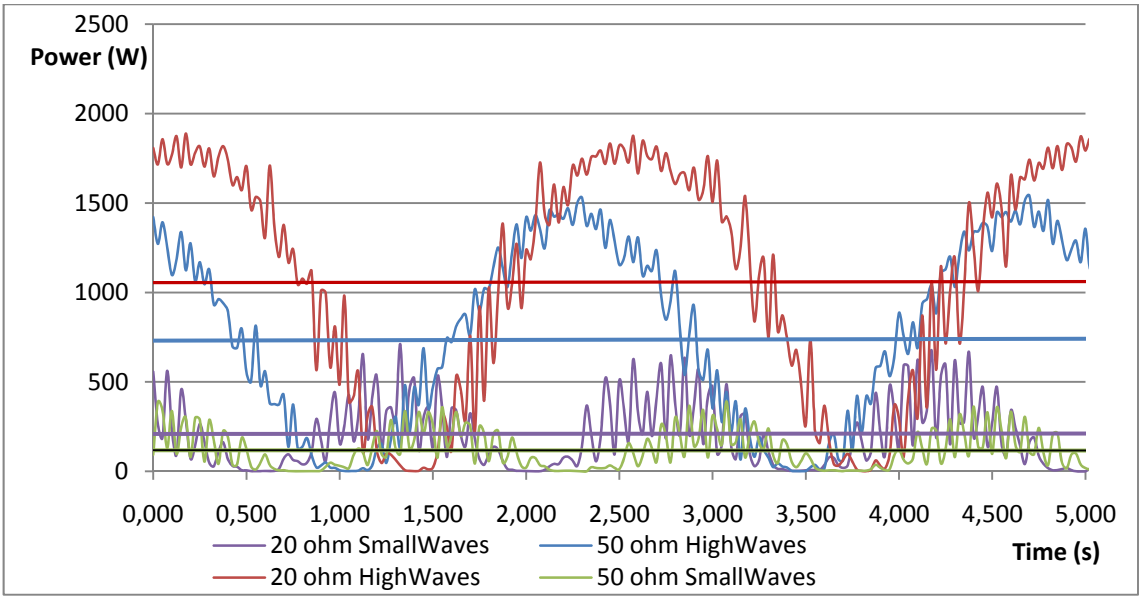

The horizontal lines represent the average generated power. There are two waves, the high waves and the small waves. The high waves are higher (amplitude A) and have a longer wavelength.

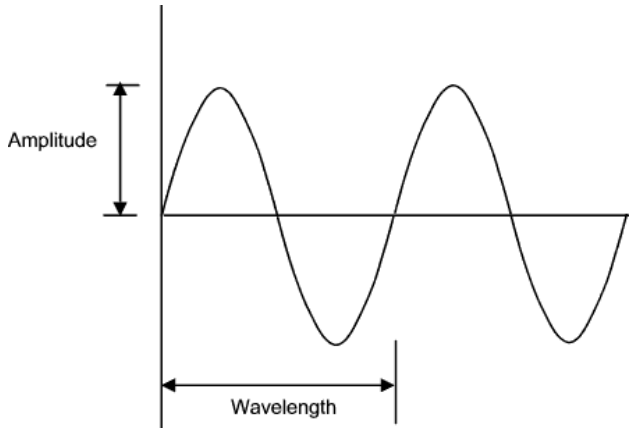

Figure 66: Basic wave

These are the wave properties:

Waves	Lampda m	T s	H m	$v_{average}$ m/s	v_{max} m/s
small	13,0	2,9	1,0	0,34	1,08
high	36,0	4,8	4,7	0,98	3,08

Out of the period T and height H it is possible to calculate the maximum vertical speed v_{max} the buoy will have. This is important, because of the mechanical restrictions of the system. The maximum speed is calculated by a derivation of the sine.

As we can see in the measurements, the generated power is varies a lot. This is the same for the voltage and current. In the next graph, induced voltage is given for the small waves with a 50ohm load.

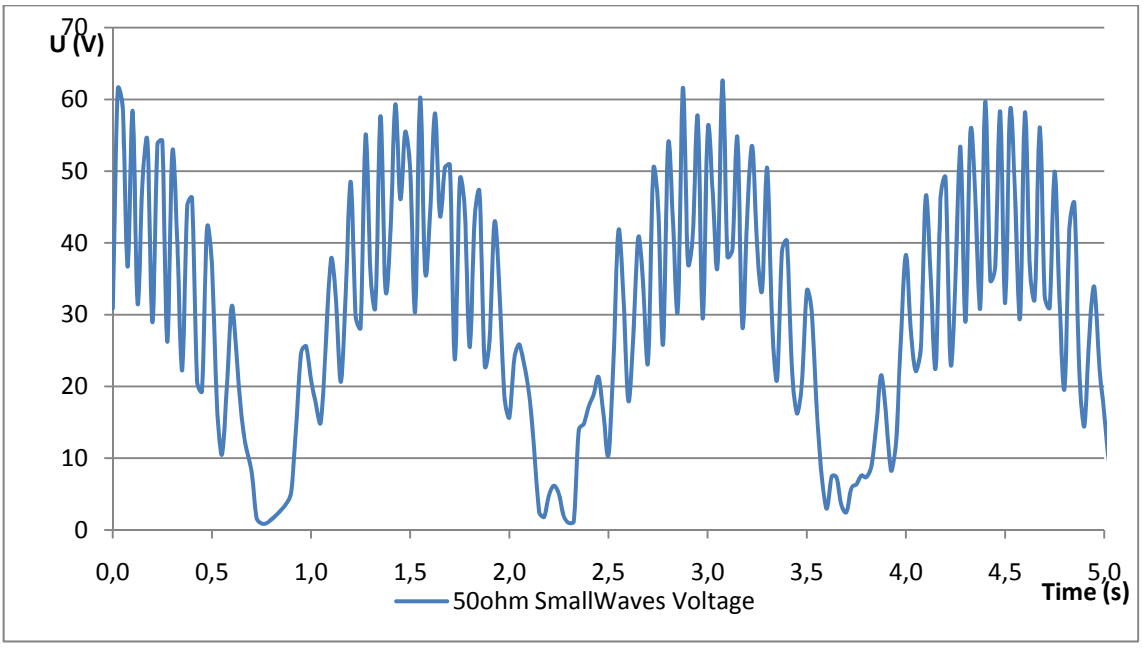

In the measurement, we can see clearly that the induced voltage is not as smooth as we want. By thinking about the reason for this; there were three main possibilities:

1) The servo motor is driven by little steps, so the peaks are an effect of this.
2) The diode bridge influences the measured voltage.
3) The generator is winded in such a way that it causes this effect.

To solve this we removed the diode bridge and let the servo motor run very slow (= changes with small steps). The result was still the same, so eliminating possibilities 1 & 2; we can assume that the generator windings are causing this phenomenon.

Because voltage and current both have this disturbance, the effect strengthens itself when we calculate the power (basically $3.U.I$)

8.3 Fixed load at changing speed

Because it is not easy to control changing load constantly, a fixed load might be a more realistic solution. If so, there are some losses by not using the optimal load. In order to investigate this, we performed a simulation and did some measurements.

8.3.1 Fixed load - Model simulation

This is a model simulation for the same high waves as used in 8.2. The model simulation says that there will be losses, as shown. The red line shows the simulation with an optimized load for each speed. The black line is with a fixed load.

Red - Rph = 0..14,55 ohm
Black - Rph = 14,55 ohm

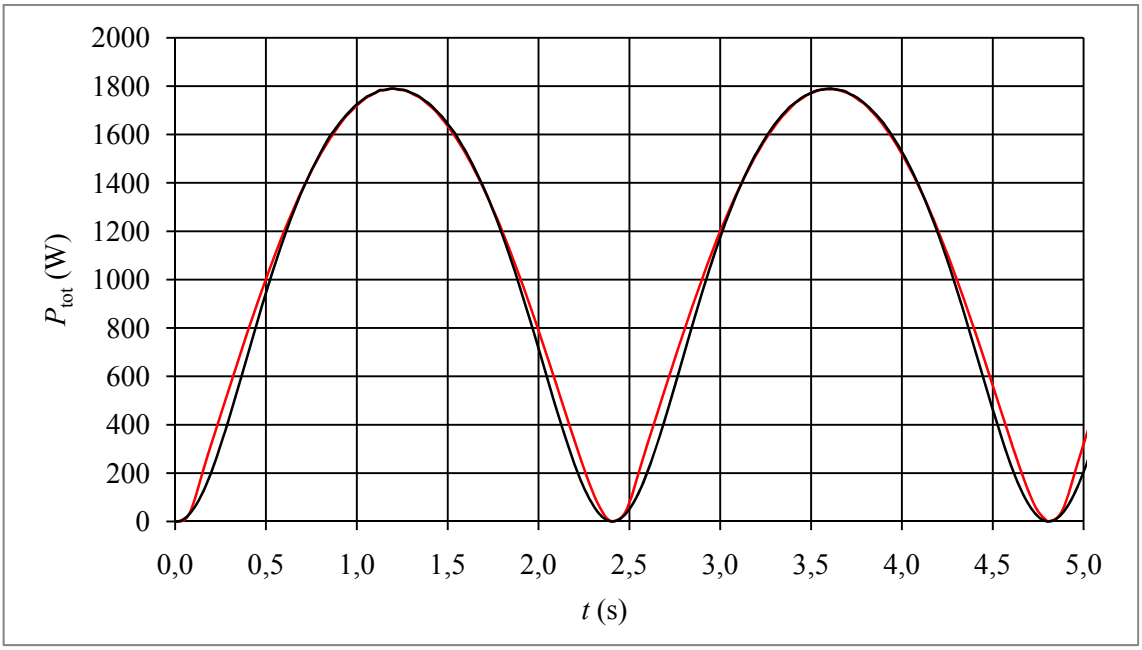

Calculation of the average power of both the fixed load and the varying load gives:

Average power fixed load: $P_{avg,fix}$= 1053,46 W

Average power optimized load: $P_{avg,opt}$ =1209,59 W

We notice a difference of 156,13 W.

8.3.2 Fixed load – Measurements

When we keep the load constant at 14,55Ω the black line shows us the measured power during a test drive. We can see a small difference between the theoretical simulated value (red line).

When we calculate the average power out of the measurements and the simulation data, this is given:

Average power simulation: $P_{avg,sim}$ = 1046,58 W

Average power measurements: $P_{avg,mes}$ = 1073,19 W

We notice a difference of 26,61 W.

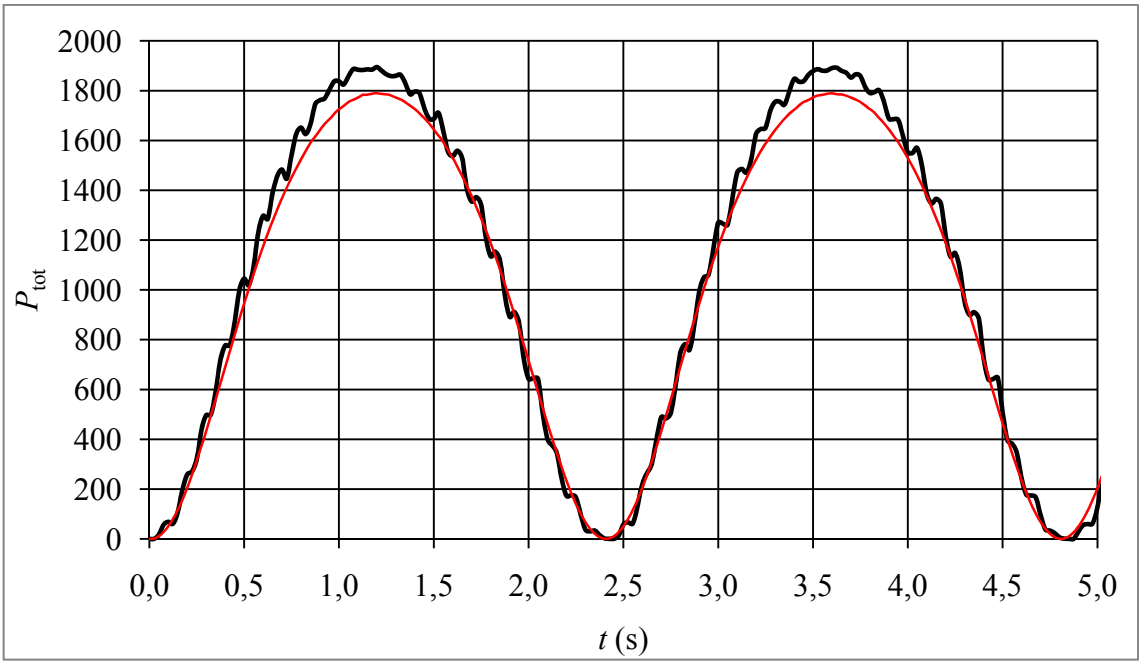

9 CONCLUSIONS

There are enough possibilities to extract wave energy. The technology is surely worth further investment.

When working in this field, we have to keep in mind that theoretical models are not always reliable, and it is difficult to compare them with the reality if there are no practical examples available. Nevertheless, theoretical models -if dimensioned correctly- are very important to estimate the result. Theoretical modeling and simulation is a very time consuming activity, but indispensable in this field.

Since the ASWEC project has now a test setting in the lab, the project has made progress. In the future it will be easier to do practical measurements. The next step is undoubtedly trying to get energy into the grid.

Nonetheless, further research is required to optimize the boost converter. Now simulation programs show the usefulness of the boost converter in the project, further dimensioning and later controlling of the boost converter is necessary.

Measurements on the test setting have showed that the dimensioning of the load can change the energy extraction. Research on how the load can be constantly optimized may be useful.

While using the servo motor control program, we have to keep in mind that the computer running the program has to be powerful enough. It is proven that the measurements of a powerful computer are more precise than the one from a less powerful computer. The main reason may be that the powerful computer can take much more measuring points due to a faster processor.

The PSpice simulations of the boost converter have shown that the boost converter is useful. However, other things may be useful to improve the DC voltage even more. The use of a flywheel might be the first choice. When using this, the axis is expected to have no stops anymore, which makes sure the generator keeps on generating (lower) power. The more power there is at the input of the boost converter, the better it is working. Simulations have shown the boost converter is not able to keep up the output voltage while the input voltage is dropping to zero. The flywheel can help to increase the input voltage when needed.

Combined with the flywheel, a capacitance might also be useful. The advantage with the boost converter might be that the capacitor can be smaller than before. So, we are still avoiding the use of an expensive super capacitor.

In all the simulations, the boost converter has no control. The next step in the development of the boost converter might be the design of the control. This should ensure the boost converter is only working in the points where the voltage is dropping, and the more the voltage drops, the more the converter has to boost. A good control can help to make the DC-voltage smoother.

Theoretically, the switching frequency of the boost converter can improve the results. In this thesis only 1 kHz and 10 kHz is simulated. Further research to find an optimal switching frequency might be useful.

Since the generator is acting very inductive in the simulations (comparable to a current source), calculations made to calculate the boost converter's inductance and the optimized load might be irrelevant in this situation.

10 REFERENCES

[1] Book: João Cruz, 2008, *Ocean Wave Energy – Current status and future perspectives*, Springer

[2] Book: Godfrey Boyle, 2004, *Renewable Energy – Power for a sustainable future, 2nd edition,* Oxford

[3] Book: William D'haeseleer, 2005, *Energie vandaag en morgen. Beschouwingen over energievoorziening en -gebruik*, ACCO

[4] Book: Mohan/ Undeland/ Robbins, 2003, *Power Electronics: Converters, Applications, and Design, 3rd edition*, WILEY

[5] L. Ran, P. Tavner, M. Mueller, N. Baker & S. Mc Donald, "*Power Conversion and Control for a Low Speed, Permanent Magnet, Direct-Drive, Wave Energy Converter"*, Power Electronics Machines and Drives, Dublin 2006.

[6] Paper: Z.Nie, P.C.J. Clifton & R.A. McMahon, 2008, *Wave Energy Emulator and AC/DC Rectifiers for Direct Drive Wave Energy Converters,* Cambridge University Engineering Department, England

[7] Paper: Gunnar Asplund, *Sustainable energy systems with HVDC transmission*

[8] Course: G. Merlevede, *Inleiding tot de vermogenselektronica,* KHBO